EUROPEAN ORGANISATION FOR NUCLEAR RESEARCH (CERN)

Submitted to: JHEP

CERN-EP-2018-168
13th August 2018

Search for charged Higgs bosons decaying into top and bottom quarks at $\sqrt{s} = 13$ TeV with the ATLAS detector

The ATLAS Collaboration

A search for charged Higgs bosons heavier than the top quark and decaying via $H^{\pm} \to tb$ is presented. The data analysed corresponds to 36.1 fb^{-1} of pp collisions at $\sqrt{s} = 13$ TeV and was recorded with the ATLAS detector at the LHC in 2015 and 2016. The production of a charged Higgs boson in association with a top quark and a bottom quark, $pp \to tbH^{\pm}$, is explored in the mass range from $m_{H^{\pm}} = 200$ to 2000 GeV using multi-jet final states with one or two electrons or muons. Events are categorised according to the multiplicity of jets and how likely these are to have originated from hadronisation of a bottom quark. Multivariate techniques are used to discriminate between signal and background events. No significant excess above the background-only hypothesis is observed and exclusion limits are derived for the production cross-section times branching ratio of a charged Higgs boson as a function of its mass, which range from 2.9 pb at $m_{H^{\pm}} = 200$ GeV to 0.070 pb at $m_{H^{\pm}} = 2000$ GeV. The results are interpreted in two benchmark scenarios of the Minimal Supersymmetric Standard Model.

Contents

1 Introduction

Following the discovery of a Higgs boson, H, with a mass of around 125 GeV and consistent with the Standard Model (SM) [1–3] at the Large Hadron Collider (LHC) in 2012 [4] a key question is whether this Higgs boson is the only Higgs boson, or the first observed physical state of an extended Higgs sector. No charged fundamental scalar boson exists in the SM, but many beyond the Standard Model (BSM) scenarios contain an extended Higgs sector with at least one set of charged Higgs bosons, H^+ and H^-, in particular two-Higgs-doublet models (2HDM) [5–8] and models containing Higgs triplets [9–13].

The production mechanisms and decay modes of a charged Higgs boson[1] depend on its mass, m_{H^+}. This analysis searches for heavy charged Higgs bosons with $m_{H^+} > m_t + m_b$, where m_t and m_b are the masses of the top and bottom quarks, respectively. The dominant production mode is expected to be in association with a top quark and a bottom quark (tbH^+), as illustrated in Figure 1. In the 2HDM, H^+ production and decay at tree level depend on its mass and two parameters: $\tan\beta$ and α, which are the ratio of the vacuum expectation values of the two Higgs doublets and the mixing angle between the CP-even Higgs bosons, respectively. The dominant decay mode for heavy charged Higgs bosons is $H^+ \to tb$ in a broad range of models [14, 15]. In particular, this is the preferred decay mode in both the decoupling limit scenario and the alignment limit $\cos(\beta-\alpha) \approx 0$, where the lightest CP-even neutral Higgs boson of the extended Higgs sector has properties similar to those of the SM Higgs boson [7]. For lower m_{H^+}, the dominant decay mode is $H^+ \to \tau\nu$. It is also predicted that this decay mode becomes more relevant as the value of $\tan\beta$

[1] For simplicity in the following, charged Higgs bosons are denoted H^+, with the charge-conjugate H^- always implied. Similarly, the difference between quarks and antiquarks, q and $\bar{q}$, is generally understood from the context, so that e.g. $H^+ \to tb$ means both $H^+ \to t\bar{b}$ and $H^- \to \bar{t}b$.

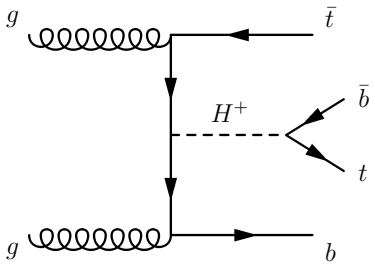

Figure 1: Leading-order Feynman diagram for the production of a heavy charged Higgs boson ($m_{H^+} > m_t + m_b$) in association with a top quark and a bottom quark (tbH^+).

increases, irrespective of m_{H^+}. Therefore, the $H^+ \to tb$ and $H^+ \to \tau\nu$ decays naturally complement each other in searches for charged Higgs bosons.

Limits on charged Higgs boson production have been obtained by many experiments, such as the LEP experiments with upper limits on H^+ production in the mass range 40–100 GeV [16], and CDF and DØ at the Tevatron that set upper limits on the branching ratio $\mathcal{B}(t \to bH^+)$ for 80 GeV $< m_{H^+} <$ 150 GeV [17, 18]. The CMS Collaboration has performed direct searches for heavy charged Higgs bosons in 8 TeV proton–proton (pp) collisions. By assuming the branching ratio $\mathcal{B}(H^+ \to tb) = 1$, an upper limit of 2.0–0.13 pb was obtained for the production cross-section $\sigma(pp \to tbH^+)$ for 180 GeV $< m_{H^+} <$ 600 GeV [19]. The ATLAS Collaboration has searched for similar heavy charged Higgs boson production in the $H^+ \to tb$ decay channel at 8 TeV, setting upper limits on the production cross-section times the $H^+ \to tb$ branching ratio of 6–0.2 pb for 200 GeV $< m_{H^+} <$ 600 GeV [20]. Indirect constraints can be obtained from the measurement of flavour-physics observables sensitive to charged Higgs boson exchange. Such observables include the relative branching ratios of B or K meson decays, B meson mixing parameters, the ratio of the Z decay partial widths $\Gamma(Z \to b\bar{b})/\Gamma(Z \to \text{hadrons})$, as well as the measurements of $b \to s\gamma$ decays [21, 22]. The relative branching ratio $\mathcal{R}(D^{(*)}) = \mathcal{B}(B \to D^{(*)}\tau\nu)/\mathcal{B}(B \to D^{(*)}\ell\nu)$, where ℓ denotes e or μ, are especially sensitive to contributions from new physics. Measurements from BaBar [23] exclude H^+ for all m_{H^+} and $\tan\beta$ values in a Type-II 2HDM. However, more recent measurements from Belle [24–26] and LHCb [27] place a weaker constraint on the allowed range of $m_{H^+}/\tan\beta$ values. A global fit combining the most recent flavour-physics results [22] sets a lower limit at 95% confidence level on the charged Higgs boson mass of $m_{H^+} \gtrsim 600$ GeV for $\tan\beta > 1$ and $m_{H^+} \gtrsim 650$ GeV for lower $\tan\beta$ values, assuming a Type-II 2HDM.

This paper presents a search for H^+ production in the $H^+ \to tb$ decay mode using pp collisions at $\sqrt{s} = 13$ TeV. Events with one charged lepton ($\ell = e, \mu$) and jets in the final state (ℓ+jets final state) and events with two charged leptons and jets in the final state ($\ell\ell$ final state) are considered. Exclusive regions are defined according to the number of jets and those that are tagged as originating from the hadronisation of a b-quark. In order to separate the signal from the SM background, multivariate discriminants are employed in the regions where the signal contributions are expected to be largest. Limits on the $H^+ \to tb$ production cross-section are set by means of a simultaneous fit of binned distributions of multivariate discriminants in the signal-rich regions and inclusive event yields in the signal-depleted regions. The results are interpreted in two benchmark scenarios of the Minimal Supersymmetric Standard Model (MSSM): the $m_h^{\text{mod}-}$ scenario [28] and the hMSSM [29]. Both scenarios exploit the MSSM in such a way that the light CP-even Higgs boson can be interpreted as the observed Higgs boson with $m_H = 125$ GeV. Limits on the value of $\tan\beta$ are extracted as a function of the charged Higgs boson mass. Finally, the

excluded range of m_{H^+} and tanβ values from the $H^+ \to tb$ and $H^+ \to \tau\nu$ [30] searches at $\sqrt{s} = 13$ TeVare superimposed, providing a summary of the ATLAS sensitivity to H^+ through the two decay modes.

The paper is organised as follows. Section 2 briefly describes the ATLAS detector. The samples of simulated events used for the analysis are summarised in Section 3. Section 4 presents the reconstruction of objects in ATLAS and the event selection. Section 5 describes the analysis strategy while systematic uncertainties are discussed in Section 6. The statistical analysis of the data is described in Section 7 and the results are presented in Section 8. Finally, a summary is given in Section 9.

2 ATLAS detector

The ATLAS detector [31] at the LHC is a multipurpose particle detector with a forward–backward symmetric cylindrical geometry and near 4π coverage around the collision point.[2] The ATLAS detector consists of an inner tracking detector (ID) surrounded by a thin superconducting solenoid producing a 2 T axial magnetic field, electromagnetic (EM) and hadronic calorimeters, and an external muon spectrometer (MS) incorporating three large toroid magnet assemblies. The ID contains a high-granularity silicon pixel detector, including an insertable B-layer [32] added in 2014 as a new innermost layer, and a silicon microstrip tracker, providing precision tracking in the pseudorapidity range $|\eta| < 2.5$. The silicon detectors are complemented by a transition radiation tracker providing tracking and electron identification information for $|\eta| < 2.0$. The EM sampling calorimeter uses lead as the absorber material and liquid argon (LAr) as the active medium, and is divided into barrel ($|\eta| < 1.47$) and endcap ($1.37 < |\eta| < 3.20$) regions. Hadron calorimetry is also based on the sampling technique, with scintillator tiles or LAr as the active medium, and with steel, copper, or tungsten as the absorber material. The calorimeters cover $|\eta| < 4.9$. The MS measures the deflection of muons with $|\eta| < 2.7$ using multiple layers of high-precision tracking chambers located in a toroidal field in the central and endcap regions of ATLAS. The field integral of the toroids ranges between 2.0 and 6.0 T m across most of the detector. The MS is also instrumented with separate trigger chambers covering $|\eta| < 2.4$. A two-level trigger system, with the first level implemented in custom hardware and followed by a software-based second level, is used to reduce the trigger rate to around 1 kHz for offline storage [33].

3 Signal and background modelling

The tbH^+ process was modelled with MadGraph5_aMC@NLO (MG5_aMC) [34] at next-to-leading order (NLO) in QCD [35] using a four-flavour scheme (4FS) implementation with the NNPDF2.3NLO [36] parton distribution function (PDF).[3] Parton showering and hadronisation were modelled by Pythia 8.186 [37]

[2] ATLAS uses a right-handed coordinate system with its origin at the nominal interaction point (IP) in the centre of the detector and the z-axis along the beam pipe. The x-axis points from the IP to the centre of the LHC ring, and the y-axis points upwards. Cylindrical coordinates (r, ϕ) are used in the transverse plane, ϕ being the azimuthal angle around the z-axis. The pseudorapidity is defined in terms of the polar angle θ as $\eta = -\ln\tan(\theta/2)$. Angular distance is measured in units of $\Delta R \equiv \sqrt{(\Delta\eta)^2 + (\Delta\phi)^2}$ (pseudorapidity and azimuthal angle). Alternatively, the distance $\Delta R_y \equiv \sqrt{(\Delta y)^2 + (\Delta\phi)^2}$ is used, where $y = 0.5 \ln\left[(E + p_z)/(E - p_z)\right]$ is the rapidity of a particle of energy E and momentum component p_z along the beam axis.

[3] Five-flavour scheme (5FS) PDFs consider b-quarks as a source of incoming partons and the b-quarks are therefore assumed to be massless. In contrast, 4FS PDFs only include lighter quarks and gluons, allowing the b-quark mass to be taken into account properly in the matrix element calculation.

with the A14 [38] set of underlying-event (UE) related parameters tuned to ATLAS data (tune). For the simulation of the tbH^+ process, the narrow-width approximation was used. This assumption has a negligible impact on the analysis for the models considered in this paper, as the experimental resolution is much larger than the H^+ natural width. Interference with the SM $t\bar{t} + b\bar{b}$ background is neglected.

Altogether 18 H^+ mass hypotheses are used, with 25 GeV mass steps between an H^+ mass of 200 GeV and 300 GeV, 50 GeV steps between 300 GeV and 400 GeV, 100 GeV steps between 400 GeV and 1000 GeV and 200 GeV steps from 1000 GeV to 2000 GeV. The step sizes are selected to match the expected resolution of the H^+ signal. The samples were processed with a fast simulation of the ATLAS detector [39]. Unless otherwise indicated, the cross-section of the signal is set to 1 pb, for easy rescaling to various model predictions. Only the H^+ decay into tb is considered, and the top quark decays according to the SM predictions.

The nominal sample used to model the $t\bar{t}$ background was generated using the Powheg-Box v2 NLO-in-QCD generator [40–43], referred to as Powheg in the remainder of this article, with the NNPDF3.0NLO PDF set [44]. The h_{damp} parameter, which controls the transverse momentum p_{T} of the first additional emission beyond the Born configuration, was set to 1.5 times the top quark mass [45]. Parton shower and hadronisation were modelled by Pythia 8.210 [46] with the A14 UE tune. The sample was normalised to the top++2.0 [47] theoretical cross-section of 832^{+46}_{-51} pb, calculated at next-to-next-to-leading order (NNLO) in QCD including resummation of next-to-next-to-leading logarithmic (NNLL) soft gluon terms [48–52]. The generation of the $t\bar{t}$ sample was performed inclusively, with all possible flavours of additional jets produced. The decay of c- and b-hadrons was simulated with the EvtGen v1.2.0 [53] program. The $t\bar{t}$ + jets background is categorised according to the flavour of additional jets in the event, using the same procedure as described in Ref. [54]. The $t\bar{t}$ + additional heavy-flavour (HF) jets background is subdivided into the categories $t\bar{t} + \geq 1b$ and $t\bar{t} + \geq 1c$, depending on whether the additional HF jets originate from hadrons containing b- or c-quarks. Particle jets were reconstructed from stable particles (mean lifetime $\tau > 3 \times 10^{-11}$ seconds) at generator level using the anti-k_t algorithm [55] with a radius parameter of 0.4, and were required to have $p_{\text{T}} > 15$ GeV and $|\eta| < 2.5$. If at least one particle-level jet in the event is matched ($\Delta R < 0.3$) to a b-hadron (not originating from a t-decay) with $p_{\text{T}} > 5$ GeV, the event is categorised as $t\bar{t} + \geq 1b$. In the remaining events, if at least one jet is matched to a c-hadron (not originating from a W decay) but no b-hadron, the event is categorised as $t\bar{t} + \geq 1c$. Events with $t\bar{t}$ + jets that belong to neither the $t\bar{t} + \geq 1b$ nor $t\bar{t} + \geq 1c$ category are called $t\bar{t}$ + light events.

For the $t\bar{t} + \geq 1b$ process, subcategories are defined in accord with the matching between particle-level jets and the b-hadrons not from t-decay: events where exactly two jets are matched to b-hadrons ($t\bar{t} + b\bar{b}$), events where exactly one jet is matched to a b-hadron ($t\bar{t} + b$), events where exactly one jet is matched to two or more b-hadrons ($t\bar{t} + B$), and all other events ($t\bar{t} + \geq 3b$). Events where the additional HF jets can only be matched to b-hadrons from multi-parton interactions and final-state gluon radiation are considered separately and labelled as $t\bar{t} + b$ (MPI/FSR).

To model the irreducible $t\bar{t} + \geq 1b$ background to the highest available precision, the $t\bar{t} + \geq 1b$ events from the nominal Powheg+Pythia8 simulation are reweighted to an NLO prediction of $t\bar{t}b\bar{b}$ including parton showering and hadronisation from Sherpa 2.1.1 [56, 57] with OpenLoops [58]. This sample was generated using the 4FS PDF set CT10F4 [59]. The renormalisation scale (μ_{R}) for this sample was set to the $\mu_{\text{CMMPS}} = \prod_{i=t,\bar{t},b,\bar{b}} E_{\text{T},i}^{1/4}$ [57, 60], and the factorisation (μ_{F}) and resummation (μ_{Q}) scales to $H_{\text{T}}/2 = \frac{1}{2}\sum_{i=t,\bar{t},b,\bar{b}} E_{\text{T},i}$. A first type of reweighting is performed in the $t\bar{t} + \geq 1b$ subcategories, using a method similar to the one outlined in Ref. [61]. The reweighting corrects the relative normalisation of the $t\bar{t} + \geq 1b$ subcategories to match the predictions from Sherpa, while keeping the overall $t\bar{t} + \geq 1b$

normalisation unchanged. A second type of reweighting is derived and performed on several kinematic variables sequentially. First the p_{T} of the $t\bar{t}$ system is reweighted, and secondly the p_{T} of the top quarks. The final reweighting is performed depending on the type of $t\bar{t}+\geq 1b$ events. If there is only one additional HF jet, the p_{T} of that jet is used in the final reweighting. If there is more than one additional HF jet, first the ΔR between the HF jets is reweighted and then the p_{T} of the HF dijet system. A closure test is performed on all reweighted kinematic variables, showing a reasonable level of agreement between the reweighted Powheg+Pythia8 sample and the Sherpa sample.

The Powheg-Box v1 generator was used to produce the samples of Wt single-top-quark backgrounds, with the CT10 PDF set. Overlaps between the $t\bar{t}$ and Wt final states were handled using the 'diagram removal' scheme [62]. The t-channel single-top-quark events were generated using the Powheg-Box v1 generator with the 4FS for the NLO matrix element calculations and the fixed 4FS PDF set CT10F4. The top quarks were decayed with MadSpin [63], which preserves the spin correlations. The samples were interfaced to Pythia 6.428 [64] with the Perugia 2012 UE tune [65]. The single-top-quark Wt and t-channel samples were normalised to the approximate NNLO (aNNLO) theoretical cross-section [66–68].

Samples of W/Z+jets events were generated using Sherpa 2.2.1 [56]. Matrix elements were calculated for up to 2 partons at NLO and 4 partons at LO using Comix [69] and OpenLoops and merged with the Sherpa parton shower [70] using the ME+PS@NLO prescription [71]. The NNPDF3.0NNLO PDF set was used together with a dedicated parton shower tune developed by the Sherpa authors. The W/Z+jets events were normalised to the NNLO cross-sections [72–76].

Samples of $t\bar{t}V$ ($V = W, Z$) events were generated at NLO in the matrix elements calculation using MG5_aMC with the NNPDF3.0NLO PDF set interfaced to Pythia 8.210 with the A14 UE tune. The $t\bar{t}H$ process was modelled using MG5_aMC with NLO matrix elements, NNPDF3.0NLO PDF set and factorisation and renormalisation scales set to $\mu_{\mathrm{F}} = \mu_{\mathrm{R}} = m_{\mathrm{T}}/2$, where m_{T} is defined as the scalar sum of the transverse masses $m_{\mathrm{T}} = \sqrt{p_{\mathrm{T}}^2 + m^2}$ of all final-state particles. The events were interfaced to Pythia 8.210 with the A14 UE tune. Variations in $t\bar{t}H$ production due to the extended Higgs sector are not considered in this analysis. Measurements of the $t\bar{t}H$ production cross-section have been performed by the ATLAS and CMS Collaborations [77, 78] at 13 TeV, both in agreement with the SM prediction within 25%.

The minor $tH + X$ backgrounds, consisting of the production of a single top quark in association with a Higgs boson and jets ($tHjb$), and the production of a single top quark, a W boson and a Higgs boson (WtH), are treated as one background. The $tHjb$ process was simulated with MG5_aMC interfaced to Pythia 8.210 and the CT10 PDF set, and WtH was modelled with MG5_aMC interfaced to Herwig++ [79] using the CTEQ6L1 PDF set [80]. Additional minor SM backgrounds (diboson production, single top s-channel, tZ, tWZ, $4t$, $ttWW$) were also simulated and accounted for, even though they contribute less than 1% in any analysis region.

Except where otherwise stated, all simulated event samples were produced using the full ATLAS detector simulation [81] based on Geant 4 [82]. Additional pile-up interactions were simulated with Pythia 8.186 using the A2 set of tuned parameters [83] and the MSTW2008LO PDF set [84], and overlaid onto the simulated hard-scatter event. All simulated samples were reweighted such that the average number of interactions per bunch crossing (pile-up) matches that of the data. In the simulation, the top quark mass was set to $m_t = 172.5\,\mathrm{GeV}$. Decays of b- and c-hadrons were performed by EvtGen v1.2.0, except in samples simulated by the Sherpa event generator.

The samples and their basic generation parameters are summarised in Table 1.

Table 1: Nominal simulated signal and background event samples. The generator, parton shower generator and cross-section used for normalisation are shown together with the applied PDF set and tune. The $t\bar{t}b\bar{b}$ event sample generated using Sherpa 2.1.1 is used to reweight the events from the $t\bar{t}+\geq 1b$ process in the $t\bar{t}$ + jets sample.

Physics process	Generator	Parton shower generator	Cross-section normalisation	PDF set	Tune
tbH^+	MG5_aMC	Pythia 8.186	–	NNPDF2.3NLO	A14
$t\bar{t}$ + jets	Powheg-Box v2	Pythia 8.210	NNLO+NNLL	NNPDF3.0NLO	A14
$t\bar{t}b\bar{b}$	Sherpa 2.1.1	Sherpa 2.1.1	NLO for $t\bar{t}b\bar{b}$	CT10F4	Sherpa default
$t\bar{t}V$	MG5_aMC	Pythia 8.210	NLO	NNPDF3.0	A14
$t\bar{t}H$	MG5_aMC	Pythia 8.210	NLO	NNPDF3.0NLO	A14
Single top, Wt	Powheg-Box v1	Pythia 6.428	aNNLO	CT10	Perugia 2012
Single top, t-channel	Powheg-Box v1	Pythia 6.428	aNNLO	CT10F4	Perugia 2012
W+jets	Sherpa 2.2.1	Sherpa 2.2.1	NNLO	NNPDF3.0NNLO	Sherpa default
Z+jets	Sherpa 2.2.1	Sherpa 2.2.1	NNLO	NNPDF3.0NNLO	Sherpa default

4 Object and event selection

The data used in this analysis were recorded in 2015 and 2016 from $\sqrt{s}$ = 13 TeV pp collisions with an integrated luminosity of 36.1 fb^{-1}. Only runs with stable colliding beams and in which all relevant detector components were functional are used. Events are required to have at least one reconstructed vertex with two or more tracks with $p_{\mathrm{T}} > 0.4$ GeV. The vertex with the largest sum of the squared p_{T} of associated tracks is taken as the primary vertex.

Events were recorded using single-lepton triggers, in both the ℓ+jets and $\ell\ell$ final states. To maximise the event selection efficiency, multiple triggers were used, with either low p_{T} thresholds and lepton identification and isolation requirements, or with higher p_{T} thresholds but looser identification criteria and no isolation requirements. Slightly different sets of triggers were used for 2015 and 2016 data. For muons, the lowest p_{T} threshold was 20 (26) GeV in 2015 (2016), while for electrons, triggers with a p_{T} threshold of 24 (26) GeV were used. Simulated events were also required to satisfy the trigger criteria.

Electrons are reconstructed from energy clusters in the EM calorimeter associated with tracks reconstructed in the ID [85]. Candidates in the calorimeter transition region $1.37 < |\eta_{\mathrm{cluster}}| < 1.52$ are excluded. Electrons are required to satisfy the tight identification criterion described in Ref. [85], based on shower-shape and track-matching variables. Muons are reconstructed from track segments in the MS that are matched to tracks in the ID [86]. Tracks are then re-fit using information from both detector systems. The medium identification criterion described in Ref. [86] is used to select muons. To reduce the contribution of leptons from hadronic decays (non-prompt leptons), both the electrons and muons must satisfy isolation criteria. These criteria include both track and calorimeter information, and have an efficiency of 90% for leptons with a p_{T} of 25 GeV, rising to 99% above 60 GeV, as measured in $Z \to ee$ [85] and $Z \to \mu\mu$ [86] samples. Finally, the lepton tracks must point to the primary vertex of the event: the longitudinal impact parameter z_0 must satisfy $|z_0 \sin\theta| < 0.5$ mm, while the transverse impact parameter significance must satisfy, $|d_0|/\sigma(|d_0|) < 5$ (3) for electrons (muons).

Jets are reconstructed from three-dimensional topological energy clusters [87] in the calorimeter using the anti-k_t jet algorithm [55, 88] with a radius parameter of 0.4. Each topological cluster is calibrated to the EM scale response prior to jet reconstruction. The reconstructed jets are then calibrated to the jet energy scale (JES) derived from simulation and *in situ* corrections based on $\sqrt{s}$ = 13 TeV data [89]. After

energy calibration, jets are required to have $p_{\mathrm{T}} > 25\,\mathrm{GeV}$ and $|\eta| < 2.5$. Quality criteria are imposed to identify jets arising from non-collision sources or detector noise, and events containing any such jets are removed [90]. Finally, to reduce the effect of pile-up an additional requirement using information about the tracks and the primary vertex associated to a jet (Jet Vertex Tagger) [91] is applied for jets with $p_{\mathrm{T}} < 60$ GeV and $|\eta| < 2.4$.

Jets are identified as containing the decay of a b-hadron (b-tagged) via an algorithm using multivariate techniques to combine information from the impact parameters of displaced tracks with the topological properties of secondary and tertiary decay vertices reconstructed within the jet [92, 93]. Jets are b-tagged by directly requiring the output discriminant of the b-tagging algorithm to be above a threshold. A criterion with an efficiency of 70% for b-jets in $t\bar{t}$ events is used to determine the b-jet multiplicity for all final states and H^+ masses. For this working point, the c-jet and light-jet rejection factors are 12 and 381, respectively. For $m_{H^+} \leq 300$ GeV, five exclusive efficiency bins are defined using the same b-tagging discriminant: 0–60%, 60–70%, 70–77%, 77–85% and 85–100%, following the procedure described in Ref. [94]. These step-wise efficiencies are used as input to the kinematic discriminant described in Section 5. When 'a b-tagged jet' is mentioned without any further specification, an efficiency of 70% is implied.

To avoid counting a single detector response as two objects, an overlap removal procedure is used. First, the closest jet within $\Delta R_y = 0.2$ of a selected electron is removed. If the nearest jet surviving this selection is within $\Delta R_y = 0.4$ of the electron, the electron is discarded, to ensure it is sufficiently separated from nearby jet activity. Muons are removed if they are separated from the nearest jet by $\Delta R_y < 0.4$, to reduce the background from muons from HF decays inside jets. However, if this jet has fewer than three associated tracks, the muon is kept and the jet is removed instead; this avoids an inefficiency for high-energy muons undergoing significant energy loss in the calorimeter.

The missing transverse momentum in the event is defined as the negative vector sum of the p_{T} of all the selected electrons, muons and jets described above, with an extra term added to account for energy in the event that is not associated with any of these. This extra term, referred to as the 'soft term' in the following, is calculated from ID tracks matched to the primary vertex to make it resilient to pile-up contamination [95–97]. The missing transverse momentum is not used for event selection but is an input to the multivariate discriminants.

Events are required to have at least one electron or muon. The leading lepton must be matched to a lepton with the same flavour reconstructed by the trigger algorithm within $\Delta R < 0.15$, and have a $p_{\mathrm{T}} > 27$ GeV. Additional leptons are required to have $p_{\mathrm{T}} > 10$ GeV, or > 15 GeV for events with two electrons. The latter requirement reduces the bakground due to jets and photons that are misidentified as electrons. Events in the ℓ+jets channel and the $\ell\ell$ channel are required to be mutually exclusive. Electrons or muons from τ decays are also included in the analysis.

For the ℓ+jets channel, five or more jets, of which at least two jets have to be b-tagged, are required. For the $\ell\ell$ channel, events with two leptons with opposite charge are selected, and at least three jets are required, of which two or more must be b-tagged. In the ee and $\mu\mu$ channels, the dilepton invariant mass must be > 15 GeV and outside the Z boson mass window of 83–99 GeV.

5 Analysis strategy

After the event selection, the samples in both the $\ell\ell$ and the ℓ+jets final states contain mostly $t\bar{t}$ events. Events passing the event selection are categorised into separate regions according to the number of

reconstructed jets and b-tagged jets. The regions where tbH^+ is enhanced relative to the backgrounds are referred to as signal regions (SRs), whereas the remaining regions are referred to as control regions (CRs). In the SRs, for each H^+ mass hypothesis a different discriminating variable based on boosted decision trees (BDTs) is defined. In order to separate the H^+ signal from the SM background, the binned output of this variable is used together with the total event yields in the CRs in a combined profile likelihood fit. The fit simultaneously determines both the signal and background yields, while constraining the overall background model within the assigned systematic uncertainties. The event yields in the CRs are used to constrain the background normalisation and systematic uncertainties. The profile likelihood fit, including the treatment of backgrounds in the fit, is described in detail in Section 7.

For the ℓ+jets final state, two CRs (5j2b and ≥6j2b)[4] and four SRs (5j3b, 5j≥4b, ≥6j3b and ≥6j≥4b) are defined, while in the $\ell\ell$ final state, two CRs (3j2b and ≥4j2b) and two SRs (≥4j3b and ≥4j≥4b) are defined for all mass hypotheses. In addition, for the $\ell\ell$ final state, the region with three b-tagged jets and no other jets (3j3b) is considered a SR for $m_{H^+} < 1$ TeV and a CR for $m_{H^+} \geq 1$ TeV due to the change in expected signal yield for the different H^+ mass hypotheses.

The background from processes with prompt leptons is estimated using the simulated event samples described in Section 3. For $t\bar{t}$ production, the number of events with high leading jet p_{T} is overestimated in the simulation, and a reweighting function for the leading jet p_{T} distribution is determined by comparing simulation with data in a ℓ+jets CR that requires exactly four jets and at least two b-tagged jets. This function is validated in the dilepton channel and applied to both channels.

The normalisation of the Z+HF jets backgrounds is corrected by a factor of 1.3, extracted from dedicated control regions in data, defined by requiring two opposite-charge same-flavour leptons (e^+e^- or $\mu^+\mu^-$) with an invariant mass compatible with the Z boson mass, 83 GeV $< m_{\ell\ell} <$ 99 GeV.

Processes that do not contain prompt electrons or muons from W or Z boson decays (multi-jet events) can still satisfy the selection criteria if they contain non-prompt leptons. The leading sources of non-prompt leptons are from semileptonic hadron decays or jets misidentified as leptons ('fake' leptons). These backgrounds are estimated using data. For the ℓ+jets final state a matrix method [98] is employed. An event sample that is enriched in non-prompt leptons is selected by using looser isolation or identification requirements for the lepton. These events are then weighted according to the efficiencies for both the prompt and non-prompt leptons to pass the tighter default selection. These efficiencies are measured using data in dedicated CRs. In the $\ell\ell$ final state, this background is estimated from simulations, and the normalisation is determined by comparing data and simulations in a CR of same-sign dilepton events. The contribution of multi-jet events to the $\ell\ell$ final state is found to be negligible.

The expected event yields of all SM processes and the number of events observed in the data are shown in Figure 2 for the $\ell\ell$ and the ℓ+jets final states before performing the fit to data. The expected H^+ signal yields for $m_{H^+} = 200$ GeV, assuming a cross-section times branching ratio of 1 pb, are also shown.

The training of the BDTs that are used to discriminate signal from background in the SRs is performed with the TMVA toolkit [99]. BDTs are trained separately for each value of the 18 generated H^+ masses and for each SR against all the backgrounds (ℓ+jets channel) or the $t\bar{t}$ background ($\ell\ell$ channel). For the BDT training in the ℓ+jets channel, the SRs 5j3b and 5j≥4b are treated as one region, in order to increase the number of simulated events available for training.

The BDT variables include various kinematic quantities with the optimal discrimination against the $t\bar{t}+\geq 1b$ background. For H^+ masses above 400 GeV the most important variables in the ℓ+jets final state

[4] $XjYb$ means that X jets are found in the event, and among them Y are b-tagged.

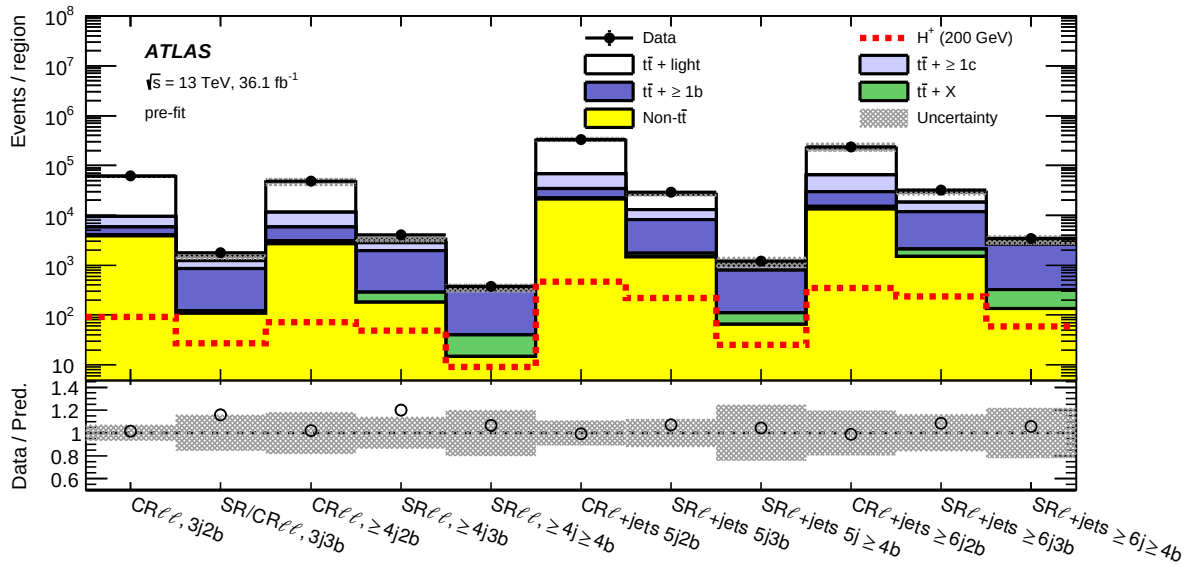

Figure 2: Comparison of predicted and observed event yields. Each background process is normalised according to its cross-section and the prediction has not been fitted to the data. The $t\bar{t}$ + X includes contributions from $t\bar{t}W$, $t\bar{t}Z$ and $t\bar{t}H$. A signal with m_{H^+} = 200 GeV, normalised to a cross-section times branching ratio for $H^+ \to tb$ of 1 pb, is shown as a dashed line. The lower panel displays the ratio of the data to the total prediction. The hatched bands show uncertainties before the fit to the data, which are dominated by systematic uncertainties as discussed in Section 6. The comparison is shown for all signal and control regions used in the analysis. For the $\ell\ell$ final state: CR 3j2b, CR/SR 3j3b, CR ≥4j2b, SR ≥4j3b, SR ≥4j≥4b. For the ℓ+jets final state: CR 5j2b, SR 5j3b, SR 5j≥4b, CR ≥6j2b, SR ≥6j3b, SR ≥6j≥4b.

are the scalar sum of the p_{T} of all jets, $H_{\mathrm{T}}^{\mathrm{jets}}$, and the leading jet p_{T}. For a mass at or below 300 GeV, a kinematic discriminant, D, as described below, is used as an input variable for the BDT. The kinematic discriminant, D, and the invariant mass of the pair of jets that are not b-tagged and have the smallest ΔR are the most important variables in the low mass range. The latter variable is not used in the 5j≥4b SR, where it is not well defined.

The kinematic discriminant, D, is a variable reflecting the probability that an event is compatible with the $H^+ \to tb$ and the $t\bar{t}$ hypotheses, and is defined as $D = P_{H^+}(\mathbf{x})/(P_{H^+}(\mathbf{x}) + P_{t\bar{t}}(\mathbf{x}))$, where $P_{H^+}(\mathbf{x})$ and $P_{t\bar{t}}(\mathbf{x})$ are probability density functions for $\mathbf{x}$ under the signal hypothesis and background ($t\bar{t}$) hypothesis, respectively. Here, the event variable $\mathbf{x}$ indicates the set of the missing transverse momentum and the four-momenta of reconstructed electrons, muons and jets.

The probability $P_{H^+}(\mathbf{x})$ is defined as the product of the probability density functions for each of the reconstructed invariant masses in the event:

- the mass of the semileptonically decaying top quark, $m_{b_\ell \ell \nu}$,
- the mass of the hadronically decaying W boson, $m_{q_1 q_2}$,
- the difference between the masses of the hadronically decaying top quark and the hadronically decaying W boson $m_{b_h q_1 q_2} - m_{q_1 q_2}$, and

- the difference between the mass of the charged Higgs boson and the mass of the leptonically or hadronically decaying top quark, $m_{b_{H^+}b_\ell\ell\nu} - m_{b_\ell\ell\nu}$ or $m_{b_{H^+}b_h q_1 q_2} - m_{b_h q_1 q_2}$, depending on whether the top quark from the charged Higgs boson decays leptonically or hadronically.

In this context q_1 or q_2 refer to the quarks from the W boson decay, ℓ and ν to the lepton and neutrino from the other W boson decay, b_h to the b-quark from the hadronic top quark decay, b_ℓ to the b-quark from the leptonic top quark decay and b_{H^+} to the b-quark directly from the H^+ decay. The probability $P_{t\bar{t}}(\mathbf{x})$ is constructed from probability density functions obtained from simulated $t\bar{t}$ events. For the SRs with five jets, $P_{t\bar{t}}(\mathbf{x})$ is defined using the same invariant masses as above. The jet that does not originate from a top quark decay is used instead of b_{H^+}. For the SRs with at least six jets the power of the discriminant is improved by using the invariant mass of the two highest-p_T jets not originating from the hadronisation of q_1, q_2, b_h or b_ℓ instead of $m_{b_{H^+}b_\ell\ell\nu} - m_{b_\ell\ell\nu}$ or $m_{b_{H^+}b_h q_1 q_2} - m_{b_h q_1 q_2}$.

The functional form of the probability density functions is obtained from simulation using the reconstructed masses of jets and leptons matched to simulated partons and leptons for H^+ and $t\bar{t}$. The neutrino four-momentum is derived with the assumption that the missing transverse momentum is solely due to the neutrino; the constraint $m_W^2 = (p_\ell + p_\nu)^2$ is used to obtain $p_{\nu,z}$. If two real solutions exist, they are sorted according to the absolute value of their p_z, i.e., $|p_{z,\nu_1}| < |p_{z,\nu_2}|$. In approximately 60% of the cases p_{z,ν_1} is closer than p_{z,ν_2} to the generator-level neutrino p_z. Two different probability density functions are constructed, one for each solution, and the probability is defined as a weighted average of the two probability density functions. The weight is taken as the fraction of the corresponding solution being closer to the generated neutrino p_z. Also, if no real solution exists, the p_x and p_y components are scaled by a common factor until the discriminant of the quadratic equation is exactly zero, yielding only one solution.

When evaluating $P_{H^+}(\mathbf{x})$ and $P_{t\bar{t}}(\mathbf{x})$ for the calculation of D, all possible parton–jet assignments are considered since the partonic origin of the jets is not known. In order to suppress the impact from parton–jet assignments that are inconsistent with the correct parton flavours, a weighted average over all parton-jet assignments is used. The value of $P_{H^+}(\mathbf{x})$ and $P_{t\bar{t}}(\mathbf{x})$ for each parton–jet assignment is weighted with a probability based on the b-tagging discriminant value of each jet. The distribution of the step-wise efficiencies of the b-tagging algorithm, as described in Section 4, is used as a probability density function, with the b-jet hypothesis for generated b-quarks and the light-jet hypothesis for other generated partons. Due to the large number of events in which q_1 and q_2 cannot be matched to different jets, the average of two different probability density functions, where either all partons can be matched to jets or only one jet can be matched to q_1 and q_2, is used. This discriminant gives better background suppression than would be obtained by adding the kinematic input variables directly to the BDT.

In the $\ell\ell$ final state, approximately ten optimal kinematic variables from the analysis objects and their combinations were selected for each SR, independently for the low-mass region ($m_{H^+} \leq 600$ GeV) and the high-mass region ($m_{H^+} > 600$ GeV). For the high-mass region, the most important variables are the scalar sum of the p_T of all jets and leptons, $H_\mathrm{T}^\mathrm{all}$, and the transverse momentum of the jet pair with maximum p_T. For the low-mass region, the smallest invariant mass formed by two b-tagged jets and the smallest invariant mass formed by a lepton and a b-tagged jet, are among the most important variables.

All BDT input variables in the ℓ+jets and $\ell\ell$ final states are listed in the Appendix. In most regions, the distributions show a reasonable level of agreement between simulation and data within the systematic and statistical uncertainties before the fit to the data (pre-fit). As examples, Figures 3 and 4 show the distribution of the observed and pre-fit expected event yields for $H_\mathrm{T}^\mathrm{jets}$ in the ℓ+jets channel and $H_\mathrm{T}^\mathrm{all}$ in the

$\ell\ell$ channel. Figure 5 shows the expected BDT output distributions, normalised to unity, for selected H^+ signal samples and the background processes in the SRs.

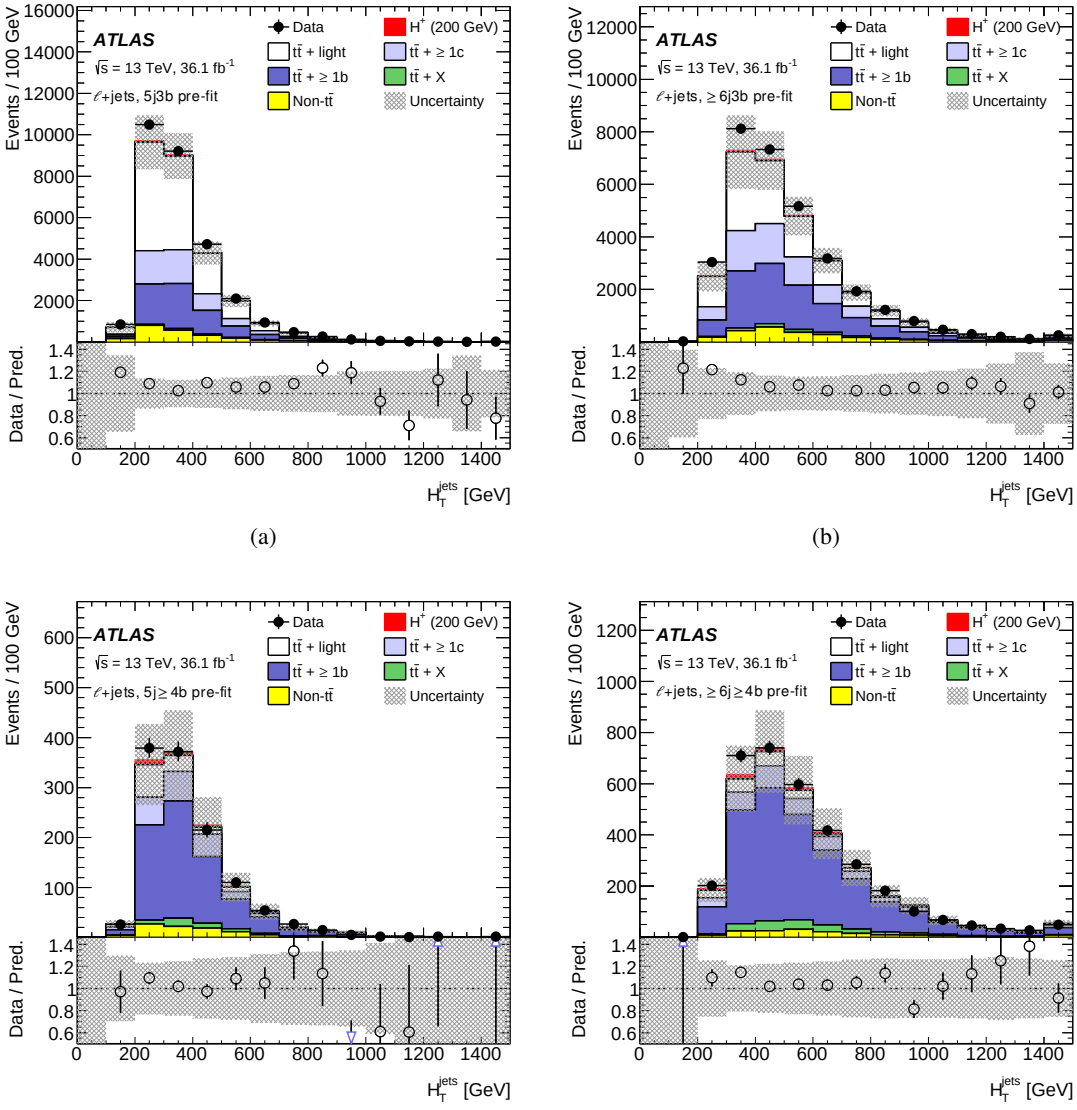

Figure 3: Distributions of the $H_{\mathrm{T}}^{\mathrm{jets}}$ variable before the fit to the data in the four SRs of the ℓ+jets channel: (a) 5j3b, (b) ≥6j3b, (c) 5j≥4b, (d) ≥6j≥4b. Each background process is normalised according to its cross-section and the normalisation of the $t\bar{t}+\geq 1b$ and $t\bar{t}+\geq 1c$ backgrounds corresponds to the prediction from Powheg+Pythia8 for the fraction of each of these components relative to the total $t\bar{t}$ prediction. The $t\bar{t}+X$ includes contributions from $t\bar{t}W$, $t\bar{t}Z$ and $t\bar{t}H$. In addition, the expectation for a 200 GeV signal is shown for a cross-section times branching ratio of 1 pb. The lower panels display the ratio of the data to the total prediction. The hatched bands show the pre-fit uncertainties. The level of agreement is improved post-fit due to the adjustment of the normalisation of the $t\bar{t}+\geq 1b$ and $t\bar{t}+\geq 1c$ backgrounds and the other nuisance parameters by the fit.

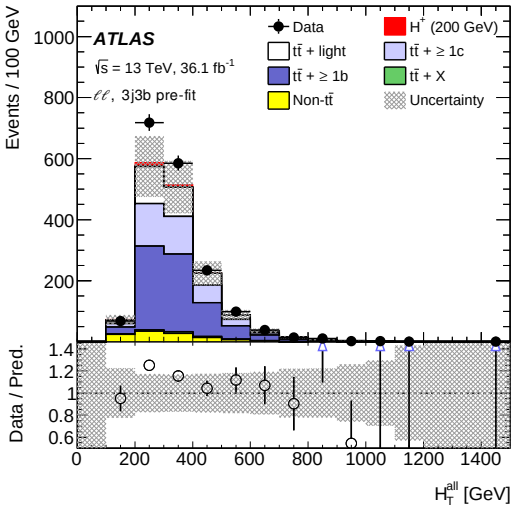

(a)

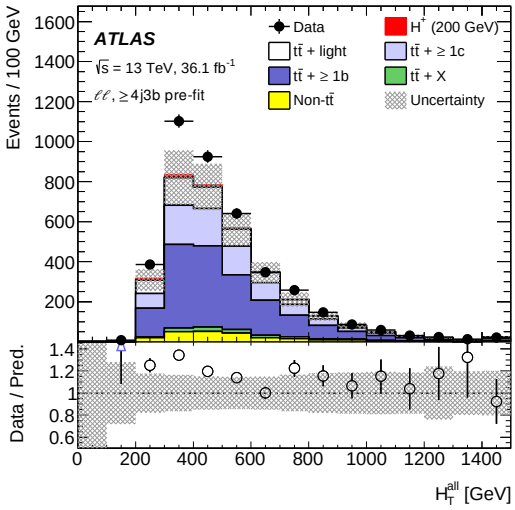

(b)

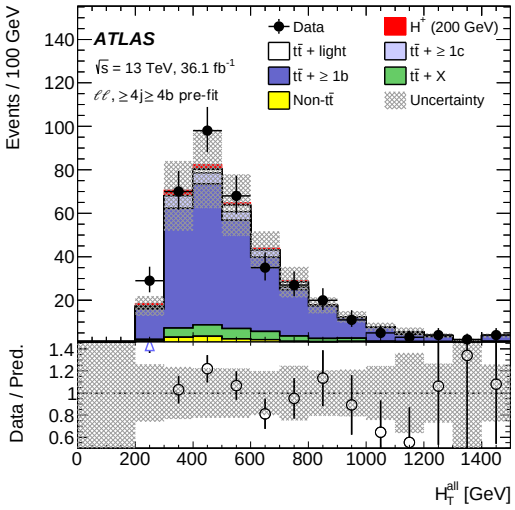

(c)

Figure 4: Distributions of the $H_{\mathrm{T}}^{\mathrm{all}}$ variable before the fit to the data in the three SRs of the $\ell\ell$ channel: (a) 3j3b, (b) ≥4j3b and (c) ≥4j≥4b. Each background process is normalised according to its cross-section and the normalisation of the $t\bar{t}+\geq 1b$ and $t\bar{t}+\geq 1c$ backgrounds corresponds to the prediction from Powheg+Pythia8 for the fraction of each of these components relative to the total $t\bar{t}$ prediction. The $t\bar{t}+X$ includes contributions from $t\bar{t}W$, $t\bar{t}Z$ and $t\bar{t}H$. In addition, the expectation for a 200 GeV signal is shown for a cross-section times branching ratio of 1 pb. The lower panels display the ratio of the data to the total prediction. The hatched bands show the pre-fit uncertainties. The level of agreement is improved post-fit due to the adjustment of the normalisation of the $t\bar{t}+\geq 1b$ and $t\bar{t}+\geq 1c$ backgrounds and the other nuisance parameters by the fit.

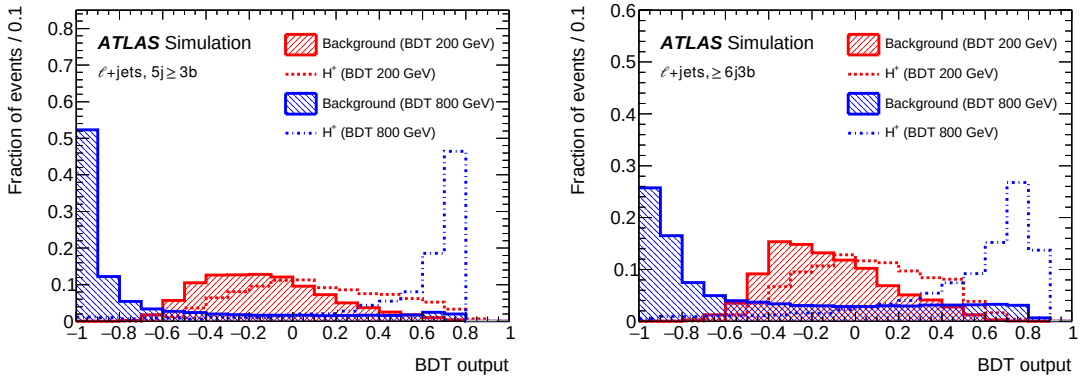

(a)

(b)

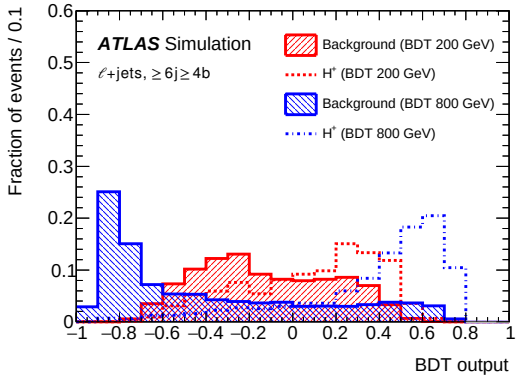

(c)

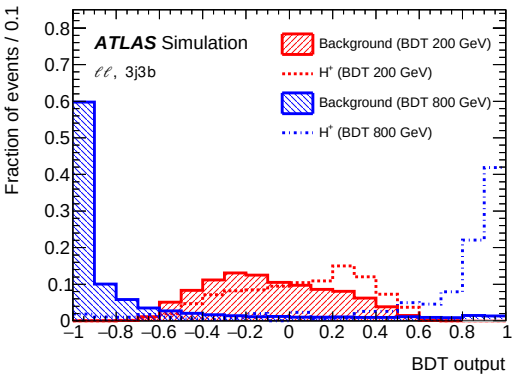

(d)

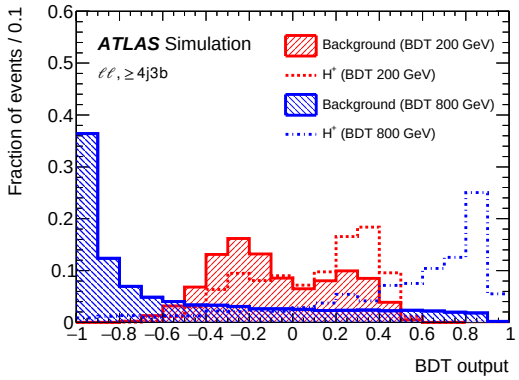

(e)

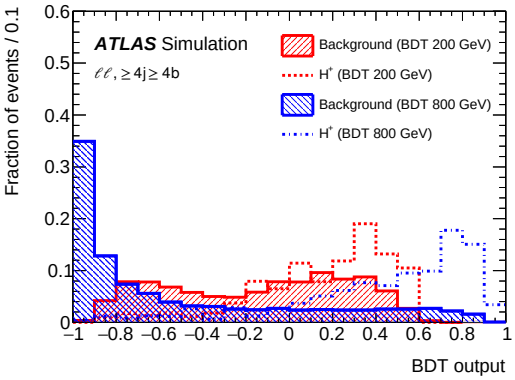

(f)

Figure 5: The expected output distributions of the BDTs employed for H^+ masses of 200 GeV and 800 GeV for SM backgrounds and H^+ signal in the three ℓ+jets and the three $\ell\ell$ SRs used in the BDT training: (a) ℓ+jets final state, 5j≥3b, (b) ℓ+jets final state, ≥6j3b, (c) ℓ+jets final state, ≥6j≥4b, (d) $\ell\ell$ final state, 3j3b, (e) $\ell\ell$ final state, ≥4j3b and (f) $\ell\ell$ final state, ≥4j≥4b. All distributions are normalised to unity.

6 Systematic uncertainties

Systematic uncertainties from various sources affect this search, such as uncertainties in the luminosity measurement, the reconstruction and calibration of physics objects, in particular b-tagged jets, and the modelling of the signal and background processes. Uncertainties can either modify the normalisation of the signal and background processes, change the shape of the final distributions, or both. An overview of the systematic uncertainties is given in Table 2. The impact of the systematic uncertainties is listed in Table 5 in Section 8.

Table 2: List of systematic uncertainties considered. 'N' indicates that the uncertainty is taken as normalisation-only for all processes and channels affected, while 'NS' means that the uncertainty applies to both normalisation and shape. The systematic uncertainties are split into several components for a more accurate treatment. Flavour-tagging uncertainties marked (*) are different for the two sets of calibrations: the step-wise efficiency calibration for $m_{H^+} \leq 300$ GeV, and the 70% efficiency point calibration elsewhere.

Systematic uncertainty	Type	Number of components
Luminosity	N	1
Pile-up	NS	1
Electron reconstruction	NS	6
Muon reconstruction	NS	13
Jet and $E_{\mathrm{T}}^{\mathrm{miss}}$ reconstruction	NS	28
Flavour tagging, 70% efficiency calibration (*)	NS	27
Flavour tagging, step-wise efficiency calibration (*)	NS	126
Signal modelling	NS	31
Background modelling, $t\bar{t}$ + jets	NS	29
Background modelling, other top	NS	25
Background modelling, non-top (ℓ+jets final state)	N	13
Background modelling, non-top ($\ell\ell$ final state)	N	4

The combined uncertainty in the integrated luminosity for the data collected in 2015 and 2016 is 2.1%, and it is applied as a normalisation uncertainty for all processes estimated using simulation. It is derived, following a methodology similar to that detailed in Ref. [100], from a preliminary calibration of the luminosity scale using x–y beam-separation scans performed in August 2015 and May 2016. A variation in the pile-up reweighting of MC events is included to cover the uncertainty in the ratio of the predicted and measured inelastic cross-sections in the fiducial volume defined by $M_X > 13\,\mathrm{GeV}$ where M_X is the mass of the hadronic system [101].

Uncertainties associated with charged leptons arise from the trigger selection, the object reconstruction, the identification, and the isolation criteria, as well as the lepton momentum scale and resolution. These are estimated by comparing $Z \to \ell^+\ell^-$ ($\ell = e, \mu$) events in data and simulation [85, 86]. Correction factors are applied to the simulation to better model the efficiencies observed in data. The charged-lepton uncertainties have a small impact on the analysis.

Uncertainties associated with jets arise from the efficiency of jet reconstruction and identification based on the JES and jet energy resolution, and on the Jet Vertex Tagger [102]. The JES and its uncertainty were derived by combining information from test-beam data, LHC collision data (*in situ* techniques) and simulation. The JES-related uncertainties are factored into 23 statistically independent components.

In the reconstruction of quantities used for the BDT, $E_{\mathrm{T}}^{\mathrm{miss}}$ is used. The $E_{\mathrm{T}}^{\mathrm{miss}}$ calculation depends on the reconstruction of leptons and jets, and the $E_{\mathrm{T}}^{\mathrm{miss}}$ uncertainties are therefore related to the uncertainties associated with these objects, which are propagated to the $E_{\mathrm{T}}^{\mathrm{miss}}$ uncertainty estimation. Uncertainties due to soft objects (not included in the calculation of the leptons and jets) are also considered [96].

Differences between data and simulation in the b-tagging efficiency for b-jets, c-jets and light jets are taken into account using correction factors. For b-jets, the corrections are derived from $t\bar{t}$ events with final states containing two leptons, and the corrections are consistent with unity within uncertainties at the level of a few percent over most of the jet p_{T} range. The mis-tag rate for c-jets is also measured in $t\bar{t}$ events, identifying hadronic decays of W bosons including c-jets. For light jets, the mis-tag rate is measured in multi-jet events using jets containing secondary vertices and tracks with impact parameters consistent with a negative lifetime. Systematic uncertainties affecting the correction factors are derived in the p_{T} and η bins used for extracting the correction factors. They are transformed into uncorrelated components using an eigenvector decomposition, taking into account the bin-to-bin correlations [92, 93, 103]. For $m_{H^+} > 300\,\mathrm{GeV}$, corrections corresponding to the fixed working point of 70% efficiency are used and a total of 6, 3 and 16 independent uncorrelated eigen-variations are considered as systematic uncertainties for b-, c- and light jets, respectively. For $m_{H^+} \leq 300\,\mathrm{GeV}$, corrections for the step-wise efficiencies are used to support the kinematic discriminant D and the number of eigen-variations is increased by a factor of five to account for the five b-tagging efficiency bins. In addition, uncertainties due to tagging the hadronic decays of τ-leptons as b-jets are considered. For $m_{H^+} > 300\,\mathrm{GeV}$, an additional uncertainty is included due to the extrapolation of scale factors for jets with $p_{\mathrm{T}} > 300$ GeV, beyond the kinematic reach of the data calibration samples used [93].

The modelling uncertainty of the H^+ signal is estimated by varying the renormalisation and factorisation scales up and down by a factor of two. The uncertainty ranges from 7% at low masses to 15% at masses above 1300 GeV for the ℓ+jets final state, and from 12% to 16.5% for the $\ell\ell$ final state. Additionally, the PDF uncertainty in the modelling is estimated using the PDF4LHC15_30 PDF set [104], which is based on a combination of the CT14 [105], MMHT14 [106] and NNPDF3.0 [44] PDF sets and contains 30 components obtained using the Hessian reduction method [107–109].

The modelling of the $t\bar{t}$ + jets background is one of the largest sources of uncertainty in the analysis and many different components are considered. The uncertainty in the inclusive $t\bar{t}$ production cross-section at NNLO+NNLL [47] is 6%, including effects from varying the factorisation and renormalisation scales, the PDF, the QCD coupling constant α_{s}, and the top quark mass. Due to the large difference between the 4FS prediction and the various 5FS predictions for the $t\bar{t} + \geq 3b$ process, an additional 50% normalisation uncertainty is assigned to this background.

The uncertainty due to the choice of NLO generator is derived by comparing the nominal Powheg sample with a sample generated using Sherpa 2.2.1 with a 5FS PDF. A Powheg sample with the same settings as in the nominal Powheg+Pythia8 sample, but using Herwig7 [79, 110] for parton showering, is used to assess the uncertainty due to the choice of parton shower and hadronisation model. Furthermore, the uncertainty due to the modelling of initial- and final-state radiation is evaluated with two different Powheg+Pythia8 samples in which the radiation is increased or decreased by halving or doubling the renormalisation and factorisation scales in addition to simultaneous changes to the h_{damp} parameter and the A14 tune parameters [111].

For the $t\bar{t} + \geq 1b$ background, an additional uncertainty is assigned by comparing the predictions from Powheg+Pythia8 and Sherpa with 4FS. This takes into account the difference between a 5FS inclusive $t\bar{t}$ prediction at NLO and a 4FS NLO $t\bar{t}b\bar{b}$ prediction. For the $t\bar{t} + \geq 1c$ background, an additional uncertainty

is derived by comparing a MG5_aMC sample that is interfaced to Herwig++ [79] with the nominal event sample. In this MG5_aMC event sample, a three-flavour scheme is employed and the $t\bar{t}c\bar{c}$ process is generated at the matrix element level [112] using the CT10F3 PDF set, while in the nominal sample the charm jets are primarily produced in the parton shower. All of these uncertainties, with the exception of the inclusive and $t\bar{t}+\geq 3b$ cross-sections, are considered to be uncorrelated amongst the $t\bar{t}+\geq 1b$, $t\bar{t}+\geq 1c$, and $t\bar{t}$ + light samples. For the modelling of the $t\bar{t}+\geq 1b$ backgrounds, the alternative samples are reweighted to the NLO prediction of $t\bar{t}b\bar{b}$ from Sherpa before the uncertainty is evaluated.

In addition, uncertainties due to the reweighting to the Sherpa NLO prediction of $t\bar{t}b\bar{b}$ are considered. For these uncertainties, the $t\bar{t}+\geq 1b$ is reweighted to different Sherpa predictions with modified scale parameters, in particular where the renormalisation scale is varied up and down by a factor of two, where the functional form of the resummation scale is changed to μ_{CMMPS} and where a global scale choice $\mu_{\text{Q}} = \mu_{\text{R}} = \mu_{\text{F}} = \mu_{\text{CMMPS}}$ is used. Two alternative PDF sets, MSTW2008NLO [84] and NNPDF2.3NLO [44], are used, and uncertainties in the underlying event and parton shower are estimated from samples with an alternative set of tuned parameters for the underlying event and an alternative shower recoil scheme. Due to the absence of b-jets from multi-parton interactions and final-state gluon radiation in the $t\bar{t}b\bar{b}$ prediction from Sherpa, a 50% uncertainty is assigned to the $t\bar{t}+b$ (MPI/FSR) category based on studies of different sets of UE tunes. An uncertainty due to the reweighting of the leading jet p_{T} is determined by comparing a reweighted event sample with an event sample without reweighting. Because the reweighting changes the normalisation for jet $p_{\text{T}} > 400$ GeV by 15%, an additional normalisation uncertainty of 15% is applied in this region. The reweighting factors are derived from the CR with exactly four jets and at least two b-tagged jets and applied to higher jet multiplicity bins. However, the effect of this extrapolation is expected to be small and is covered by the above uncertainties.

An uncertainty of 5% is assigned to the total cross-section for single top-quark production [66–68], uncorrelated between Wt and t-channel production. An additional uncertainty due to initial- and final-state radiation is estimated using samples with factorisation and renormalisation scale variations and appropriate variations of the Perugia 2012 set of tuned parameters. The parton showering and hadronisation modelling uncertainties in the single-top Wt and t-channel production are estimated by comparing with samples where the parton shower generator is Herwig++ instead of Pythia 6.428. The uncertainty in the interference between Wt and $t\bar{t}$ production at NLO [62] is assessed by comparing the default 'diagram removal' scheme with an alternative 'diagram subtraction' scheme [62, 113].

The uncertainty arising from $t\bar{t}V$ generation is estimated by comparison with samples generated with Sherpa. The uncertainty in the $t\bar{t}V$ production cross-section is about 15%, taken from the NLO predictions [15, 114–116], treated as uncorrelated between $t\bar{t}W$ and $t\bar{t}Z$ with PDF and QCD scale variations.

The $t\bar{t}H$ modelling uncertainty is assessed through an uncertainty in the cross-section, uncorrelated between QCD ($^{+5.8}_{-9.2}$%) and the PDFs (±3.6%) [15, 117–121], and the modelling of the parton shower and hadronisation by comparing Pythia8 with Herwig++. The minor $tH + X$ backgrounds, $tHjb$ and WtH are treated as one background and its cross-section uncertainty is 6% due to PDF uncertainties and another 10% due to factorisation and renormalisation scale uncertainties [15].

The uncertainties from the data-driven estimation of non-prompt leptons are based on a comparison between data and the non-prompt lepton estimates in CRs. A 50% uncertainty is assigned in the ℓ+jets final state. In the $\ell\ell$ final state, where all backgrounds with one or no prompt leptons fall into this category, including W+jets and single top production, an uncertainty of 25% is assigned.

An uncertainty of 40% is assumed for the W+jets cross-section, uncorrelated between jet bins, with an additional 30% for W+HF jets, uncorrelated for two, three and more than three HF jets. These uncertainties

are derived from variations of the renormalisation and factorisation scales and matching parameters in Sherpa simulations. An uncertainty in Z+jets of 35% is applied, uncorrelated among jet bins in the $\ell\ell$ final state. This uncertainty accounts for both the variation of the scales and matching parameters in Sherpa simulations and the data-driven correction factors applied to the Z+HF jets component. In the $\ell\ell$ final state, only the Z+jets component is estimated separately, and the W+jets background is included in the estimation of the background from non-prompt leptons.

7 Statistical analysis

In order to test for the presence of an H^+ signal, a binned maximum-likelihood fit to the data is performed simultaneously in all categories, and each mass hypothesis is tested separately. The inputs to the fit include the number of events in the CRs and the binned BDT output in the SRs. Two initially unconstrained fit parameters are used to model the normalisation of the $t\bar{t}+\geq 1b$ and $t\bar{t}+\geq 1c$ backgrounds. The procedures used to quantify the level of agreement with the background-only or background-plus-signal hypothesis and to determine exclusion limits are based on the profile likelihood ratio test and the $\mathrm{CL_s}$ method [122–124]. The parameter of interest is the signal strength, μ, defined as the product of the production cross-section $\sigma(pp \to tbH^+)$ and the branching ratio $\mathcal{B}(H^+ \to tb)$.

To estimate the signal strength, a likelihood function, $\mathcal{L}(\mu, \theta)$, is constructed as the product of Poisson probability terms. One Poisson term is included for every CR and every bin of the BDT distribution in the SRs. The expected number of events in the Poisson terms is a function of μ, and a set of nuisance parameters, θ. The nuisance parameters encode effects from the normalisation of backgrounds, including two free normalisation factors for the $t\bar{t}+\geq 1b$ and $t\bar{t}+\geq 1c$ backgrounds, the systematic uncertainties and one parameter per bin to model statistical uncertainties in the simulated samples. All nuisance parameters are constrained with Gaussian or log-normal terms. There are about 170 nuisance parameters considered in the fit, the number varying slightly across the range of mass hypotheses.

To extract the exclusion limit on $\mu = \sigma(pp \to H^+) \times \mathcal{B}(H^+ \to tb)$, the following test statistic is used:

$$\tilde{t}_\mu = \begin{cases} -2\ln \dfrac{\mathcal{L}\left(\mu, \hat{\hat{\theta}}(\mu)\right)}{\mathcal{L}\left(0, \hat{\hat{\theta}}(0)\right)} & \hat{\mu} < 0, \\ -2\ln \dfrac{\mathcal{L}\left(\mu, \hat{\hat{\theta}}(\mu)\right)}{\mathcal{L}(\hat{\mu}, \hat{\theta})} & \hat{\mu} \geq 0. \end{cases}$$

The values of the signal strength and nuisance parameters that maximise the likelihood function are represented by $\hat{\mu}$ and $\hat{\theta}$, respectively. For a given value of μ, the values of the nuisance parameters that maximise the likelihood function are represented by $\hat{\hat{\theta}}(\mu)$.

8 Results

Tables 3 and 4 show the post-fit event yields under the background-plus-signal hypothesis for a signal mass $m_{H^+} = 200\,\mathrm{GeV}$. A value of $\sigma(pp \to tbH^+) \times \mathcal{B}(H^+ \to tb) = -0.36$ pb is obtained from the fit. The corresponding post-fit distributions of the BDT discriminant in the SRs are shown in Figures 6 and 7 for a 200 GeV H^+ mass hypotheses for the ℓ+jets and $\ell\ell$ final state, respectively.

Table 3: Event yields of the SM background processes and data in all categories of the ℓ+jets final state, after the fit to the data under the background-plus-signal hypothesis (m_{H^+} = 200 GeV). The expected event yields for the H^+ signal masses of 200 GeV and 800 GeV are shown with pre-fit uncertainties and assuming a cross-section times branching ratio of 1 pb. The quoted uncertainties include both the statistical and systematic components. The uncertainties take into account correlations and constraints of the nuisance parameters. 'Other top' includes contributions from Zt as well as s- and t-channel production.

Process	CR 5j2b	SR 5j3b	SR 5j≥4b	CR ≥6j2b	SR ≥6j3b	SR ≥6j≥4b
$t\bar{t}+\geq 1b$	15 300 ± 2300	7400 ± 1000	750 ± 110	17100 ± 2800	11 100 ± 1500	2410 ± 260
$t\bar{t}+\geq 1c$	47 000 ± 12 000	6400 ± 1700	260 ± 80	55 000 ± 11 000	9400 ± 2000	450 ± 180
$t\bar{t}$ + light	226 000 ± 11 000	12 200 ± 1100	89 ± 35	132 000 ± 10 000	8500 ± 1100	260 ± 120
Non-prompt leptons	15 000 ± 6000	600 ± 500	11 ± 8	13 000 ± 6000	700 ± 400	4 ± 5
$t\bar{t}W$	340 ± 50	29 ± 4	0.66 ± 0.22	540 ± 80	72 ± 11	5.0 ± 1.2
$t\bar{t}Z$	390 ± 50	78 ± 10	12.2 ± 2.2	720 ± 90	183 ± 23	50 ± 7
Single top Wt	8900 ± 2400	690 ± 210	23 ± 13	5400 ± 1800	640 ± 260	53 ± 31
Other top	328 ± 27	28.2 ± 2.6	3.1 ± 0.6	183 ± 20	46 ± 11	14 ± 5
Diboson	410 ± 210	29 ± 15	2.0 ± 2.1	340 ± 170	37 ± 19	4.3 ± 2.5
W + jets	9000 ± 4000	540 ± 240	16 ± 9	5200 ± 2100	470 ± 200	27 ± 12
Z + jets	2100 ± 600	104 ± 35	4.9 ± 1.8	1300 ± 400	130 ± 40	11 ± 4
$t\bar{t}H$	252 ± 24	127 ± 13	30 ± 4	520 ± 50	315 ± 32	117 ± 16
tH	19.5 ± 2.4	10.6 ± 1.3	2.21 ± 0.32	27.2 ± 3.5	15.7 ± 2.0	5.0 ± 0.7
Total	328 000 ± 7000	28 400 ± 900	1220 ± 60	233 000 ± 6000	31 800 ± 800	3410 ± 150
Data	334 813	29 322	1210	234 053	32 151	3459
H^+ (200 GeV)	470 ± 50	220 ± 23	25.3 ± 3.3	340 ± 50	235 ± 34	60 ± 9
H^+ (800 GeV)	630 ± 90	390 ± 70	56 ± 12	1230 ± 190	1020 ± 170	350 ± 70

Table 4: Event yields of the SM background processes and data in all categories of the $\ell\ell$ final state, after the fit to the data under the background-plus-signal hypothesis (m_{H^+} = 200 GeV). The expected event yields for the H^+ signal masses of 200 GeV and 800 GeV are shown with pre-fit uncertainties and assuming a cross-section times branching ratio of 1 pb. The quoted uncertainties include both the statistical and systematic components. The uncertainties take into account correlations and constraints of the nuisance parameters. 'Other top' includes contributions from Zt as well as s- and t-channel production.

Process	CR 3j2b	SR/CR 3j3b	CR ≥4j2b	SR ≥4j3b	SR ≥4j≥4b
$t\bar{t}+\geq 1b$	2330 ± 330	940 ± 130	3300 ± 500	2050 ± 280	322 ± 35
$t\bar{t}+\geq 1c$	6100 ± 1300	520 ± 140	9900 ± 2000	1310 ± 290	30 ± 14
$t\bar{t}$ + light	50 700 ± 2300	260 ± 70	32 500 ± 2100	420 ± 120	4 ± 5
Non-prompt leptons	420 ± 110	6.7 ± 2.4	620 ± 160	48 ± 13	2.2 ± 0.8
$t\bar{t}W$	48 ± 7	1.48 ± 0.17	129 ± 7	9.8 ± 1.1	0.55 ± 0.21
$t\bar{t}Z$	43 ± 5	5.8 ± 1.1	174 ± 10	32.9 ± 2.0	7.0 ± 1.3
Single top Wt	1700 ± 500	40 ± 12	1110 ± 330	63 ± 26	3.9 ± 2.0
Other top	3.9 ± 0.5	0.12 ± 0.05	21.8 ± 3.5	5.8 ± 2.2	2.0 ± 0.9
Diboson	36 ± 4	1.2 ± 0.4	46 ± 6	3.1 ± 0.9	0.48 ± 0.28
Z + jets	1600 ± 500	42 ± 16	1300 ± 400	82 ± 29	5.3 ± 2.0
$t\bar{t}H$	26.2 ± 1.3	8.5 ± 0.5	116 ± 6	52.2 ± 3.5	16.0 ± 1.9
tH	1.95 ± 0.27	0.42 ± 0.10	5.7 ± 0.7	2.14 ± 0.32	0.48 ± 0.09
Total	62 800 ± 2800	1810 ± 110	49 300 ± 2300	4060 ± 200	390 ± 28
Data	62 399	1774	48 356	4047	376
H^+ (200 GeV)	92 ± 12	27 ± 4	72 ± 12	49 ± 8	9.0 ± 1.6
H^+ (800 GeV)	70 ± 12	32 ± 7	212 ± 33	157 ± 27	44 ± 9

A summary of the systematic uncertainties is given in Table 5. Depending on the particular H^+ mass hypothesis, the total systematic uncertainty is dominated by the uncertainties in the modelling of the $t\bar{t}+\geq 1b$ background, the jet flavour-tagging uncertainties and the uncertainties due to the limited size of simulated event samples.

Table 5: The summary of the effects of the systematic uncertainties on the signal strength parameter, $\mu = \sigma(pp \to H^+) \times \mathcal{B}(H^+ \to tb)$, for the combination of the ℓ+jets and $\ell\ell$ final states is shown for an H^+ signal with a mass of 200 and 800 GeV. Due to correlations between the different sources of uncertainty, the total systematic uncertainty can be different from the sum in quadrature of the individual sources. The normalisation factors for both $t\bar{t}+\geq 1b$ and $t\bar{t}+\geq 1c$ are included in the statistical component. The total uncertainty corresponds to a best-fit value of μ of -0.4 pb at $m_{H^+} = 200$ GeV and -0.02 pb at $m_{H^+} = 800$ GeV. The expected upper limit on μ is 3.05 pb at $m_{H^+} = 200$ GeV and 0.26 pb at $m_{H^+} = 800$ GeV.

Uncertainty Source	$\Delta\mu(H^+_{200})$ [pb]	$\Delta\mu(H^+_{800})$ [pb]
Jet flavour tagging	0.70	0.050
$t\bar{t}+\geq 1b$ modelling	0.65	0.008
Jet energy scale and resolution	0.44	0.031
$t\bar{t}$+light modelling	0.44	0.019
MC statistics	0.37	0.044
$t\bar{t}+\geq 1c$ modelling	0.36	0.032
Other background modelling	0.36	0.039
Luminosity	0.24	0.010
Jet-vertex assoc., pile-up modelling	0.10	0.006
Lepton, $E_{\mathrm{T}}^{\mathrm{miss}}$, ID, isol., trigger	0.08	0.003
H^+ modelling	0.03	0.006
Total systematic uncertainty	1.4	0.11
$t\bar{t}+\geq 1b$ normalisation	0.61	0.022
$t\bar{t}+\geq 1c$ normalisation	0.28	0.012
Total statistical uncertainty	0.69	0.050
Total uncertainty	1.5	0.12

The 95% confidence level (CL) upper limits on $\sigma(pp \to H^+) \times \mathcal{B}(H^+ \to tb)$ using the $\mathrm{CL_s}$ method are presented in Figure 8. The observed (expected) 95% CL upper limits on the $pp \to tbH^+$ production cross-section times the branching ratio $\mathcal{B}(H^+ \to tb)$ range from $\sigma \times \mathcal{B} = 2.9\,(3.0)$ pb at $m_{H^+} = 200$ GeV to $\sigma \times \mathcal{B} = 0.070\,(0.077)$ pb at $m_{H^+} = 2$ TeV. The compatibility of the SM hypothesis with the results obtained from the fit to the data is tested. The largest deviation from the SM hypothesis is observed at 300 GeV. Given that a negative $\hat{\mu}$ is observed under this mass hypothesis, the test statistic $t_0 = -2\ln(\mathcal{L}(0, \hat{\hat{\theta}}(0))/\mathcal{L}(\hat{\mu}, \hat{\theta}))$ is used to quantify the deviation of the fitted result from the SM expectation. A local p_0 value of 1.13% is obtained at 300 GeV, corresponding to the probability to obtain a deviation at least as large as the one observed in data provided that only SM processes are present.

Figure 9 shows 95% CL exclusion limits set on $\tan\beta$ for the $m_h^{\mathrm{mod}-}$ scenario of the MSSM [14, 15, 28] and the hMSSM [29, 125, 126]. Beyond tree level, the Higgs sector is affected by the choice of parameters in addition to Higgs boson masses and $\tan\beta$. For the $m_h^{\mathrm{mod}-}$ benchmark scenario the top-squark mixing parameter is chosen such that the mass of the lightest CP-even Higgs boson, m_h, is close to the measured mass of the Higgs boson that was discovered at the LHC. In the hMSSM scenario, instead of adjusting the

parameters of soft supersymmetry breaking, the value of m_h is used to predict the masses and couplings of the MSSM Higgs bosons.

For H^+ masses of 200–920 GeV (200–965 GeV), the observed exclusion of low values of $\tan\beta$ at 95% CL is in the range 0.5–1.91 (0.5–1.95) for the $m_h^{\text{mod}-}$ (hMSSM) scenario. The most stringent limits on $\tan\beta$ are set for H^+ masses around 250 GeV. High values of $\tan\beta$ between 36 and 60 are excluded in the H^+ mass range 200–520 GeV (220–540 GeV) for the $m_h^{\text{mod}-}$ (hMSSM) scenario. The most stringent exclusion, $\tan\beta > 36$, is at 300 GeV for both the $m_h^{\text{mod}-}$ and hMSSM benchmark scenarios. In the $m_h^{\text{mod}-}$ scenario for $\tan\beta = 0.5$, the observed (expected) exclusion of H^+ masses is $m_{H^+} < 920$ GeV ($m_{H^+} < 930$ GeV).

In comparison with a previous search for $t[b]H^+$ production followed by $H^+ \to tb$ decays [20], more stringent limits on H^+ masses for particular models and parameter choices can be set. The analysis reach is increased and now also includes H^+ masses between 600 GeV and 2 TeV. The excluded region of parameter space for the model-dependent interpretation is extended significantly for low $\tan\beta$ and an additional excluded region is added at high $\tan\beta$.

The ATLAS Collaboration has also set limits on the production of H^+ using the $H^+ \to \tau\nu$ decay with the same data [30]. The $\tau\nu$ final state can be used to set limits at high $\tan\beta$ which are more stringent than those from the tb final state, and to probe H^+ masses below 200 GeV, in both the $m_h^{\text{mod}-}$ and hMSSM scenarios. Figure 10 shows a superposition of the limits from the two final states, where the limits from the $\tau\nu$ final state exclude a larger portion of the parameter space at high $\tan\beta$ and low H^+ masses than the tb limits alone.

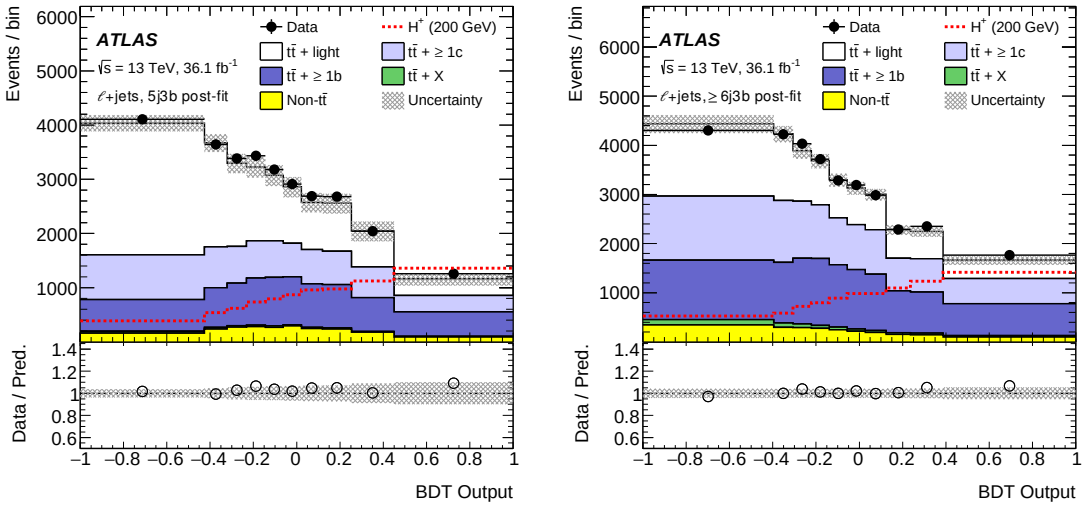

(a)

(b)

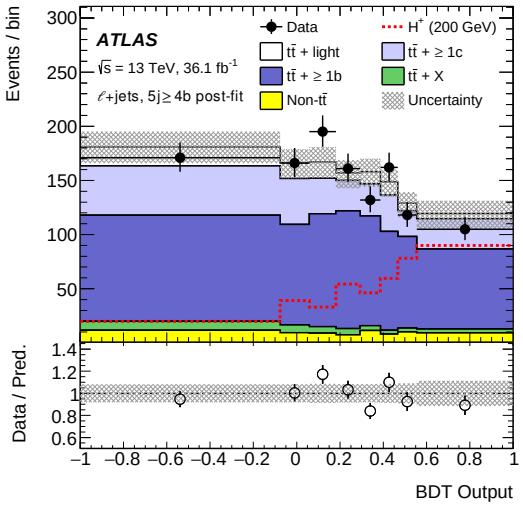

(c)

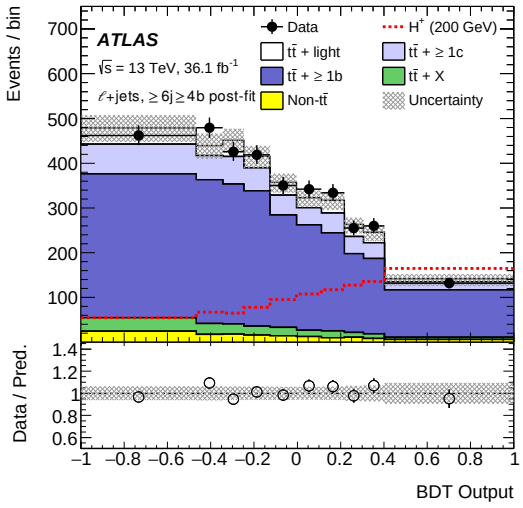

(d)

Figure 6: Distributions of the BDT output after the fit to the data in the four SRs of the ℓ+jets final state: (a) 5j3b, (b) ≥6j3b, (c) 5j≥4b and (d) ≥6j≥4b for the 200 GeV mass hypothesis. Each background process is normalised according to its post-fit cross-section. The $t\bar{t}+X$ includes contributions from $t\bar{t}W$, $t\bar{t}Z$ and $t\bar{t}H$. The total prediction of the BDT distributions includes cases where the signal obtained from the fit is negative. For this particular mass point the fitted signal strength is $\mu = -0.4 \pm 1.5$ pb. The pre-fit signal distribution is shown superimposed as a dashed line with arbitrary normalisation. The lower panels display the ratio of the data to the total prediction. The hatched bands show the post-fit uncertainties.

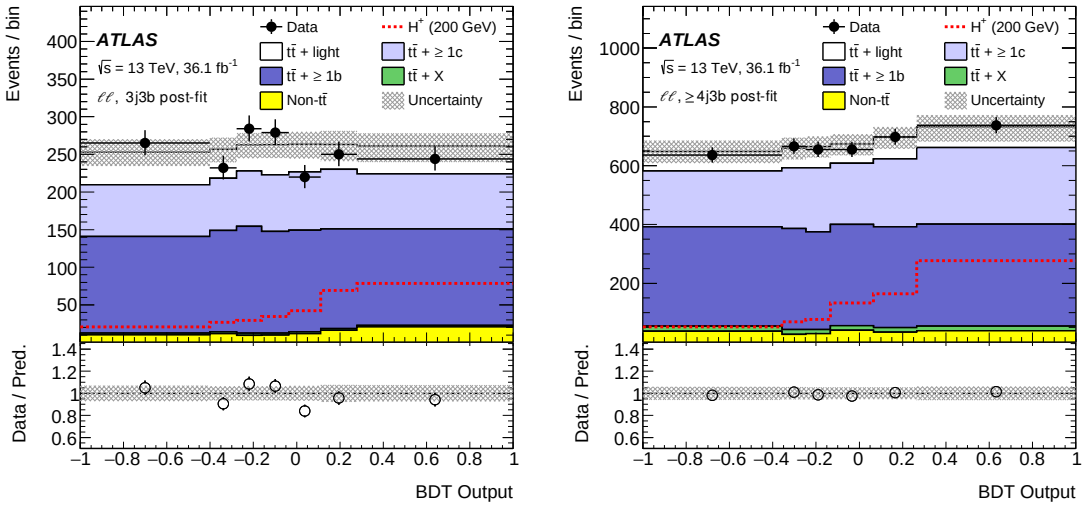

(a)

(b)

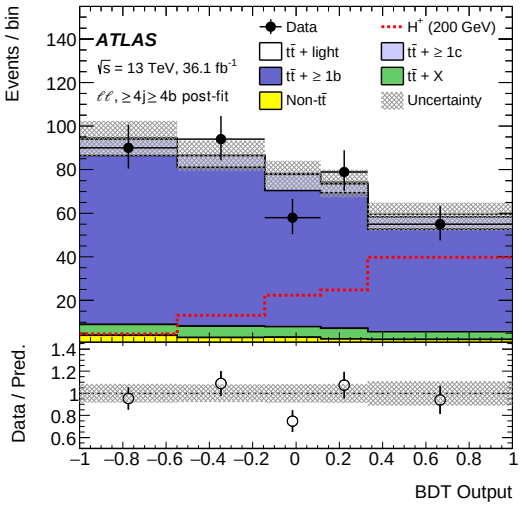

(c)

Figure 7: Distributions of the BDT output after the fit to the data in the three SRs of the $\ell\ell$ final state: (a) 3j3b, (b) ≥4j3b and (c) ≥4j≥4b for the 200 GeV mass hypothesis. Each background process is normalised according to its post-fit cross-section. The $t\bar{t}+X$ includes contributions from $t\bar{t}W$, $t\bar{t}Z$ and $t\bar{t}H$. The total prediction of the BDT distributions includes cases where the signal obtained from the fit is negative. For this particular mass point the fitted signal strength is $\mu = -0.4 \pm 1.5$ pb. The pre-fit signal distribution is shown superimposed as a dashed line with arbitrary normalisation. The lower panels display the ratio of the data to the total prediction. The hatched bands show the post-fit uncertainties.

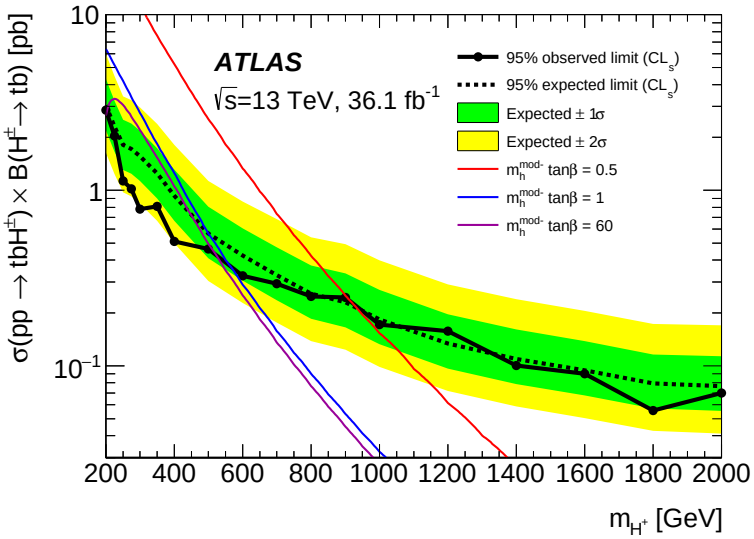

Figure 8: Expected and observed limits for the production of $H^+ \to tb$ in association with a top quark and a bottom quark. The bands surrounding the expected limit show the 68% and 95% confidence intervals. The limits are based on the combination of the ℓ+jets and $\ell\ell$ final states. Theory predictions are shown for three representative values of tanβ in the $m_h^{\text{mod}-}$ benchmark scenario [28]. Uncertainties in the predicted H^+ cross-sections or branching ratios are not considered.

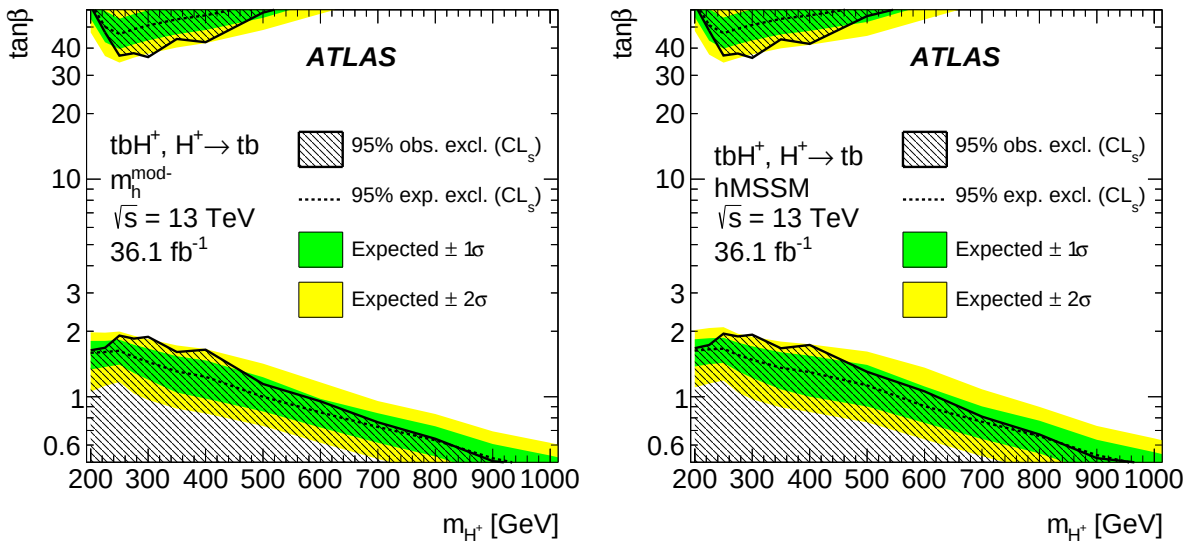

(a) (b)

Figure 9: Expected and observed limits on tanβ as a function of m_{H^+} in the $m_h^{\text{mod}-}$ [28] (left) and the hMSSM [29] (right) scenarios of the MSSM. Limits are shown for tanβ values in the range of 0.5–60, where predictions are available from both scenarios. The bands surrounding the expected limits show the 68% and 95% confidence intervals. The limits are based on the combination of the ℓ+jets and $\ell\ell$ final states. The production cross-section of $t\bar{t}H$ and tH, as well as the branching ratios of the H, are fixed to their SM values at each point in the plane. Uncertainties in the predicted H^+ cross-sections or branching ratios are not considered.

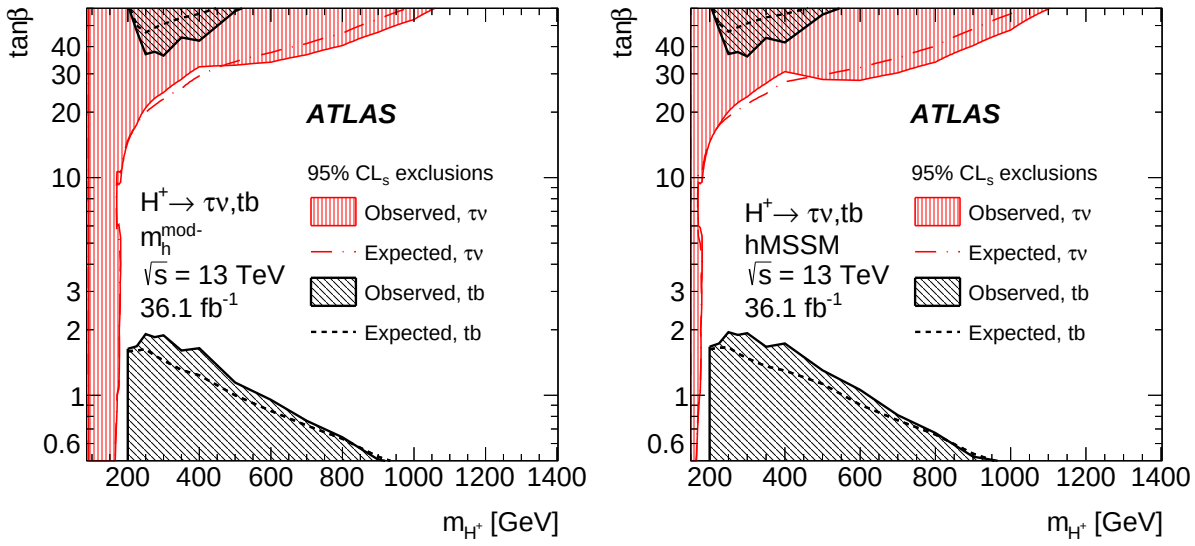

Figure 10: Expected and observed limits on tanβ as a function of m_{H^+} in the $m_h^{\text{mod}-}$ [28] (left) and the hMSSM [29] (right) scenarios of the MSSM. Limits are shown for tanβ values in the range of 0.5–60, where predictions are available from both scenarios. The limits are a superposition of the results obtained in the analysis presented here, and the ATLAS limits derived from the $H^+ \to \tau\nu$ decay [30]. The expected limits from the $\tau\nu$ final state are shown as the horizontally hatched area, with the observed limit as a dash-dotted curve. The expected limits from the tb final state are shown as diagonally hatched areas, with the observed limit as dashed lines. At low tanβ, the strongest limits are from the tb final state, whereas the exclusions at high tanβ and low H^+ masses are obtained from the $\tau\nu$ final state. The exclusion limits for the hMSSM scenario are shown only for $m_{H^+} > 150$ GeV, where the corresponding theoretical predictions are available.

9 Conclusions

A search for charged Higgs bosons is performed using a data sample corresponding to an integrated luminosity of 36.1 fb^{-1} from pp collisions at $\sqrt{s} = 13$ TeV, recorded by the ATLAS detector at the LHC. The search for $pp \to tbH^+$ is performed in the H^+ mass range 200–2000 GeV. The analysis uses multivariate techniques in the signal regions to enhance the separation of signal from background and utilises control regions to reduce the effect of large uncertainties in background predictions.

No significant excess above the expected SM background is found and observed (expected) 95% CL upper limits are set on the $pp \to tbH^+$ production cross-section times the branching ratio $\mathcal{B}(H^+ \to tb)$, which range from $\sigma \times \mathcal{B} = 2.9$ (3.0) pb at $m_{H^+} = 200$ GeV to $\sigma \times \mathcal{B} = 0.070$ (0.077) pb at $m_{H^+} = 2$ TeV.

In the context of the $m_h^{\text{mod}-}$ (hMSSM) scenario of the MSSM, some values of tanβ, in the range 0.5–1.91 (0.5–1.95), are excluded for H^+ masses of 200–920 (200–965) GeV. For H^+ masses between 200 and 520 GeV (220 and 540 GeV), high values of tanβ are excluded, e.g. tan$\beta > 36$ is excluded at 300 GeV.

Additionally, taking into consideration the $H^+ \to \tau\nu$ decay, even stricter exclusions can be made at high tanβ and low H^+ masses. In the context of the hMSSM, the H^+ mass range up to 1100 GeV is excluded at tan$\beta = 60$, and all tanβ values are excluded for m_{H^+} below 160 GeV.

Acknowledgements

We thank CERN for the very successful operation of the LHC, as well as the support staff from our institutions without whom ATLAS could not be operated efficiently.

We acknowledge the support of ANPCyT, Argentina; YerPhI, Armenia; ARC, Australia; BMWFW and FWF, Austria; ANAS, Azerbaijan; SSTC, Belarus; CNPq and FAPESP, Brazil; NSERC, NRC and CFI, Canada; CERN; CONICYT, Chile; CAS, MOST and NSFC, China; COLCIENCIAS, Colombia; MSMT CR, MPO CR and VSC CR, Czech Republic; DNRF and DNSRC, Denmark; IN2P3-CNRS, CEA-DRF/IRFU, France; SRNSFG, Georgia; BMBF, HGF, and MPG, Germany; GSRT, Greece; RGC, Hong Kong SAR, China; ISF, I-CORE and Benoziyo Center, Israel; INFN, Italy; MEXT and JSPS, Japan; CNRST, Morocco; NWO, Netherlands; RCN, Norway; MNiSW and NCN, Poland; FCT, Portugal; MNE/IFA, Romania; MES of Russia and NRC KI, Russian Federation; JINR; MESTD, Serbia; MSSR, Slovakia; ARRS and MIZŠ, Slovenia; DST/NRF, South Africa; MINECO, Spain; SRC and Wallenberg Foundation, Sweden; SERI, SNSF and Cantons of Bern and Geneva, Switzerland; MOST, Taiwan; TAEK, Turkey; STFC, United Kingdom; DOE and NSF, United States of America. In addition, individual groups and members have received support from BCKDF, the Canada Council, CANARIE, CRC, Compute Canada, FQRNT, and the Ontario Innovation Trust, Canada; EPLANET, ERC, ERDF, FP7, Horizon 2020 and Marie Skłodowska-Curie Actions, European Union; Investissements d'Avenir Labex and Idex, ANR, Région Auvergne and Fondation Partager le Savoir, France; DFG and AvH Foundation, Germany; Herakleitos, Thales and Aristeia programmes co-financed by EU-ESF and the Greek NSRF; BSF, GIF and Minerva, Israel; BRF, Norway; CERCA Programme Generalitat de Catalunya, Generalitat Valenciana, Spain; the Royal Society and Leverhulme Trust, United Kingdom.

The crucial computing support from all WLCG partners is acknowledged gratefully, in particular from CERN, the ATLAS Tier-1 facilities at TRIUMF (Canada), NDGF (Denmark, Norway, Sweden), CC-IN2P3 (France), KIT/GridKA (Germany), INFN-CNAF (Italy), NL-T1 (Netherlands), PIC (Spain), ASGC

(Taiwan), RAL (UK) and BNL (USA), the Tier-2 facilities worldwide and large non-WLCG resource providers. Major contributors of computing resources are listed in Ref. [127].

Appendix

In this appendix, the full list of variables used as inputs to the BDTs, described in Section 5, is reported.

Table 6: Input variables to the classification BDT in the ℓ+jets and $\ell\ell$ channels. The symbols j, b, u, ℓ and $E_{\mathrm{T}}^{\mathrm{miss}}$ represent the four-momenta of jets, b-tagged jets, non-b-tagged jets, the lepton and the missing transverse momentum. All numbered indices refer to ordering in transverse momentum, with 1 as leading. The SRs where the variables are used are indicated for the $\ell\ell$ channel. In the ℓ+jets channels the variables are used for all channels. In the ℓ+jets channel the discriminant, D, is only used for charged Higgs boson masses $m_{H^+} \leq 300$ GeV. For the $\ell\ell$ channel a very large set of kinematic variables using combinations of the analysis objects was examined, and approximately ten optimal variables were selected for each SR independently for the low-mass region ($m_{H^+} \leq 600$ GeV) and the high-mass region ($m_{H^+} > 600$ GeV).

ℓ+jets channel	
$p_{\mathrm{T}}(j_1)$	Leading jet transverse momentum
$m(b\text{-pair}^{\Delta R^{\mathrm{min}}})$	Invariant mass of pair of b-tagged jets with smallest ΔR
$p_{\mathrm{T}}(j_5)$	Transverse momentum of fifth jet
H_2	Second Fox–Wolfram moment [128] calculated using all jets and leptons
$\Delta R^{\mathrm{avg}}(b\text{-pair})$	Average ΔR between all b-tagged jet pairs in the event
$\Delta R(\ell, b\text{-pair}^{\Delta R^{\mathrm{min}}})$	ΔR between the lepton and the b-tagged jet pair with smallest ΔR
$m(u\text{-pair}^{\Delta R^{\mathrm{min}}})$	Invariant mass of the non-b-tagged jet-pair with minimum ΔR
$H_{\mathrm{T}}^{\mathrm{jets}}$	Scalar sum of all jets transverse momenta
$m(b\text{-pair}^{p_{\mathrm{T}}^{\mathrm{max}}})$	Invariant mass of the b-tagged jet pair with maximum transverse momentum
$m^{\mathrm{max}}(b\text{-pair})$	Largest invariant mass of any two b-tagged jets
$m^{\mathrm{max}}(j\text{-triplet})$	Largest invariant mass of any three jets
D	Kinematic discriminant based on mass templates (for $m_{H^+} \leq 300$ GeV)

$\ell\ell$ channel, $m \leq 600$ GeV		3j3b	≥4j3b	≥4j≥4b
$m((j,b)^{p_{\mathrm{T}}^{\mathrm{max}}})$	Inv. mass of the jet and b-tagged jet with largest p_{T}	✓		
$\Delta E(j_3, \ell_2)$	Energy difference between the third jet and the subleading lepton	✓		
$E(j_3)$	Energy of third jet	✓		
$\Delta m(j_1+j_2, j_1+j_3+\ell_2+E_{\mathrm{T}}^{\mathrm{miss}})$	Inv. mass difference between j_1+j_2 and $j_1+j_3+\ell_2+E_{\mathrm{T}}^{\mathrm{miss}}$	✓		
$\Delta R(j_2, j_1+\ell_2+E_{\mathrm{T}}^{\mathrm{miss}})$	Angular difference between subleading jet and $j_1+\ell_2+E_{\mathrm{T}}^{\mathrm{miss}}$	✓		
$p_{\mathrm{T}}(b_1)$	p_{T} of leading b-tagged jet	✓		
$p_{\mathrm{T}}((\ell,b)^{\Delta\eta^{\mathrm{max}}})$	p_{T} of the pair of lepton and b-tagged jet with largest $\Delta\eta$	✓		
$m((\ell,b)^{\Delta\phi^{\mathrm{min}}})$	Inv. mass of the pair of lepton and b-tagged jet with smallest $\Delta\phi$		✓	
$\Delta E(b_1, \ell_1+E_{\mathrm{T}}^{\mathrm{miss}})$	Energy difference between the leading b-tagged jet and $\ell_1+E_{\mathrm{T}}^{\mathrm{miss}}$		✓	
$\Delta m(j_2+j_3, j_1+\ell_1+\ell_2)$	Inv. mass difference between j_2+j_3 and $j_1+\ell_1+\ell_2$		✓	
$\Delta m(\ell_1+j_3+E_{\mathrm{T}}^{\mathrm{miss}}, j_1+j_2+\ell_2)$	Inv. mass difference between $\ell_1+j_3+E_{\mathrm{T}}^{\mathrm{miss}}$ and $j_1+j_2+\ell_2$		✓	
$\Delta p_{\mathrm{T}}(j_1, j_3)$	p_{T} difference between leading and third jet		✓	✓
$m^{\mathrm{min}}(b\text{-pair})$	Smallest invariant mass of any b-tagged jet pair		✓	✓
$m^{\mathrm{min}}(\ell, b)$	Smallest invariant mass of any pair of lepton and b-tagged jet		✓	✓
$p_{\mathrm{T}}(b_2+\ell_1+\ell_2+E_{\mathrm{T}}^{\mathrm{miss}})$	p_{T} of $b_2+\ell_1+\ell_2+E_{\mathrm{T}}^{\mathrm{miss}}$			✓
$\Delta R(\ell_2, j_2+j_3+\ell_1+E_{\mathrm{T}}^{\mathrm{miss}})$	Angular difference between ℓ_2 and $j_2+j_3+\ell_1+E_{\mathrm{T}}^{\mathrm{miss}}$			✓
$H_{\mathrm{T}}^{\mathrm{all}}$	Scalar sum of all jets and leptons transverse energy			✓

$\ell\ell$ channel, $m > 600$ GeV		3j3b	≥4j3b	≥4j≥4b
$p_{\mathrm{T}}((\ell,b)^{\Delta\eta^{\mathrm{min}}})$	p_{T} of the pair of lepton and b-tagged jet with smallest $\Delta\eta$	✓		✓
$\Delta p_{\mathrm{T}}(j_1, j_3)$	p_{T} difference between leading and third jets	✓		✓
$\Delta m(j_2+\ell_1+E_{\mathrm{T}}^{\mathrm{miss}}, j_1+j_3+\ell_1)$	Inv. mass difference between $j_2+\ell_1+E_{\mathrm{T}}^{\mathrm{miss}}$ and $j_1+j_3+\ell_1$	✓		
$p_{\mathrm{T}}((\ell,b)^{\Delta R^{\mathrm{min}}})$	p_{T} of the pair of lepton and b-tagged jet with smallest ΔR	✓		
$m(j\text{-pair}^{\Delta\eta^{\mathrm{min}}})$	Inv. mass of the jet pair with smallest $\Delta\eta$	✓		
$\Delta p_{\mathrm{T}}(j_1, j_2+E_{\mathrm{T}}^{\mathrm{miss}})$	p_{T} difference between leading jet and $j_2+E_{\mathrm{T}}^{\mathrm{miss}}$	✓		
$p_{\mathrm{T}}(j_1+j_2+j_3+\ell_1)$	p_{T} of $j_1+j_2+j_3+\ell_1$	✓		
$\Delta E(\ell_1+E_{\mathrm{T}}^{\mathrm{miss}}, j_1+j_2)$	Energy difference between $\ell_1+E_{\mathrm{T}}^{\mathrm{miss}}$ and j_1+j_2	✓		
$E(j_1)$	Energy of the leading jet	✓	✓	
$p_{\mathrm{T}}^{\mathrm{max}}(j\text{-pair})$	Maximum p_{T} of any jet pair	✓	✓	
$m(b_1+b_2+\ell_1+\ell_2+E_{\mathrm{T}}^{\mathrm{miss}})$	Inv. mass of $b_1+b_2+\ell_1+\ell_2+E_{\mathrm{T}}^{\mathrm{miss}}$		✓	
$p_{\mathrm{T}}((\ell,b)^{\Delta\eta^{\mathrm{min}}})$	p_{T} of the lepton-b-jet pair with smallest separation in η		✓	
$\Delta p_{\mathrm{T}}(\ell_2, u_1+b_2+E_{\mathrm{T}}^{\mathrm{miss}})$	p_{T} difference between subleading lepton and $u_1+b_2+E_{\mathrm{T}}^{\mathrm{miss}}$		✓	
$\Delta p_{\mathrm{T}}(\ell_2, u_1+b_1+E_{\mathrm{T}}^{\mathrm{miss}})$	p_{T} difference between subleading lepton and $u_1+b_1+E_{\mathrm{T}}^{\mathrm{miss}}$		✓	
$\Delta p_{\mathrm{T}}(\ell_2, \ell_1+E_{\mathrm{T}}^{\mathrm{miss}})$	p_{T} difference between subleading lepton and $\ell_1+E_{\mathrm{T}}^{\mathrm{miss}}$		✓	
$\Delta p_{\mathrm{T}}(j_1, j_3+\ell_1+E_{\mathrm{T}}^{\mathrm{miss}})$	p_{T} difference between leading jet and $j_3+\ell_1+E_{\mathrm{T}}^{\mathrm{miss}}$		✓	
$\Delta E(\ell_1, j_2+E_{\mathrm{T}}^{\mathrm{miss}})$	Energy difference between leading lepton and $j_2+E_{\mathrm{T}}^{\mathrm{miss}}$		✓	
$m^{\mathrm{min}}(b\text{-pair})$	Smallest invariant mass of any b-tagged jet pair		✓	✓
$H_{\mathrm{T}}^{\mathrm{all}}$	Scalar sum of all jets and leptons transverse momenta			✓
$p_{\mathrm{T}}(j_3+\ell_1)$	p_{T} of $j_3+\ell_1$			✓
$\Delta p_{\mathrm{T}}(b_2, b_1+\ell_2)$	p_{T} difference between subleading b-tagged jet and $b_1+\ell_2$			✓
$\Delta p_{\mathrm{T}}(j_2, j_3+\ell_1+E_{\mathrm{T}}^{\mathrm{miss}})$	p_{T} difference between subleading jet and $j_3+\ell_1+E_{\mathrm{T}}^{\mathrm{miss}}$			✓
$\Delta E(j_3, j_2+\ell_1+\ell_2+E_{\mathrm{T}}^{\mathrm{miss}})$	Energy difference between third jet and $j_2+\ell_1+\ell_2+E_{\mathrm{T}}^{\mathrm{miss}}$			✓
$\Delta m(j_2+\ell_2+E_{\mathrm{T}}^{\mathrm{miss}}, j_1+\ell_2+E_{\mathrm{T}}^{\mathrm{miss}})$	Inv. mass difference between $j_2+\ell_2+E_{\mathrm{T}}^{\mathrm{miss}}$ and $j_1+\ell_2+E_{\mathrm{T}}^{\mathrm{miss}}$			✓

References

[1] ATLAS Collaboration, *Observation of a new particle in the search for the Standard Model Higgs boson with the ATLAS detector at the LHC*, Phys. Lett. B **716** (2012) 1, arXiv: 1207.7214 [hep-ex].

[2] CMS Collaboration, *Observation of a new boson at a mass of 125 GeV with the CMS experiment at the LHC*, Phys. Lett. B **716** (2012) 30, arXiv: 1207.7235 [hep-ex].

[3] ATLAS and CMS Collaborations, *Combined Measurement of the Higgs Boson Mass in pp Collisions at $\sqrt{s} = 7$ and 8 TeV with the ATLAS and CMS Experiments*, Phys. Rev. Lett. **114** (2015) 191803, arXiv: 1503.07589 [hep-ex].

[4] L. Evans and P. Bryant, *LHC Machine*, JINST **3** (2008) S08001.

[5] T. D. Lee, *A Theory of Spontaneous T Violation*, Phys. Rev. D **8** (1973) 1226.

[6] A. G. Akeroyd et al., *Prospects for charged Higgs searches at the LHC*, Eur. Phys. J. C **77** (2017) 276, arXiv: 1607.01320 [hep-ph].

[7] J. F. Gunion and H. E. Haber, *The CP conserving two Higgs doublet model: The approach to the decoupling limit*, Phys. Rev. D **67** (2003) 075019, arXiv: hep-ph/0207010.

[8] G. C. Branco et al., *Theory and phenomenology of two-Higgs-doublet models*, Phys. Rept. **516** (2012) 1, arXiv: 1106.0034 [hep-ph].

[9] T. P. Cheng and L.-F. Li, *Neutrino masses, mixings and oscillations in SU(2)×U(1) models of electroweak interactions*, Phys. Rev. D **22** (1980) 2860.

[10] J. Schechter and J. W. F. Valle, *Neutrino masses in SU(2)×U(1) theories*, Phys. Rev. D **22** (1980) 2227.

[11] G. Lazarides, Q. Shafi and C. Wetterich, *Proton lifetime and fermion masses in an SO(10) model*, Nucl. Phys. B **181** (1981) 287.

[12] R. N. Mohapatra and G. Senjanovic, *Neutrino masses and mixings in gauge models with spontaneous parity violation*, Phys. Rev. D **23** (1981) 165.

[13] M. Magg and C. Wetterich, *Neutrino mass problem and gauge hierarchy*, Phys. Lett. B **94** (1980) 61.

[14] J. R. Andersen et al., *Handbook of LHC Higgs Cross Sections: 3. Higgs Properties*, ed. by S. Heinemeyer, C. Mariotti, G. Passarino and R. Tanaka, CERN-2013-004, FERMILAB-CONF-13-667-T, 2013, arXiv: 1307.1347 [hep-ph], URL: https://cds.cern.ch/record/1559921.

[15] D. de Florian et al., *Handbook of LHC Higgs Cross Sections: 4. Deciphering the Nature of the Higgs Sector*, FERMILAB-FN-1025-T, CERN-2017-002-M, 2016, arXiv: 1610.07922 [hep-ph], URL: https://inspirehep.net/record/1494411.

[16] ALEPH, DELPHI, L3 and OPAL Collaborations, LEP working group for Higgs boson searches: *Search for charged Higgs bosons: combined results using LEP data*, Eur. Phys. J. C **73** (2013) 2463, arXiv: 1301.6065 [hep-ex].

[17] CDF Collaboration, *Search for charged Higgs bosons in decays of top quarks in $p\bar{p}$ collisions at $\sqrt{s} = 1.96$ TeV*, Phys. Rev. Lett. **103** (2009) 101803, arXiv: 0907.1269 [hep-ex].

[18] DØ Collaboration, *Search for charged Higgs bosons in top quark decays*, Phys. Lett. B **682** (2009) 278, arXiv: 0908.1811 [hep-ex].

[19] CMS Collaboration, *Search for a charged Higgs boson in pp collisions at $\sqrt{s} = 8$ TeV*, JHEP **11** (2015) 018, arXiv: 1508.07774 [hep-ex].

[20] ATLAS Collaboration, *Search for charged Higgs bosons in the $H^{\pm} \to tb$ decay channel in pp collisions at $\sqrt{s} = 8$ TeV using the ATLAS detector*, JHEP **03** (2016) 127, arXiv: 1512.03704 [hep-ex].

[21] O. Deschamps et al., *Two Higgs doublet model of type II facing flavor physics data*, Phys. Rev. D **82** (2010) 073012, arXiv: 0907.5135 [hep-ph].

[22] A. Arbey, F. Mahmoudi, O. Stål and T. Stefaniak, *Status of the charged Higgs boson in two Higgs doublet models*, Eur. Phys. J. C **78** (2018) 182, arXiv: 1706.07414 [hep-ph].

[23] BaBar Collaboration, *Measurement of an excess of $\bar{B} \to D^{(*)}\tau^-\bar{\nu}_\tau$ decays and implications for charged Higgs bosons*, Phys. Rev. D **88** (2013) 072012, arXiv: 1303.0571 [hep-ex].

[24] Belle Collaboration, *Measurement of the τ lepton polarization and $R(D^*)$ in the decay $\bar{B} \to D^*\tau^-\bar{\nu}_\tau$ with one-prong hadronic τ decays at Belle*, Phys. Rev. D **97** (2018) 012004, arXiv: 1709.00129 [hep-ex].

[25] Belle Collaboration, *Measurement of the branching ratio of $\bar{B}^0 \to D^{*+}\tau^-\bar{\nu}_\tau$ relative to $\bar{B}^0 \to D^{*+}\ell^-\bar{\nu}_\ell$ decays with a semileptonic tagging method*, Phys. Rev. D **94** (2016) 072007, arXiv: 1607.07923 [hep-ex].

[26] Belle Collaboration, *Measurement of the branching ratio of $\bar{B} \to D^{(*)}\tau^-\bar{\nu}_\tau$ relative to $\bar{B} \to D^{(*)}\ell^-\bar{\nu}_\ell$ decays with hadronic tagging at Belle*, Phys. Rev. D **92** (2015) 072014, arXiv: 1507.03233 [hep-ex].

[27] LHCb Collaboration, *Test of lepton flavor universality by the measurement of the $B^0 \to D^{*-}\tau^+\nu_\tau$ branching fraction using three-prong τ decays*, Phys. Rev. D **97** (2018) 072013, arXiv: 1711.02505 [hep-ex].

[28] M. Carena, S. Heinemeyer, O. Stål, C. E. M. Wagner and G. Weiglein, *MSSM Higgs boson searches at the LHC: benchmark scenarios after the discovery of a Higgs-like particle*, Eur. Phys. J. C **73** (2013) 2552, arXiv: 1302.7033 [hep-ph].

[29] A. Djouadi et al., *The post-Higgs MSSM scenario: habemus MSSM?*, Eur. Phys. J. **C73** (2013) 2650, arXiv: 1307.5205 [hep-ph].

[30] ATLAS Collaboration, *Search for charged Higgs bosons decaying via $H^{\pm} \to \tau^{\pm}\nu_\tau$ in the τ+jets and τ+lepton final states with 36.1 fb^{-1} of pp collision data recorded at $\sqrt{s} = 13$ TeV with the ATLAS experiment*, (2018), arXiv: 1807.07915 [hep-ex].

[31] ATLAS Collaboration, *The ATLAS Experiment at the CERN Large Hadron Collider*, JINST **3** (2008) S08003.

[32] ATLAS Collaboration, *ATLAS Insertable B-Layer Technical Design Report*, ATLAS-TDR-19, 2010, URL: https://cds.cern.ch/record/1291633.

[33] ATLAS Collaboration, *Performance of the ATLAS trigger system in 2015*, Eur. Phys. J. C **77** (2017) 317, arXiv: 1611.09661 [hep-ex].

[34] J. Alwall et al., *The automated computation of tree-level and next-to-leading order differential cross sections, and their matching to parton shower simulations*, JHEP **07** (2014) 079, arXiv: 1405.0301 [hep-ph].

[35] C. Degrande, M. Ubiali, M. Wiesemann and M. Zaro, *Heavy charged Higgs boson production at the LHC*, JHEP **10** (2015) 145, arXiv: 1507.02549 [hep-ph].

[36] R. D. Ball et al., *Parton distributions with LHC data*, Nucl. Phys. B **867** (2013) 244, arXiv: 1207.1303 [hep-ph].

[37] T. Sjöstrand, S. Mrenna and P. Z. Skands, *A brief introduction to PYTHIA 8.1*, Comput. Phys. Commun. **178** (2008) 852, arXiv: 0710.3820 [hep-ph].

[38] ATLAS Collaboration, *ATLAS Pythia 8 tunes to* 7 *TeV data*, ATL-PHYS-PUB-2014-021, 2014, URL: https://cds.cern.ch/record/1966419.

[39] ATLAS Collaboration, *The simulation principle and performance of the ATLAS fast calorimeter simulation FastCaloSim*, ATL-PHYS-PUB-2010-013, 2010, URL: https://cds.cern.ch/record/1300517.

[40] P. Nason, *A New method for combining NLO QCD with shower Monte Carlo algorithms*, JHEP **11** (2004) 040, arXiv: hep-ph/0409146.

[41] S. Frixione, P. Nason and C. Oleari, *Matching NLO QCD computations with Parton Shower simulations: the POWHEG method*, JHEP **11** (2007) 070, arXiv: 0709.2092 [hep-ph].

[42] S. Alioli, P. Nason, C. Oleari and E. Re, *A general framework for implementing NLO calculations in shower Monte Carlo programs: the POWHEG BOX*, JHEP **06** (2010) 043, arXiv: 1002.2581 [hep-ph].

[43] J. M. Campbell, R. K. Ellis, P. Nason and E. Re, *Top-pair production and decay at NLO matched with parton showers*, JHEP **04** (2015) 114, arXiv: 1412.1828 [hep-ph].

[44] R. D. Ball et al., *Parton distributions for the LHC Run II*, JHEP **04** (2015) 040, arXiv: 1410.8849 [hep-ph].

[45] ATLAS Collaboration, *Studies on top-quark Monte Carlo modelling for Top2016*, ATL-PHYS-PUB-2016-020, 2016, URL: https://cds.cern.ch/record/2216168.

[46] T. Sjöstrand et al., *An introduction to PYTHIA 8.2*, Comput. Phys. Commun. **191** (2015) 159, arXiv: 1410.3012 [hep-ph].

[47] M. Czakon and A. Mitov, *Top++: A program for the calculation of the top-pair cross-section at hadron colliders*, Comput. Phys. Commun. **185** (2014) 2930, arXiv: 1112.5675 [hep-ph].

[48] M. Cacciari, M. Czakon, M. Mangano, A. Mitov and P. Nason, *Top-pair production at hadron colliders with next-to-next-to-leading logarithmic soft-gluon resummation*, Phys. Lett. B **710** (2012) 612, arXiv: 1111.5869 [hep-ph].

[49] P. Bärnreuther, M. Czakon and A. Mitov, *Percent Level Precision Physics at the Tevatron: First Genuine NNLO QCD Corrections to $q\bar{q} \to t\bar{t} + X$*, Phys. Rev. Lett. **109** (2012) 132001, arXiv: 1204.5201 [hep-ph].

[50] M. Czakon and A. Mitov, *NNLO corrections to top-pair production at hadron colliders: the all-fermionic scattering channels*, JHEP **12** (2012) 054, arXiv: 1207.0236 [hep-ph].

[51] M. Czakon and A. Mitov, *NNLO corrections to top-pair production at hadron colliders: the quark-gluon reaction*, JHEP **01** (2013) 080, arXiv: 1210.6832 [hep-ph].

[52] M. Czakon, P. Fiedler and A. Mitov, *Total Top-Quark Pair-Production Cross Section at Hadron Colliders Through $O(\alpha_S^4)$*, Phys. Rev. Lett. **110** (2013) 252004, arXiv: 1303.6254 [hep-ph].

[53] D. J. Lange, *The EvtGen particle decay simulation package*, Nucl. Instrum. Meth. A **462** (2001) 152.

[54] ATLAS Collaboration, *Search for the Standard Model Higgs boson produced in association with top quarks and decaying into $b\bar{b}$ in pp collisions at $\sqrt{s} = 8$ TeV with the ATLAS detector*, Eur. Phys. J. C **75** (2015) 349, arXiv: 1503.05066 [hep-ex].

[55] M. Cacciari, G. P. Salam and G. Soyez, *The anti-k_t jet clustering algorithm*, JHEP **04** (2008) 063, arXiv: 0802.1189 [hep-ph].

[56] T. Gleisberg et al., *Event generation with SHERPA 1.1*, JHEP **02** (2009) 007, arXiv: 0811.4622 [hep-ph].

[57] F. Cascioli, P. Maierhöfer, N. Moretti, S. Pozzorini and F. Siegert, *NLO matching for $t\bar{t}b\bar{b}$ production with massive b-quarks*, Phys. Lett. B **734** (2014) 210, arXiv: 1309.5912 [hep-ph].

[58] F. Cascioli, P. Maierhofer and S. Pozzorini, *Scattering Amplitudes with Open Loops*, Phys. Rev. Lett. **108** (2012) 111601, arXiv: 1111.5206 [hep-ph].

[59] H.-L. Lai et al., *New parton distributions for collider physics*, Phys. Rev. D **82** (2010) 074024, arXiv: 1007.2241 [hep-ph].

[60] N. Moretti, *Precise Predictions for Top-quark Pair Production in Association with Multiple Jets*, University of Zurich, Faculty of Science, PhD thesis, 2016, URL: https://doi.org/10.5167/uzh-127073.

[61] ATLAS Collaboration, *Search for the Standard Model Higgs boson produced in association with top quarks and decaying into a $b\bar{b}$ pair in pp collisions at $\sqrt{s} = 13$ TeV with the ATLAS detector*, Phys. Rev. D **97** (2018) 072016, arXiv: 1712.08895 [hep-ex].

[62] S. Frixione, E. Laenen, P. Motylinski, B. R. Webber and C. D. White, *Single-top hadroproduction in association with a W boson*, JHEP **07** (2008) 029, arXiv: 0805.3067 [hep-ph].

[63] P. Artoisenet, R. Frederix, O. Mattelaer and R. Rietkerk, *Automatic spin-entangled decays of heavy resonances in Monte Carlo simulations*, JHEP **03** (2013) 015, arXiv: 1212.3460 [hep-ph].

[64] T. Sjöstrand, S. Mrenna and P. Z. Skands, *PYTHIA 6.4 physics and manual*, JHEP **05** (2006) 026, arXiv: hep-ph/0603175.

[65] P. Z. Skands, *Tuning Monte Carlo generators: The Perugia tunes*, Phys. Rev. D **82** (2010) 074018, arXiv: 1005.3457 [hep-ph].

[66] N. Kidonakis, *Two-loop soft anomalous dimensions for single top quark associated production with a W^- or H^-*, Phys. Rev. D **82** (2010) 054018, arXiv: 1005.4451 [hep-ph].

[67] N. Kidonakis, *NNLL resummation for s-channel single top quark production*, Phys. Rev. D **81** (2010) 054028, arXiv: 1001.5034 [hep-ph].

[68] N. Kidonakis, *Next-to-next-to-leading-order collinear and soft gluon corrections for t-channel single top quark production*, Phys. Rev. D **83** (2011) 091503, arXiv: 1103.2792 [hep-ph].

[69] T. Gleisberg and S. Höche, *Comix, a new matrix element generator*, JHEP **12** (2008) 039, arXiv: 0808.3674 [hep-ph].

[70] S. Schumann and F. Krauss, *A Parton shower algorithm based on Catani-Seymour dipole factorisation*, JHEP **03** (2008) 038, arXiv: 0709.1027 [hep-ph].

[71] S. Höche, F. Krauss, M. Schönherr and F. Siegert, *QCD matrix elements + parton showers: The NLO case*, JHEP **04** (2013) 027, arXiv: 1207.5030 [hep-ph].

[72] K. Melnikov and F. Petriello, *Electroweak gauge boson production at hadron colliders through $O(\alpha_S^4)$*, Phys. Rev. D **74** (2006) 114017, arXiv: hep-ph/0609070.

[73] R. Gavin, Y. Li, F. Petriello and S. Quackenbush, *FEWZ 2.0: A code for hadronic Z production at next-to-next-to-leading order*, Comput. Phys. Commun. **182** (2011) 2388, arXiv: 1011.3540 [hep-ph].

[74] Y. Li and F. Petriello, *Combining QCD and electroweak corrections to dilepton production in FEWZ*, Phys. Rev. D **86** (2012) 094034, arXiv: 1208.5967 [hep-ph].

[75] D. Bardin et al., *SANC integrator in the progress: QCD and EW contributions*, JETP Lett. **96** (2012) 285, arXiv: 1207.4400 [hep-ph].

[76] A. B. Arbuzov, R. R. Sadykov and Z. Was, *QED bremsstrahlung in decays of electroweak bosons*, Eur. Phys. J. C **73** (2013) 2625, arXiv: 1212.6783 [hep-ph].

[77] ATLAS Collaboration, *Observation of Higgs boson production in association with a top quark pair at the LHC with the ATLAS detector*, (2018), arXiv: 1806.00425 [hep-ex].

[78] CMS Collaboration, *Observation of $t\bar{t}H$ production*, Phys. Rev. Lett. **120** (2018) 231801, arXiv: 1804.02610 [hep-ex].

[79] M. Bahr et al., *Herwig++ physics and manual*, Eur. Phys. J. C **58** (2008) 639, arXiv: 0803.0883 [hep-ph].

[80] J. Pumplin et al., *New generation of parton distributions with uncertainties from global QCD analysis*, JHEP **07** (2002) 012, arXiv: hep-ph/0201195.

[81] ATLAS Collaboration, *The ATLAS Simulation Infrastructure*, Eur. Phys. J. C **70** (2010) 823, arXiv: 1005.4568 [physics.ins-det].

[82] S. Agostinelli et al., *GEANT4 – a simulation toolkit*, Nucl. Instrum. Meth. A **506** (2003) 250.

[83] ATLAS Collaboration, *Summary of ATLAS Pythia 8 tunes*, ATL-PHYS-PUB-2012-003, 2012, URL: https://cds.cern.ch/record/2160731.

[84] A. D. Martin, W. J. Stirling, R. S. Thorne and G. Watt, *Parton distributions for the LHC*, Eur. Phys. J. C **63** (2009) 189, arXiv: 0901.0002 [hep-ph].

[85] ATLAS Collaboration, *Electron efficiency measurements with the ATLAS detector using the 2015 LHC proton–proton collision data*, ATLAS-CONF-2016-024, 2016, URL: https://cds.cern.ch/record/2157687.

[86] ATLAS Collaboration, *Muon reconstruction performance of the ATLAS detector in proton–proton collision data at* $\sqrt{s} = 13$ *TeV*, Eur. Phys. J. C **76** (2016) 292, arXiv: 1603.05598 [hep-ex].

[87] ATLAS Collaboration, *Topological cell clustering in the ATLAS calorimeters and its performance in LHC Run 1*, Eur. Phys. J. C **77** (2017) 490, arXiv: 1603.02934 [hep-ex].

[88] M. Cacciari, G. P. Salam and G. Soyez, *FastJet user manual*, Eur. Phys. J. C **72** (2012) 1896, arXiv: 1111.6097 [hep-ph].

[89] ATLAS Collaboration, *Jet energy scale measurements and their systematic uncertainties in proton–proton collisions at* $\sqrt{s} = 13$ *TeV with the ATLAS detector*, Phys. Rev. D **96** (2017) 072002, arXiv: 1703.09665 [hep-ex].

[90] ATLAS Collaboration, *Selection of jets produced in* 13 *TeV proton–proton collisions with the ATLAS detector*, ATLAS-CONF-2015-029, 2015, URL: https://cds.cern.ch/record/2037702.

[91] ATLAS Collaboration, *Performance of pile-up mitigation techniques for jets in pp collisions at* $\sqrt{s} = 8$ *TeV using the ATLAS detector*, Eur. Phys. J. C **76** (2016) 581, arXiv: 1510.03823 [hep-ex].

[92] ATLAS Collaboration, *Performance of b-jet identification in the ATLAS experiment*, JINST **11** (2016) P04008, arXiv: 1512.01094 [hep-ex].

[93] ATLAS Collaboration, *Optimisation of the ATLAS b-tagging performance for the 2016 LHC Run*, ATL-PHYS-PUB-2016-012, 2016, URL: https://cds.cern.ch/record/2160731.

[94] ATLAS Collaboration, *Search for the* $b\bar{b}$ *decay of the Standard Model Higgs boson in associated* $(W/Z)H$ *production with the ATLAS detector*, JHEP **01** (2015) 069, arXiv: 1409.6212 [hep-ex].

[95] ATLAS Collaboration, *Performance of algorithms that reconstruct missing transverse momentum in* $\sqrt{s} = 8$ *TeV proton–proton collisions in the ATLAS detector*, Eur. Phys. J. C **77** (2017) 241, arXiv: 1609.09324 [hep-ex].

[96] ATLAS Collaboration, *Performance of missing transverse momentum reconstruction with the ATLAS detector using proton–proton collisions at* $\sqrt{s} = 13$ *TeV*, (2018), arXiv: 1802.08168 [hep-ex].

[97] ATLAS Collaboration,
E_T^{miss} performance in the ATLAS detector using 2015-2016 LHC p-p collisions,
ATLAS-CONF-2018-023, 2018, URL: http://cds.cern.ch/record/2625233.

[98] ATLAS Collaboration, *Estimation of non-prompt and fake lepton backgrounds in final states with top quarks produced in proton–proton collisions at $\sqrt{s}$ = 8 TeV with the ATLAS Detector*,
ATLAS-CONF-2014-058, 2014, URL: https://cds.cern.ch/record/1951336.

[99] A. Höcker et al., *TMVA - Toolkit for Multivariate Data Analysis*, PoS **ACAT** (2007) 040,
arXiv: physics/0703039.

[100] ATLAS Collaboration,
Luminosity determination in pp collisions at $\sqrt{s}$ = 8 TeV using the ATLAS detector at the LHC,
Eur. Phys. J. C **76** (2016) 653, arXiv: 1608.03953 [hep-ex].

[101] ATLAS Collaboration, *Measurement of the Inelastic Proton–Proton Cross Section at $\sqrt{s}$ = 13 TeV with the ATLAS Detector at the LHC*, Phys. Rev. Lett. **117** (2016) 182002,
arXiv: 1606.02625 [hep-ex].

[102] ATLAS Collaboration, *Jet energy resolution in proton–proton collisions at $\sqrt{s}$ = 7 TeV recorded in 2010 with the ATLAS detector*, Eur. Phys. J. C **73** (2013) 2306, arXiv: 1210.6210 [hep-ex].

[103] ATLAS Collaboration, *Measurement of b-tagging efficiency of c-jets in $t\bar{t}$ events using a likelihood approach wth the ATLAS detector*, ATLAS-CONF-2018-001, 2018,
URL: https://cds.cern.ch/record/2306649.

[104] J. Butterworth et al., *PDF4LHC recommendations for LHC Run II*, J. Phys. G **43** (2016) 023001,
arXiv: 1510.03865 [hep-ph].

[105] S. Dulat et al.,
New parton distribution functions from a global analysis of quantum chromodynamics,
Phys. Rev. D **93** (2016) 033006, arXiv: 1506.07443 [hep-ph].

[106] L. A. Harland-Lang, A. D. Martin, P. Motylinski and R. S. Thorne,
Parton distributions in the LHC era: MMHT 2014 PDFs, Eur. Phys. J. C **75** (2015) 204,
arXiv: 1412.3989 [hep-ph].

[107] J. Gao and P. Nadolsky, *A meta-analysis of parton distribution functions*, JHEP **07** (2014) 035,
arXiv: 1401.0013 [hep-ph].

[108] S. Carrazza, S. Forte, Z. Kassabov, J. I. Latorre and J. Rojo,
An unbiased Hessian representation for Monte Carlo PDFs, Eur. Phys. J. C **75** (2015) 369,
arXiv: 1505.06736 [hep-ph].

[109] G. Watt and R. S. Thorne, *Study of Monte Carlo approach to experimental uncertainty propagation with MSTW 2008 PDFs*, JHEP **08** (2012) 052, arXiv: 1205.4024 [hep-ph].

[110] J. Bellm et al., *Herwig 7.0/Herwig++ 3.0 release note*, Eur. Phys. J. C **76** (2016) 196,
arXiv: 1512.01178 [hep-ph].

[111] ATLAS Collaboration,
Simulation of top-quark production for the ATLAS experiment at $\sqrt{s}$ = 13 TeV,
ATL-PHYS-PUB-2016-004, 2016, URL: https://cds.cern.ch/record/2120417.

[112] ATLAS Collaboration, *Studies of $t\bar{t}c\bar{c}$ production with MadGraph5_aMC@NLO and Herwig++ for the ATLAS experiment*, ATL-PHYS-PUB-2016-011, 2016,
URL: https://cds.cern.ch/record/2153876.

[113] E. Re,
Single-top Wt-channel production matched with parton showers using the POWHEG method,
Eur. Phys. J. C **71** (2011) 1547, arXiv: 1009.2450 [hep-ph].

[114] A. Kardos, Z. Trocsanyi and C. Papadopoulos,
Top quark pair production in association with a Z-boson at NLO accuracy,
Phys. Rev. D **85** (2012) 054015, arXiv: 1111.0610 [hep-ph].

[115] A. Lazopoulos, T. McElmurry, K. Melnikov and F. Petriello,
Next-to-leading order QCD corrections to $t\bar{t}Z$ production at the LHC,
Phys. Lett. B **666** (2008) 62, arXiv: 0804.2220 [hep-ph].

[116] J. M. Campbell and R. K. Ellis, *$t\bar{t}W^{\pm}$ production and decay at NLO*, JHEP **07** (2012) 052,
arXiv: 1204.5678 [hep-ph].

[117] R. Raitio and W. W. Wada,
Higgs-boson production at large transverse momentum in quantum chromodynamics,
Phys. Rev. D **19** (1979) 941.

[118] W. Beenakker et al., *NLO QCD corrections to $t\bar{t}H$ production in hadron collisions*,
Nucl. Phys. B **653** (2003) 151, arXiv: hep-ph/0211352.

[119] S. Dawson, C. Jackson, L. H. Orr, L. Reina and D. Wackeroth, *Associated Higgs production with top quarks at the large hadron collider: NLO QCD corrections*, Phys. Rev. D **68** (2003) 034022,
arXiv: hep-ph/0305087.

[120] Y. Zhang, W.-G. Ma, R.-Y. Zhang, C. Chen and L. Guo,
QCD NLO and EW NLO corrections to $t\bar{t}H$ production with top quark decays at hadron collider,
Phys. Lett. B **738** (2014) 1, arXiv: 1407.1110 [hep-ph].

[121] S. Frixione, V. Hirschi, D. Pagani, H.-S. Shao and M. Zaro,
Electroweak and QCD corrections to top-pair hadroproduction in association with heavy bosons,
JHEP **06** (2015) 184, arXiv: 1504.03446 [hep-ph].

[122] G. Cowan, K. Cranmer, E. Gross and O. Vitells,
Asymptotic formulae for likelihood-based tests of new physics, Eur. Phys. J. C **71** (2011) 1554,
arXiv: 1007.1727 [physics.data-an], Erratum: Eur. Phys. J. C **73** (2013) 2501.

[123] A. L. Read, *Presentation of search results: the CL_S technique*, J. Phys. G **28** (2002) 2693.

[124] T. Junk, *Confidence level computation for combining searches with small statistics*,
Nucl. Instrum. Meth. A **434** (1999) 435, arXiv: hep-ex/9902006.

[125] A. Djouadi, L. Maiani, A. Polosa, J. Quevillon and V. Riquer,
Fully covering the MSSM Higgs sector at the LHC, JHEP **06** (2015) 168,
arXiv: 1502.05653 [hep-ph].

[126] E. Bagnaschi et al., *Benchmark scenarios for low* $\tan\beta$ *in the MSSM*, LHCHXSWG-2015-002,
2015, URL: https://cds.cern.ch/record/2039911.

[127] ATLAS Collaboration, *ATLAS Computing Acknowledgements 2016–2017*,
ATL-GEN-PUB-2016-002, URL: https://cds.cern.ch/record/2202407.

[128] C. Bernaciak, M. S. A. Buschmann, A. Butter and T. Plehn,
Fox-Wolfram moments in Higgs physics, Phys. Rev. D **87** (2013) 073014,
arXiv: 1212.4436 [hep-ph].

The ATLAS Collaboration

M. Aaboud[34d], G. Aad[99], B. Abbott[124], O. Abdinov[13,*], B. Abeloos[128], D.K. Abhayasinghe[91], S.H. Abidi[164], O.S. AbouZeid[39], N.L. Abraham[153], H. Abramowicz[158], H. Abreu[157], Y. Abulaiti[6], B.S. Acharya[64a,64b,n], S. Adachi[160], L. Adamczyk[81a], J. Adelman[119], M. Adersberger[112], A. Adiguzel[12c,ag], T. Adye[141], A.A. Affolder[143], Y. Afik[157], C. Agheorghiesei[27c], J.A. Aguilar-Saavedra[136f,136a], F. Ahmadov[77,ae], G. Aielli[71a,71b], S. Akatsuka[83], T.P.A. Åkesson[94], E. Akilli[52], A.V. Akimov[108], G.L. Alberghi[23b,23a], J. Albert[173], P. Albicocco[49], M.J. Alconada Verzini[86], S. Alderweireldt[117], M. Aleksa[35], I.N. Aleksandrov[77], C. Alexa[27b], T. Alexopoulos[10], M. Alhroob[124], B. Ali[138], G. Alimonti[66a], J. Alison[36], S.P. Alkire[145], C. Allaire[128], B.M.M. Allbrooke[153], B.W. Allen[127], P.P. Allport[21], A. Aloisio[67a,67b], A. Alonso[39], F. Alonso[86], C. Alpigiani[145], A.A. Alshehri[55], M.I. Alstaty[99], B. Alvarez Gonzalez[35], D. Álvarez Piqueras[171], M.G. Alviggi[67a,67b], B.T. Amadio[18], Y. Amaral Coutinho[78b], L. Ambroz[131], C. Amelung[26], D. Amidei[103], S.P. Amor Dos Santos[136a,136c], S. Amoroso[44], C.S. Amrouche[52], C. Anastopoulos[146], L.S. Ancu[52], N. Andari[21], T. Andeen[11], C.F. Anders[59b], J.K. Anders[20], K.J. Anderson[36], A. Andreazza[66a,66b], V. Andrei[59a], C.R. Anelli[173], S. Angelidakis[37], I. Angelozzi[118], A. Angerami[38], A.V. Anisenkov[120b,120a], A. Annovi[69a], C. Antel[59a], M.T. Anthony[146], M. Antonelli[49], D.J.A. Antrim[168], F. Anulli[70a], M. Aoki[79], J.A. Aparisi Pozo[171], L. Aperio Bella[35], G. Arabidze[104], J.P. Araque[136a], V. Araujo Ferraz[78b], R. Araujo Pereira[78b], A.T.H. Arce[47], R.E. Ardell[91], F.A. Arduh[86], J-F. Arguin[107], S. Argyropoulos[75], A.J. Armbruster[35], L.J. Armitage[90], A Armstrong[168], O. Arnaez[164], H. Arnold[118], M. Arratia[31], O. Arslan[24], A. Artamonov[109,*], G. Artoni[131], S. Artz[97], S. Asai[160], N. Asbah[44], A. Ashkenazi[158], E.M. Asimakopoulou[169], L. Asquith[153], K. Assamagan[29], R. Astalos[28a], R.J. Atkin[32a], M. Atkinson[170], N.B. Atlay[148], K. Augsten[138], G. Avolio[35], R. Avramidou[58a], M.K. Ayoub[15a], G. Azuelos[107,as], A.E. Baas[59a], M.J. Baca[21], H. Bachacou[142], K. Bachas[65a,65b], M. Backes[131], P. Bagnaia[70a,70b], M. Bahmani[82], H. Bahrasemani[149], A.J. Bailey[171], J.T. Baines[141], M. Bajic[39], C. Bakalis[10], O.K. Baker[180], P.J. Bakker[118], D. Bakshi Gupta[93], E.M. Baldin[120b,120a], P. Balek[177], F. Balli[142], W.K. Balunas[133], J. Balz[97], E. Banas[82], A. Bandyopadhyay[24], S. Banerjee[178,j], A.A.E. Bannoura[179], L. Barak[158], W.M. Barbe[37], E.L. Barberio[102], D. Barberis[53b,53a], M. Barbero[99], T. Barillari[113], M-S. Barisits[35], J. Barkeloo[127], T. Barklow[150], N. Barlow[31], R. Barnea[157], S.L. Barnes[58c], B.M. Barnett[141], R.M. Barnett[18], Z. Barnovska-Blenessy[58a], A. Baroncelli[72a], G. Barone[26], A.J. Barr[131], L. Barranco Navarro[171], F. Barreiro[96], J. Barreiro Guimarães da Costa[15a], R. Bartoldus[150], A.E. Barton[87], P. Bartos[28a], A. Basalaev[134], A. Bassalat[128], R.L. Bates[55], S.J. Batista[164], S. Batlamous[34e], J.R. Batley[31], M. Battaglia[143], M. Bauce[70a,70b], F. Bauer[142], K.T. Bauer[168], H.S. Bawa[150,l], J.B. Beacham[122], M.D. Beattie[87], T. Beau[132], P.H. Beauchemin[167], P. Bechtle[24], H.C. Beck[51], H.P. Beck[20,q], K. Becker[50], M. Becker[97], C. Becot[44], A. Beddall[12d], A.J. Beddall[12a], V.A. Bednyakov[77], M. Bedognetti[118], C.P. Bee[152], T.A. Beermann[35], M. Begalli[78b], M. Begel[29], A. Behera[152], J.K. Behr[44], A.S. Bell[92], G. Bella[158], L. Bellagamba[23b], A. Bellerive[33], M. Bellomo[157], P. Bellos[9], K. Belotskiy[110], N.L. Belyaev[110], O. Benary[158,*], D. Benchekroun[34a], M. Bender[112], N. Benekos[10], Y. Benhammou[158], E. Benhar Noccioli[180], J. Benitez[75], D.P. Benjamin[47], M. Benoit[52], J.R. Bensinger[26], S. Bentvelsen[118], L. Beresford[131], M. Beretta[49], D. Berge[44], E. Bergeaas Kuutmann[169], N. Berger[5], L.J. Bergsten[26], J. Beringer[18], S. Berlendis[7], N.R. Bernard[100], G. Bernardi[132], C. Bernius[150], F.U. Bernlochner[24], T. Berry[91], P. Berta[97], C. Bertella[15a], G. Bertoli[43a,43b], I.A. Bertram[87], G.J. Besjes[39], O. Bessidskaia Bylund[43a,43b], M. Bessner[44], N. Besson[142], A. Bethani[98], S. Bethke[113], A. Betti[24], A.J. Bevan[90], J. Beyer[113], R.M. Bianchi[135], O. Biebel[112], D. Biedermann[19], R. Bielski[98], K. Bierwagen[97], N.V. Biesuz[69a,69b], M. Biglietti[72a], T.R.V. Billoud[107], M. Bindi[51], A. Bingul[12d], C. Bini[70a,70b], S. Biondi[23b,23a], M. Birman[177], T. Bisanz[51], J.P. Biswal[158], C. Bittrich[46],

D.M. Bjergaard[47], J.E. Black[150], K.M. Black[25], T. Blazek[28a], I. Bloch[44], C. Blocker[26], A. Blue[55], U. Blumenschein[90], Dr. Blunier[144a], G.J. Bobbink[118], V.S. Bobrovnikov[120b,120a], S.S. Bocchetta[94], A. Bocci[47], D. Boerner[179], D. Bogavac[112], A.G. Bogdanchikov[120b,120a], C. Bohm[43a], V. Boisvert[91], P. Bokan[169,51], T. Bold[81a], A.S. Boldyrev[111], A.E. Bolz[59b], M. Bomben[132], M. Bona[90], J.S. Bonilla[127], M. Boonekamp[142], A. Borisov[140], G. Borissov[87], J. Bortfeldt[35], D. Bortoletto[131], V. Bortolotto[71a,61b,61c,71b], D. Boscherini[23b], M. Bosman[14], J.D. Bossio Sola[30], K. Bouaouda[34a], J. Boudreau[135], E.V. Bouhova-Thacker[87], D. Boumediene[37], C. Bourdarios[128], S.K. Boutle[55], A. Boveia[122], J. Boyd[35], I.R. Boyko[77], A.J. Bozson[91], J. Bracinik[21], N. Brahimi[99], A. Brandt[8], G. Brandt[179], O. Brandt[59a], F. Braren[44], U. Bratzler[161], B. Brau[100], J.E. Brau[127], W.D. Breaden Madden[55], K. Brendlinger[44], A.J. Brennan[102], L. Brenner[44], R. Brenner[169], S. Bressler[177], B. Brickwedde[97], D.L. Briglin[21], D. Britton[55], D. Britzger[59b], I. Brock[24], R. Brock[104], G. Brooijmans[38], T. Brooks[91], W.K. Brooks[144b], E. Brost[119], J.H Broughton[21], P.A. Bruckman de Renstrom[82], D. Bruncko[28b], A. Bruni[23b], G. Bruni[23b], L.S. Bruni[118], S. Bruno[71a,71b], B.H. Brunt[31], M. Bruschi[23b], N. Bruscino[135], P. Bryant[36], L. Bryngemark[44], T. Buanes[17], Q. Buat[35], P. Buchholz[148], A.G. Buckley[55], I.A. Budagov[77], F. Buehrer[50], M.K. Bugge[130], O. Bulekov[110], D. Bullock[8], T.J. Burch[119], S. Burdin[88], C.D. Burgard[118], A.M. Burger[5], B. Burghgrave[119], K. Burka[82], S. Burke[141], I. Burmeister[45], J.T.P. Burr[131], D. Büscher[50], V. Büscher[97], E. Buschmann[51], P. Bussey[55], J.M. Butler[25], C.M. Buttar[55], J.M. Butterworth[92], P. Butti[35], W. Buttinger[35], A. Buzatu[155], A.R. Buzykaev[120b,120a], G. Cabras[23b,23a], S. Cabrera Urbán[171], D. Caforio[138], H. Cai[170], V.M.M. Cairo[2], O. Cakir[4a], N. Calace[52], P. Calafiura[18], A. Calandri[99], G. Calderini[132], P. Calfayan[63], G. Callea[40b,40a], L.P. Caloba[78b], S. Calvente Lopez[96], D. Calvet[37], S. Calvet[37], T.P. Calvet[152], M. Calvetti[69a,69b], R. Camacho Toro[132], S. Camarda[35], P. Camarri[71a,71b], D. Cameron[130], R. Caminal Armadans[100], C. Camincher[35], S. Campana[35], M. Campanelli[92], A. Camplani[39], A. Campoverde[148], V. Canale[67a,67b], M. Cano Bret[58c], J. Cantero[125], T. Cao[158], Y. Cao[170], M.D.M. Capeans Garrido[35], I. Caprini[27b], M. Caprini[27b], M. Capua[40b,40a], R.M. Carbone[38], R. Cardarelli[71a], F.C. Cardillo[50], I. Carli[139], T. Carli[35], G. Carlino[67a], B.T. Carlson[135], L. Carminati[66a,66b], R.M.D. Carney[43a,43b], S. Caron[117], E. Carquin[144b], S. Carrá[66a,66b], G.D. Carrillo-Montoya[35], D. Casadei[32b], M.P. Casado[14,f], A.F. Casha[164], M. Casolino[14], D.W. Casper[168], R. Castelijn[118], F.L. Castillo[171], V. Castillo Gimenez[171], N.F. Castro[136a,136e], A. Catinaccio[35], J.R. Catmore[130], A. Cattai[35], J. Caudron[24], V. Cavaliere[29], E. Cavallaro[14], D. Cavalli[66a], M. Cavalli-Sforza[14], V. Cavasinni[69a,69b], E. Celebi[12b], F. Ceradini[72a,72b], L. Cerda Alberich[171], A.S. Cerqueira[78a], A. Cerri[153], L. Cerrito[71a,71b], F. Cerutti[18], A. Cervelli[23b,23a], S.A. Cetin[12b], A. Chafaq[34a], D Chakraborty[119], S.K. Chan[57], W.S. Chan[118], Y.L. Chan[61a], J.D. Chapman[31], D.G. Charlton[21], C.C. Chau[33], C.A. Chavez Barajas[153], S. Che[122], A. Chegwidden[104], S. Chekanov[6], S.V. Chekulaev[165a], G.A. Chelkov[77,ar], M.A. Chelstowska[35], C. Chen[58a], C.H. Chen[76], H. Chen[29], J. Chen[58a], J. Chen[38], S. Chen[133], S.J. Chen[15c], X. Chen[15b,aq], Y. Chen[80], Y-H. Chen[44], H.C. Cheng[103], H.J. Cheng[15d], A. Cheplakov[77], E. Cheremushkina[140], R. Cherkaoui El Moursli[34e], E. Cheu[7], K. Cheung[62], L. Chevalier[142], V. Chiarella[49], G. Chiarelli[69a], G. Chiodini[65a], A.S. Chisholm[35], A. Chitan[27b], I. Chiu[160], Y.H. Chiu[173], M.V. Chizhov[77], K. Choi[63], A.R. Chomont[128], S. Chouridou[159], Y.S. Chow[118], V. Christodoulou[92], M.C. Chu[61a], J. Chudoba[137], A.J. Chuinard[101], J.J. Chwastowski[82], L. Chytka[126], D. Cinca[45], V. Cindro[89], I.A. Cioară[24], A. Ciocio[18], F. Cirotto[67a,67b], Z.H. Citron[177], M. Citterio[66a], A. Clark[52], M.R. Clark[38], P.J. Clark[48], C. Clement[43a,43b], Y. Coadou[99], M. Cobal[64a,64c], A. Coccaro[53b,53a], J. Cochran[76], A.E.C. Coimbra[177], L. Colasurdo[117], B. Cole[38], A.P. Colijn[118], J. Collot[56], P. Conde Muiño[136a,136b], E. Coniavitis[50], S.H. Connell[32b], I.A. Connelly[98], S. Constantinescu[27b], F. Conventi[67a,at], A.M. Cooper-Sarkar[131], F. Cormier[172], K.J.R. Cormier[164], M. Corradi[70a,70b], E.E. Corrigan[94], F. Corriveau[101,ac], A. Cortes-Gonzalez[35], M.J. Costa[171], D. Costanzo[146], G. Cottin[31], G. Cowan[91], B.E. Cox[98], J. Crane[98], K. Cranmer[121], S.J. Crawley[55], R.A. Creager[133], G. Cree[33], S. Crépé-Renaudin[56], F. Crescioli[132], M. Cristinziani[24], V. Croft[121],

G. Crosetti[40b,40a], A. Cueto[96], T. Cuhadar Donszelmann[146], A.R. Cukierman[150], J. Cúth[97], S. Czekierda[82], P. Czodrowski[35], M.J. Da Cunha Sargedas De Sousa[58b,136b], C. Da Via[98], W. Dabrowski[81a], T. Dado[28a,x], S. Dahbi[34e], T. Dai[103], F. Dallaire[107], C. Dallapiccola[100], M. Dam[39], G. D'amen[23b,23a], J. Damp[97], J.R. Dandoy[133], M.F. Daneri[30], N.P. Dang[178,j], N.D Dann[98], M. Danninger[172], V. Dao[35], G. Darbo[53b], S. Darmora[8], O. Dartsi[5], A. Dattagupta[127], T. Daubney[44], S. D'Auria[55], W. Davey[24], C. David[44], T. Davidek[139], D.R. Davis[47], E. Dawe[102], I. Dawson[146], K. De[8], R. De Asmundis[67a], A. De Benedetti[124], M. De Beurs[118], S. De Castro[23b,23a], S. De Cecco[70a,70b], N. De Groot[117], P. de Jong[118], H. De la Torre[104], F. De Lorenzi[76], A. De Maria[51,s], D. De Pedis[70a], A. De Salvo[70a], U. De Sanctis[71a,71b], A. De Santo[153], K. De Vasconcelos Corga[99], J.B. De Vivie De Regie[128], C. Debenedetti[143], D.V. Dedovich[77], N. Dehghanian[3], M. Del Gaudio[40b,40a], J. Del Peso[96], Y. Delabat Diaz[44], D. Delgove[128], F. Deliot[142], C.M. Delitzsch[7], M. Della Pietra[67a,67b], D. Della Volpe[52], A. Dell'Acqua[35], L. Dell'Asta[25], M. Delmastro[5], C. Delporte[128], P.A. Delsart[56], D.A. DeMarco[164], S. Demers[180], M. Demichev[77], S.P. Denisov[140], D. Denysiuk[118], L. D'Eramo[132], D. Derendarz[82], J.E. Derkaoui[34d], F. Derue[132], P. Dervan[88], K. Desch[24], C. Deterre[44], K. Dette[164], M.R. Devesa[30], P.O. Deviveiros[35], A. Dewhurst[141], S. Dhaliwal[26], F.A. Di Bello[52], A. Di Ciaccio[71a,71b], L. Di Ciaccio[5], W.K. Di Clemente[133], C. Di Donato[67a,67b], A. Di Girolamo[35], B. Di Micco[72a,72b], R. Di Nardo[100], K.F. Di Petrillo[57], A. Di Simone[50], R. Di Sipio[164], D. Di Valentino[33], C. Diaconu[99], M. Diamond[164], F.A. Dias[39], T. Dias Do Vale[136a], M.A. Diaz[144a], J. Dickinson[18], E.B. Diehl[103], J. Dietrich[19], S. Díez Cornell[44], A. Dimitrievska[18], J. Dingfelder[24], F. Dittus[35], F. Djama[99], T. Djobava[156b], J.I. Djuvsland[59a], M.A.B. Do Vale[78c], M. Dobre[27b], D. Dodsworth[26], C. Doglioni[94], J. Dolejsi[139], Z. Dolezal[139], M. Donadelli[78d], J. Donini[37], A. D'onofrio[90], M. D'Onofrio[88], J. Dopke[141], A. Doria[67a], M.T. Dova[86], A.T. Doyle[55], E. Drechsler[51], E. Dreyer[149], T. Dreyer[51], Y. Du[58b], J. Duarte-Campderros[158], F. Dubinin[108], M. Dubovsky[28a], A. Dubreuil[52], E. Duchovni[177], G. Duckeck[112], A. Ducourthial[132], O.A. Ducu[107,w], D. Duda[113], A. Dudarev[35], A.C. Dudder[97], E.M. Duffield[18], L. Duflot[128], M. Dührssen[35], C. Dülsen[179], M. Dumancic[177], A.E. Dumitriu[27b,d], A.K. Duncan[55], M. Dunford[59a], A. Duperrin[99], H. Duran Yildiz[4a], M. Düren[54], A. Durglishvili[156b], D. Duschinger[46], B. Dutta[44], D. Duvnjak[1], M. Dyndal[44], S. Dysch[98], B.S. Dziedzic[82], C. Eckardt[44], K.M. Ecker[113], R.C. Edgar[103], T. Eifert[35], G. Eigen[17], K. Einsweiler[18], T. Ekelof[169], M. El Kacimi[34c], R. El Kosseifi[99], V. Ellajosyula[99], M. Ellert[169], F. Ellinghaus[179], A.A. Elliot[90], N. Ellis[35], J. Elmsheuser[29], M. Elsing[35], D. Emeliyanov[141], Y. Enari[160], J.S. Ennis[175], M.B. Epland[47], J. Erdmann[45], A. Ereditato[20], S. Errede[170], M. Escalier[128], C. Escobar[171], O. Estrada Pastor[171], A.I. Etienvre[142], E. Etzion[158], H. Evans[63], A. Ezhilov[134], M. Ezzi[34e], F. Fabbri[55], L. Fabbri[23b,23a], V. Fabiani[117], G. Facini[92], R.M. Faisca Rodrigues Pereira[136a], R.M. Fakhrutdinov[140], S. Falciano[70a], P.J. Falke[5], S. Falke[5], J. Faltova[139], Y. Fang[15a], M. Fanti[66a,66b], A. Farbin[8], A. Farilla[72a], E.M. Farina[68a,68b], T. Farooque[104], S. Farrell[18], S.M. Farrington[175], P. Farthouat[35], F. Fassi[34e], P. Fassnacht[35], D. Fassouliotis[9], M. Faucci Giannelli[48], A. Favareto[53b,53a], W.J. Fawcett[52], L. Fayard[128], O.L. Fedin[134,o], W. Fedorko[172], M. Feickert[41], S. Feigl[130], L. Feligioni[99], C. Feng[58b], E.J. Feng[35], M. Feng[47], M.J. Fenton[55], A.B. Fenyuk[140], L. Feremenga[8], J. Ferrando[44], A. Ferrari[169], P. Ferrari[118], R. Ferrari[68a], D.E. Ferreira de Lima[59b], A. Ferrer[171], D. Ferrere[52], C. Ferretti[103], F. Fiedler[97], A. Filipčič[89], F. Filthaut[117], K.D. Finelli[25], M.C.N. Fiolhais[136a,136c,a], L. Fiorini[171], C. Fischer[14], W.C. Fisher[104], N. Flaschel[44], I. Fleck[148], P. Fleischmann[103], R.R.M. Fletcher[133], T. Flick[179], B.M. Flierl[112], L.M. Flores[133], L.R. Flores Castillo[61a], N. Fomin[17], G.T. Forcolin[98], A. Formica[142], F.A. Förster[14], A.C. Forti[98], A.G. Foster[21], D. Fournier[128], H. Fox[87], S. Fracchia[146], P. Francavilla[69a,69b], M. Franchini[23b,23a], S. Franchino[59a], D. Francis[35], L. Franconi[130], M. Franklin[57], M. Frate[168], M. Fraternali[68a,68b], D. Freeborn[92], S.M. Fressard-Batraneanu[35], B. Freund[107], W.S. Freund[78b], D. Froidevaux[35], J.A. Frost[131], C. Fukunaga[161], E. Fullana Torregrosa[171], T. Fusayasu[114], J. Fuster[171], O. Gabizon[157], A. Gabrielli[23b,23a], A. Gabrielli[18], G.P. Gach[81a], S. Gadatsch[52], P. Gadow[113],

G. Gagliardi[53b,53a], L.G. Gagnon[107], C. Galea[27b], B. Galhardo[136a,136c], E.J. Gallas[131], B.J. Gallop[141], P. Gallus[138], G. Galster[39], R. Gamboa Goni[90], K.K. Gan[122], S. Ganguly[177], J. Gao[58a], Y. Gao[88], Y.S. Gao[150,l], C. García[171], J.E. García Navarro[171], J.A. García Pascual[15a], M. Garcia-Sciveres[18], R.W. Gardner[36], N. Garelli[150], V. Garonne[130], K. Gasnikova[44], A. Gaudiello[53b,53a], G. Gaudio[68a], I.L. Gavrilenko[108], A. Gavrilyuk[109], C. Gay[172], G. Gaycken[24], E.N. Gazis[10], C.N.P. Gee[141], J. Geisen[51], M. Geisen[97], M.P. Geisler[59a], K. Gellerstedt[43a,43b], C. Gemme[53b], M.H. Genest[56], C. Geng[103], S. Gentile[70a,70b], S. George[91], D. Gerbaudo[14], G. Gessner[45], S. Ghasemi[148], M. Ghasemi Bostanabad[173], M. Ghneimat[24], B. Giacobbe[23b], S. Giagu[70a,70b], N. Giangiacomi[23b,23a], P. Giannetti[69a], A. Giannini[67a,67b], S.M. Gibson[91], M. Gignac[143], D. Gillberg[33], G. Gilles[179], D.M. Gingrich[3,as], M.P. Giordani[64a,64c], F.M. Giorgi[23b], P.F. Giraud[142], P. Giromini[57], G. Giugliarelli[64a,64c], D. Giugni[66a], F. Giuli[131], M. Giulini[59b], S. Gkaitatzis[159], I. Gkialas[9,i], E.L. Gkougkousis[14], P. Gkountoumis[10], L.K. Gladilin[111], C. Glasman[96], J. Glatzer[14], P.C.F. Glaysher[44], A. Glazov[44], M. Goblirsch-Kolb[26], J. Godlewski[82], S. Goldfarb[102], T. Golling[52], D. Golubkov[140], A. Gomes[136a,136b,136d], R. Goncalves Gama[78a], R. Gonçalo[136a], G. Gonella[50], L. Gonella[21], A. Gongadze[77], F. Gonnella[21], J.L. Gonski[57], S. González de la Hoz[171], S. Gonzalez-Sevilla[52], L. Goossens[35], P.A. Gorbounov[109], H.A. Gordon[29], B. Gorini[35], E. Gorini[65a,65b], A. Gorišek[89], A.T. Goshaw[47], C. Gössling[45], M.I. Gostkin[77], C.A. Gottardo[24], C.R. Goudet[128], D. Goujdami[34c], A.G. Goussiou[145], N. Govender[32b,b], C. Goy[5], E. Gozani[157], I. Grabowska-Bold[81a], P.O.J. Gradin[169], E.C. Graham[88], J. Gramling[168], E. Gramstad[130], S. Grancagnolo[19], V. Gratchev[134], P.M. Gravila[27f], F.G. Gravili[65a,65b], C. Gray[55], H.M. Gray[18], Z.D. Greenwood[93,ai], C. Grefe[24], K. Gregersen[92], I.M. Gregor[44], P. Grenier[150], K. Grevtsov[44], J. Griffiths[8], A.A. Grillo[143], K. Grimm[150], S. Grinstein[14,y], Ph. Gris[37], J.-F. Grivaz[128], S. Groh[97], E. Gross[177], J. Grosse-Knetter[51], G.C. Grossi[93], Z.J. Grout[92], C. Grud[103], A. Grummer[116], L. Guan[103], W. Guan[178], J. Guenther[35], A. Guerguichon[128], F. Guescini[165a], D. Guest[168], R. Gugel[50], B. Gui[122], T. Guillemin[5], S. Guindon[35], U. Gul[55], C. Gumpert[35], J. Guo[58c], W. Guo[103], Y. Guo[58a,r], Z. Guo[99], R. Gupta[41], S. Gurbuz[12c], G. Gustavino[124], B.J. Gutelman[157], P. Gutierrez[124], C. Gutschow[92], C. Guyot[142], M.P. Guzik[81a], C. Gwenlan[131], C.B. Gwilliam[88], A. Haas[121], C. Haber[18], H.K. Hadavand[8], N. Haddad[34e], A. Hadef[58a], S. Hageböck[24], M. Hagihara[166], H. Hakobyan[181,*], M. Haleem[174], J. Haley[125], G. Halladjian[104], G.D. Hallewell[99], K. Hamacher[179], P. Hamal[126], K. Hamano[173], A. Hamilton[32a], G.N. Hamity[146], K. Han[58a,ah], L. Han[58a], S. Han[15d], K. Hanagaki[79,u], M. Hance[143], D.M. Handl[112], B. Haney[133], R. Hankache[132], P. Hanke[59a], E. Hansen[94], J.B. Hansen[39], J.D. Hansen[39], M.C. Hansen[24], P.H. Hansen[39], K. Hara[166], A.S. Hard[178], T. Harenberg[179], S. Harkusha[105], P.F. Harrison[175], N.M. Hartmann[112], Y. Hasegawa[147], A. Hasib[48], S. Hassani[142], S. Haug[20], R. Hauser[104], L. Hauswald[46], L.B. Havener[38], M. Havranek[138], C.M. Hawkes[21], R.J. Hawkings[35], D. Hayden[104], C. Hayes[152], C.P. Hays[131], J.M. Hays[90], H.S. Hayward[88], S.J. Haywood[141], M.P. Heath[48], V. Hedberg[94], L. Heelan[8], S. Heer[24], K.K. Heidegger[50], J. Heilman[33], S. Heim[44], T. Heim[18], B. Heinemann[44,an], J.J. Heinrich[112], L. Heinrich[121], C. Heinz[54], J. Hejbal[137], L. Helary[35], A. Held[172], S. Hellesund[130], S. Hellman[43a,43b], C. Helsens[35], R.C.W. Henderson[87], Y. Heng[178], S. Henkelmann[172], A.M. Henriques Correia[35], G.H. Herbert[19], H. Herde[26], V. Herget[174], Y. Hernández Jiménez[32c], H. Herr[97], M.G. Herrmann[112], G. Herten[50], R. Hertenberger[112], L. Hervas[35], T.C. Herwig[133], G.G. Hesketh[92], N.P. Hessey[165a], J.W. Hetherly[41], S. Higashino[79], E. Higón-Rodriguez[171], K. Hildebrand[36], E. Hill[173], J.C. Hill[31], K.K. Hill[29], K.H. Hiller[44], S.J. Hillier[21], M. Hils[46], I. Hinchliffe[18], M. Hirose[129], D. Hirschbuehl[179], B. Hiti[89], O. Hladik[137], D.R. Hlaluku[32c], X. Hoad[48], J. Hobbs[152], N. Hod[165a], M.C. Hodgkinson[146], A. Hoecker[35], M.R. Hoeferkamp[116], F. Hoenig[112], D. Hohn[24], D. Hohov[128], T.R. Holmes[36], M. Holzbock[112], M. Homann[45], S. Honda[166], T. Honda[79], T.M. Hong[135], A. Hönle[113], B.H. Hooberman[170], W.H. Hopkins[127], Y. Horii[115], P. Horn[46], A.J. Horton[149], L.A. Horyn[36], J-Y. Hostachy[56], A. Hostiuc[145], S. Hou[155], A. Hoummada[34a], J. Howarth[98], J. Hoya[86], M. Hrabovsky[126], J. Hrdinka[35], I. Hristova[19], J. Hrivnac[128], A. Hrynevich[106],

T. Hryn'ova[5], P.J. Hsu[62], S.-C. Hsu[145], Q. Hu[29], S. Hu[58c], Y. Huang[15a], Z. Hubacek[138], F. Hubaut[99], M. Huebner[24], F. Huegging[24], T.B. Huffman[131], E.W. Hughes[38], M. Huhtinen[35], R.F.H. Hunter[33], P. Huo[152], A.M. Hupe[33], N. Huseynov[77,ae], J. Huston[104], J. Huth[57], R. Hyneman[103], G. Iacobucci[52], G. Iakovidis[29], I. Ibragimov[148], L. Iconomidou-Fayard[128], Z. Idrissi[34e], P. Iengo[35], R. Ignazzi[39], O. Igonkina[118,aa], R. Iguchi[160], T. Iizawa[52], Y. Ikegami[79], M. Ikeno[79], D. Iliadis[159], N. Ilic[150], F. Iltzsche[46], G. Introzzi[68a,68b], M. Iodice[72a], K. Iordanidou[38], V. Ippolito[70a,70b], M.F. Isacson[169], N. Ishijima[129], M. Ishino[160], M. Ishitsuka[162], W. Islam[125], C. Issever[131], S. Istin[12c,am], F. Ito[166], J.M. Iturbe Ponce[61a], R. Iuppa[73a,73b], A. Ivina[177], H. Iwasaki[79], J.M. Izen[42], V. Izzo[67a], P. Jacka[137], P. Jackson[1], R.M. Jacobs[24], V. Jain[2], G. Jäkel[179], K.B. Jakobi[97], K. Jakobs[50], S. Jakobsen[74], T. Jakoubek[137], D.O. Jamin[125], D.K. Jana[93], R. Jansky[52], J. Janssen[24], M. Janus[51], P.A. Janus[81a], G. Jarlskog[94], N. Javadov[77,ae], T. Javůrek[50], M. Javurkova[50], F. Jeanneau[142], L. Jeanty[18], J. Jejelava[156a,af], A. Jelinskas[175], P. Jenni[50,c], J. Jeong[44], S. Jézéquel[5], H. Ji[178], J. Jia[152], H. Jiang[76], Y. Jiang[58a], Z. Jiang[150,p], S. Jiggins[50], F.A. Jimenez Morales[37], J. Jimenez Pena[171], S. Jin[15c], A. Jinaru[27b], O. Jinnouchi[162], H. Jivan[32c], P. Johansson[146], K.A. Johns[7], C.A. Johnson[63], W.J. Johnson[145], K. Jon-And[43a,43b], R.W.L. Jones[87], S.D. Jones[153], S. Jones[7], T.J. Jones[88], J. Jongmanns[59a], P.M. Jorge[136a,136b], J. Jovicevic[165a], X. Ju[178], J.J. Junggeburth[113], A. Juste Rozas[14,y], A. Kaczmarska[82], M. Kado[128], H. Kagan[122], M. Kagan[150], T. Kaji[176], E. Kajomovitz[157], C.W. Kalderon[94], A. Kaluza[97], S. Kama[41], A. Kamenshchikov[140], L. Kanjir[89], Y. Kano[160], V.A. Kantserov[110], J. Kanzaki[79], B. Kaplan[121], L.S. Kaplan[178], D. Kar[32c], M.J. Kareem[165b], E. Karentzos[10], S.N. Karpov[77], Z.M. Karpova[77], V. Kartvelishvili[87], A.N. Karyukhin[140], K. Kasahara[166], L. Kashif[178], R.D. Kass[122], A. Kastanas[151], Y. Kataoka[160], C. Kato[160], J. Katzy[44], K. Kawade[80], K. Kawagoe[85], T. Kawamoto[160], G. Kawamura[51], E.F. Kay[88], V.F. Kazanin[120b,120a], R. Keeler[173], R. Kehoe[41], J.S. Keller[33], E. Kellermann[94], J.J. Kempster[21], J. Kendrick[21], O. Kepka[137], S. Kersten[179], B.P. Kerševan[89], R.A. Keyes[101], M. Khader[170], F. Khalil-Zada[13], A. Khanov[125], A.G. Kharlamov[120b,120a], T. Kharlamova[120b,120a], A. Khodinov[163], T.J. Khoo[52], E. Khramov[77], J. Khubua[156b], S. Kido[80], M. Kiehn[52], C.R. Kilby[91], S.H. Kim[166], Y.K. Kim[36], N. Kimura[64a,64c], O.M. Kind[19], B.T. King[88], D. Kirchmeier[46], J. Kirk[141], A.E. Kiryunin[113], T. Kishimoto[160], D. Kisielewska[81a], V. Kitali[44], O. Kivernyk[5], E. Kladiva[28b], T. Klapdor-Kleingrothaus[50], M.H. Klein[103], M. Klein[88], U. Klein[88], K. Kleinknecht[97], P. Klimek[119], A. Klimentov[29], R. Klingenberg[45,*], T. Klingl[24], T. Klioutchnikova[35], F.F. Klitzner[112], P. Kluit[118], S. Kluth[113], E. Kneringer[74], E.B.F.G. Knoops[99], A. Knue[50], A. Kobayashi[160], D. Kobayashi[85], T. Kobayashi[160], M. Kobel[46], M. Kocian[150], P. Kodys[139], T. Koffas[33], E. Koffeman[118], N.M. Köhler[113], T. Koi[150], M. Kolb[59b], I. Koletsou[5], T. Kondo[79], N. Kondrashova[58c], K. Köneke[50], A.C. König[117], T. Kono[79], R. Konoplich[121,aj], V. Konstantinides[92], N. Konstantinidis[92], B. Konya[94], R. Kopeliansky[63], S. Koperny[81a], K. Korcyl[82], K. Kordas[159], A. Korn[92], I. Korolkov[14], E.V. Korolkova[146], O. Kortner[113], S. Kortner[113], T. Kosek[139], V.V. Kostyukhin[24], A. Kotwal[47], A. Koulouris[10], A. Kourkoumeli-Charalampidi[68a,68b], C. Kourkoumelis[9], E. Kourlitis[146], V. Kouskoura[29], A.B. Kowalewska[82], R. Kowalewski[173], T.Z. Kowalski[81a], C. Kozakai[160], W. Kozanecki[142], A.S. Kozhin[140], V.A. Kramarenko[111], G. Kramberger[89], D. Krasnopevtsev[110], M.W. Krasny[132], A. Krasznahorkay[35], D. Krauss[113], J.A. Kremer[81a], J. Kretzschmar[88], P. Krieger[164], K. Krizka[18], K. Kroeninger[45], H. Kroha[113], J. Kroll[137], J. Kroll[133], J. Krstic[16], U. Kruchonak[77], H. Krüger[24], N. Krumnack[76], M.C. Kruse[47], T. Kubota[102], S. Kuday[4b], J.T. Kuechler[179], S. Kuehn[35], A. Kugel[59a], F. Kuger[174], T. Kuhl[44], V. Kukhtin[77], R. Kukla[99], Y. Kulchitsky[105], S. Kuleshov[144b], Y.P. Kulinich[170], M. Kuna[56], T. Kunigo[83], A. Kupco[137], T. Kupfer[45], O. Kuprash[158], H. Kurashige[80], L.L. Kurchaninov[165a], Y.A. Kurochkin[105], M.G. Kurth[15d], E.S. Kuwertz[173], M. Kuze[162], J. Kvita[126], T. Kwan[101], A. La Rosa[113], J.L. La Rosa Navarro[78d], L. La Rotonda[40b,40a], F. La Ruffa[40b,40a], C. Lacasta[171], F. Lacava[70a,70b], J. Lacey[44], D.P.J. Lack[98], H. Lacker[19], D. Lacour[132], E. Ladygin[77], R. Lafaye[5], B. Laforge[132], T. Lagouri[32c], S. Lai[51], S. Lammers[63], W. Lampl[7], E. Lançon[29],

U. Landgraf[50], M.P.J. Landon[90], M.C. Lanfermann[52], V.S. Lang[44], J.C. Lange[14], R.J. Langenberg[35], A.J. Lankford[168], F. Lanni[29], K. Lantzsch[24], A. Lanza[68a], A. Lapertosa[53b,53a], S. Laplace[132], J.F. Laporte[142], T. Lari[66a], F. Lasagni Manghi[23b,23a], M. Lassnig[35], T.S. Lau[61a], A. Laudrain[128], M. Lavorgna[67a,67b], A.T. Law[143], P. Laycock[88], M. Lazzaroni[66a,66b], B. Le[102], O. Le Dortz[132], E. Le Guirriec[99], E.P. Le Quilleuc[142], M. LeBlanc[7], T. LeCompte[6], F. Ledroit-Guillon[56], C.A. Lee[29], G.R. Lee[144a], L. Lee[57], S.C. Lee[155], B. Lefebvre[101], M. Lefebvre[173], F. Legger[112], C. Leggett[18], N. Lehmann[179], G. Lehmann Miotto[35], W.A. Leight[44], A. Leisos[159,v], M.A.L. Leite[78d], R. Leitner[139], D. Lellouch[177], B. Lemmer[51], K.J.C. Leney[92], T. Lenz[24], B. Lenzi[35], R. Leone[7], S. Leone[69a], C. Leonidopoulos[48], G. Lerner[153], C. Leroy[107], R. Les[164], A.A.J. Lesage[142], C.G. Lester[31], M. Levchenko[134], J. Levêque[5], D. Levin[103], L.J. Levinson[177], D. Lewis[90], B. Li[103], C-Q. Li[58a], H. Li[58b], L. Li[58c], Q. Li[15d], Q.Y. Li[58a], S. Li[58d,58c], X. Li[58c], Y. Li[148], Z. Liang[15a], B. Liberti[71a], A. Liblong[164], K. Lie[61c], S. Liem[118], A. Limosani[154], C.Y. Lin[31], K. Lin[104], T.H. Lin[97], R.A. Linck[63], B.E. Lindquist[152], A.L. Lionti[52], E. Lipeles[133], A. Lipniacka[17], M. Lisovyi[59b], T.M. Liss[170,ap], A. Lister[172], A.M. Litke[143], J.D. Little[8], B. Liu[76], B.L Liu[6], H.B. Liu[29], H. Liu[103], J.B. Liu[58a], J.K.K. Liu[131], K. Liu[132], M. Liu[58a], P. Liu[18], Y. Liu[15a], Y.L. Liu[58a], Y.W. Liu[58a], M. Livan[68a,68b], A. Lleres[56], J. Llorente Merino[15a], S.L. Lloyd[90], C.Y. Lo[61b], F. Lo Sterzo[41], E.M. Lobodzinska[44], P. Loch[7], A. Loesle[50], K.M. Loew[26], T. Lohse[19], K. Lohwasser[146], M. Lokajicek[137], B.A. Long[25], J.D. Long[170], R.E. Long[87], L. Longo[65a,65b], K.A. Looper[122], J.A. Lopez[144b], I. Lopez Paz[14], A. Lopez Solis[146], J. Lorenz[112], N. Lorenzo Martinez[5], M. Losada[22], P.J. Lösel[112], X. Lou[44], X. Lou[15a], A. Lounis[128], J. Love[6], P.A. Love[87], J.J. Lozano Bahilo[171], H. Lu[61a], M. Lu[58a], N. Lu[103], Y.J. Lu[62], H.J. Lubatti[145], C. Luci[70a,70b], A. Lucotte[56], C. Luedtke[50], F. Luehring[63], I. Luise[132], W. Lukas[74], L. Luminari[70a], B. Lund-Jensen[151], M.S. Lutz[100], P.M. Luzi[132], D. Lynn[29], R. Lysak[137], E. Lytken[94], F. Lyu[15a], V. Lyubushkin[77], H. Ma[29], L.L. Ma[58b], Y. Ma[58b], G. Maccarrone[49], A. Macchiolo[113], C.M. Macdonald[146], J. Machado Miguens[133,136b], D. Madaffari[171], R. Madar[37], W.F. Mader[46], A. Madsen[44], N. Madysa[46], J. Maeda[80], K. Maekawa[160], S. Maeland[17], T. Maeno[29], A.S. Maevskiy[111], V. Magerl[50], C. Maidantchik[78b], T. Maier[112], A. Maio[136a,136b,136d], O. Majersky[28a], S. Majewski[127], Y. Makida[79], N. Makovec[128], B. Malaescu[132], Pa. Malecki[82], V.P. Maleev[134], F. Malek[56], U. Mallik[75], D. Malon[6], C. Malone[31], S. Maltezos[10], S. Malyukov[35], J. Mamuzic[171], G. Mancini[49], I. Mandić[89], J. Maneira[136a], L. Manhaes de Andrade Filho[78a], J. Manjarres Ramos[46], K.H. Mankinen[94], A. Mann[112], A. Manousos[74], B. Mansoulie[142], J.D. Mansour[15a], M. Mantoani[51], S. Manzoni[66a,66b], G. Marceca[30], L. March[52], L. Marchese[131], G. Marchiori[132], M. Marcisovsky[137], C.A. Marin Tobon[35], M. Marjanovic[37], D.E. Marley[103], F. Marroquim[78b], Z. Marshall[18], M.U.F Martensson[169], S. Marti-Garcia[171], C.B. Martin[122], T.A. Martin[175], V.J. Martin[48], B. Martin dit Latour[17], M. Martinez[14,y], V.I. Martinez Outschoorn[100], S. Martin-Haugh[141], V.S. Martoiu[27b], A.C. Martyniuk[92], A. Marzin[35], L. Masetti[97], T. Mashimo[160], R. Mashinistov[108], J. Masik[98], A.L. Maslennikov[120b,120a], L.H. Mason[102], L. Massa[71a,71b], P. Massarotti[67a,67b], P. Mastrandrea[5], A. Mastroberardino[40b,40a], T. Masubuchi[160], P. Mättig[179], J. Maurer[27b], B. Maček[89], S.J. Maxfield[88], D.A. Maximov[120b,120a], R. Mazini[155], I. Maznas[159], S.M. Mazza[143], N.C. Mc Fadden[116], G. Mc Goldrick[164], S.P. Mc Kee[103], A. McCarn[103], T.G. McCarthy[113], L.I. McClymont[92], E.F. McDonald[102], J.A. Mcfayden[35], G. Mchedlidze[51], M.A. McKay[41], K.D. McLean[173], S.J. McMahon[141], P.C. McNamara[102], C.J. McNicol[175], R.A. McPherson[173,ac], J.E. Mdhluli[32c], Z.A. Meadows[100], S. Meehan[145], T.M. Megy[50], S. Mehlhase[112], A. Mehta[88], T. Meideck[56], B. Meirose[42], D. Melini[171,g], B.R. Mellado Garcia[32c], J.D. Mellenthin[51], M. Melo[28a], F. Meloni[44], A. Melzer[24], S.B. Menary[98], E.D. Mendes Gouveia[136a], L. Meng[88], X.T. Meng[103], A. Mengarelli[23b,23a], S. Menke[113], E. Meoni[40b,40a], S. Mergelmeyer[19], C. Merlassino[20], P. Mermod[52], L. Merola[67a,67b], C. Meroni[66a], F.S. Merritt[36], A. Messina[70a,70b], J. Metcalfe[6], A.S. Mete[168], C. Meyer[133], J. Meyer[157], J-P. Meyer[142], H. Meyer Zu Theenhausen[59a], F. Miano[153], R.P. Middleton[141], L. Mijović[48], G. Mikenberg[177], M. Mikestikova[137], M. Mikuž[89], M. Milesi[102],

A. Milic[164], D.A. Millar[90], D.W. Miller[36], A. Milov[177], D.A. Milstead[43a,43b], A.A. Minaenko[140], M. Miñano Moya[171], I.A. Minashvili[156b], A.I. Mincer[121], B. Mindur[81a], M. Mineev[77], Y. Minegishi[160], Y. Ming[178], L.M. Mir[14], A. Mirto[65a,65b], K.P. Mistry[133], T. Mitani[176], J. Mitrevski[112], V.A. Mitsou[171], A. Miucci[20], P.S. Miyagawa[146], A. Mizukami[79], J.U. Mjörnmark[94], T. Mkrtchyan[181], M. Mlynarikova[139], T. Moa[43a,43b], K. Mochizuki[107], P. Mogg[50], S. Mohapatra[38], S. Molander[43a,43b], R. Moles-Valls[24], M.C. Mondragon[104], K. Mönig[44], J. Monk[39], E. Monnier[99], A. Montalbano[149], J. Montejo Berlingen[35], F. Monticelli[86], S. Monzani[66a], R.W. Moore[3], N. Morange[128], D. Moreno[22], M. Moreno Llácer[35], P. Morettini[53b], M. Morgenstern[118], S. Morgenstern[46], D. Mori[149], T. Mori[160], M. Morii[57], M. Morinaga[176], V. Morisbak[130], A.K. Morley[35], G. Mornacchi[35], A.P. Morris[92], J.D. Morris[90], L. Morvaj[152], P. Moschovakos[10], M. Mosidze[156b], H.J. Moss[146], J. Moss[150,m], K. Motohashi[162], R. Mount[150], E. Mountricha[35], E.J.W. Moyse[100], S. Muanza[99], F. Mueller[113], J. Mueller[135], R.S.P. Mueller[112], D. Muenstermann[87], P. Mullen[55], G.A. Mullier[20], F.J. Munoz Sanchez[98], P. Murin[28b], W.J. Murray[175,141], A. Murrone[66a,66b], M. Muškinja[89], C. Mwewa[32a], A.G. Myagkov[140,ak], J. Myers[127], M. Myska[138], B.P. Nachman[18], O. Nackenhorst[45], K. Nagai[131], K. Nagano[79], Y. Nagasaka[60], K. Nagata[166], M. Nagel[50], E. Nagy[99], A.M. Nairz[35], Y. Nakahama[115], K. Nakamura[79], T. Nakamura[160], I. Nakano[123], H. Nanjo[129], F. Napolitano[59a], R.F. Naranjo Garcia[44], R. Narayan[11], D.I. Narrias Villar[59a], I. Naryshkin[134], T. Naumann[44], G. Navarro[22], R. Nayyar[7], H.A. Neal[103], P.Y. Nechaeva[108], T.J. Neep[142], A. Negri[68a,68b], M. Negrini[23b], S. Nektarijevic[117], C. Nellist[51], M.E. Nelson[131], S. Nemecek[137], P. Nemethy[121], M. Nessi[35,e], M.S. Neubauer[170], M. Neumann[179], P.R. Newman[21], T.Y. Ng[61c], Y.S. Ng[19], H.D.N. Nguyen[99], T. Nguyen Manh[107], E. Nibigira[37], R.B. Nickerson[131], R. Nicolaidou[142], J. Nielsen[143], N. Nikiforou[11], V. Nikolaenko[140,ak], I. Nikolic-Audit[132], K. Nikolopoulos[21], P. Nilsson[29], Y. Ninomiya[79], A. Nisati[70a], N. Nishu[58c], R. Nisius[113], I. Nitsche[45], T. Nitta[176], T. Nobe[160], Y. Noguchi[83], M. Nomachi[129], I. Nomidis[132], M.A. Nomura[29], T. Nooney[90], M. Nordberg[35], N. Norjoharuddeen[131], T. Novak[89], O. Novgorodova[46], R. Novotny[138], L. Nozka[126], K. Ntekas[168], E. Nurse[92], F. Nuti[102], F.G. Oakham[33,as], H. Oberlack[113], T. Obermann[24], J. Ocariz[132], A. Ochi[80], I. Ochoa[38], J.P. Ochoa-Ricoux[144a], K. O'Connor[26], S. Oda[85], S. Odaka[79], S. Oerdek[51], A. Oh[98], S.H. Oh[47], C.C. Ohm[151], H. Oide[53b,53a], H. Okawa[166], Y. Okazaki[83], Y. Okumura[160], T. Okuyama[79], A. Olariu[27b], L.F. Oleiro Seabra[136a], S.A. Olivares Pino[144a], D. Oliveira Damazio[29], J.L. Oliver[1], M.J.R. Olsson[36], A. Olszewski[82], J. Olszowska[82], D.C. O'Neil[149], A. Onofre[136a,136e], K. Onogi[115], P.U.E. Onyisi[11], H. Oppen[130], M.J. Oreglia[36], Y. Oren[158], D. Orestano[72a,72b], E.C. Orgill[98], N. Orlando[61b], A.A. O'Rourke[44], R.S. Orr[164], B. Osculati[53b,53a,*], V. O'Shea[55], R. Ospanov[58a], G. Otero y Garzon[30], H. Otono[85], M. Ouchrif[34d], F. Ould-Saada[130], A. Ouraou[142], Q. Ouyang[15a], M. Owen[55], R.E. Owen[21], V.E. Ozcan[12c], N. Ozturk[8], J. Pacalt[126], H.A. Pacey[31], K. Pachal[149], A. Pacheco Pages[14], L. Pacheco Rodriguez[142], C. Padilla Aranda[14], S. Pagan Griso[18], M. Paganini[180], G. Palacino[63], S. Palazzo[40b,40a], S. Palestini[35], M. Palka[81b], D. Pallin[37], I. Panagoulias[10], C.E. Pandini[35], J.G. Panduro Vazquez[91], P. Pani[35], G. Panizzo[64a,64c], L. Paolozzi[52], T.D. Papadopoulou[10], K. Papageorgiou[9,i], A. Paramonov[6], D. Paredes Hernandez[61b], S.R. Paredes Saenz[131], B. Parida[58c], A.J. Parker[87], K.A. Parker[44], M.A. Parker[31], F. Parodi[53b,53a], J.A. Parsons[38], U. Parzefall[50], V.R. Pascuzzi[164], J.M.P. Pasner[143], E. Pasqualucci[70a], S. Passaggio[53b], F. Pastore[91], P. Pasuwan[43a,43b], S. Pataraia[97], J.R. Pater[98], A. Pathak[178,j], T. Pauly[35], B. Pearson[113], M. Pedersen[130], L. Pedraza Diaz[117], R. Pedro[136a,136b], S.V. Peleganchuk[120b,120a], O. Penc[137], C. Peng[15d], H. Peng[58a], B.S. Peralva[78a], M.M. Perego[142], A.P. Pereira Peixoto[136a], D.V. Perepelitsa[29], F. Peri[19], L. Perini[66a,66b], H. Pernegger[35], S. Perrella[67a,67b], V.D. Peshekhonov[77,*], K. Peters[44], R.F.Y. Peters[98], B.A. Petersen[35], T.C. Petersen[39], E. Petit[56], A. Petridis[1], C. Petridou[159], P. Petroff[128], E. Petrolo[70a], M. Petrov[131], F. Petrucci[72a,72b], M. Pettee[180], N.E. Pettersson[100], A. Peyaud[142], R. Pezoa[144b], T. Pham[102], F.H. Phillips[104], P.W. Phillips[141], G. Piacquadio[152], E. Pianori[18], A. Picazio[100], M.A. Pickering[131], R. Piegaia[30], J.E. Pilcher[36], A.D. Pilkington[98], M. Pinamonti[71a,71b], J.L. Pinfold[3], M. Pitt[177], M-A. Pleier[29],

V. Pleskot[139], E. Plotnikova[77], D. Pluth[76], P. Podberezko[120b,120a], R. Poettgen[94], R. Poggi[52], L. Poggioli[128], I. Pogrebnyak[104], D. Pohl[24], I. Pokharel[51], G. Polesello[68a], A. Poley[44], A. Policicchio[70a,70b], R. Polifka[35], A. Polini[23b], C.S. Pollard[44], V. Polychronakos[29], D. Ponomarenko[110], L. Pontecorvo[70a], G.A. Popeneciu[27d], D.M. Portillo Quintero[132], S. Pospisil[138], K. Potamianos[44], I.N. Potrap[77], C.J. Potter[31], H. Potti[11], T. Poulsen[94], J. Poveda[35], T.D. Powell[146], M.E. Pozo Astigarraga[35], P. Pralavorio[99], S. Prell[76], D. Price[98], M. Primavera[65a], S. Prince[101], N. Proklova[110], K. Prokofiev[61c], F. Prokoshin[144b], S. Protopopescu[29], J. Proudfoot[6], M. Przybycien[81a], A. Puri[170], P. Puzo[128], J. Qian[103], Y. Qin[98], A. Quadt[51], M. Queitsch-Maitland[44], A. Qureshi[1], P. Rados[102], F. Ragusa[66a,66b], G. Rahal[95], J.A. Raine[98], S. Rajagopalan[29], A. Ramirez Morales[90], T. Rashid[128], S. Raspopov[5], M.G. Ratti[66a,66b], D.M. Rauch[44], F. Rauscher[112], S. Rave[97], B. Ravina[146], I. Ravinovich[177], J.H. Rawling[98], M. Raymond[35], A.L. Read[130], N.P. Readioff[56], M. Reale[65a,65b], D.M. Rebuzzi[68a,68b], A. Redelbach[174], G. Redlinger[29], R. Reece[143], R.G. Reed[32c], K. Reeves[42], L. Rehnisch[19], J. Reichert[133], A. Reiss[97], C. Rembser[35], H. Ren[15d], M. Rescigno[70a], S. Resconi[66a], E.D. Resseguie[133], S. Rettie[172], E. Reynolds[21], O.L. Rezanova[120b,120a], P. Reznicek[139], E. Ricci[73a,73b], R. Richter[113], S. Richter[92], E. Richter-Was[81b], O. Ricken[24], M. Ridel[132], P. Rieck[113], C.J. Riegel[179], O. Rifki[44], M. Rijssenbeek[152], A. Rimoldi[68a,68b], M. Rimoldi[20], L. Rinaldi[23b], G. Ripellino[151], B. Ristić[87], E. Ritsch[35], I. Riu[14], J.C. Rivera Vergara[144a], F. Rizatdinova[125], E. Rizvi[90], C. Rizzi[14], R.T. Roberts[98], S.H. Robertson[101,ac], A. Robichaud-Veronneau[101], D. Robinson[31], J.E.M. Robinson[44], A. Robson[55], E. Rocco[97], C. Roda[69a,69b], Y. Rodina[99], S. Rodriguez Bosca[171], A. Rodriguez Perez[14], D. Rodriguez Rodriguez[171], A.M. Rodríguez Vera[165b], S. Roe[35], C.S. Rogan[57], O. Røhne[130], R. Röhrig[113], C.P.A. Roland[63], J. Roloff[57], A. Romaniouk[110], M. Romano[23b,23a], N. Rompotis[88], M. Ronzani[121], L. Roos[132], S. Rosati[70a], K. Rosbach[50], P. Rose[143], N-A. Rosien[51], E. Rossi[44], E. Rossi[67a,67b], L.P. Rossi[53b], L. Rossini[66a,66b], J.H.N. Rosten[31], R. Rosten[14], M. Rotaru[27b], J. Rothberg[145], D. Rousseau[128], D. Roy[32c], A. Rozanov[99], Y. Rozen[157], X. Ruan[32c], F. Rubbo[150], F. Rühr[50], A. Ruiz-Martinez[171], Z. Rurikova[50], N.A. Rusakovich[77], H.L. Russell[101], J.P. Rutherfoord[7], E.M. Rüttinger[44,k], Y.F. Ryabov[134], M. Rybar[170], G. Rybkin[128], S. Ryu[6], A. Ryzhov[140], G.F. Rzehorz[51], P. Sabatini[51], G. Sabato[118], S. Sacerdoti[128], H.F-W. Sadrozinski[143], R. Sadykov[77], F. Safai Tehrani[70a], P. Saha[119], M. Sahinsoy[59a], A. Sahu[179], M. Saimpert[44], M. Saito[160], T. Saito[160], H. Sakamoto[160], A. Sakharov[121,aj], D. Salamani[52], G. Salamanna[72a,72b], J.E. Salazar Loyola[144b], D. Salek[118], P.H. Sales De Bruin[169], D. Salihagic[113], A. Salnikov[150], J. Salt[171], D. Salvatore[40b,40a], F. Salvatore[153], A. Salvucci[61a,61b,61c], A. Salzburger[35], J. Samarati[35], D. Sammel[50], D. Sampsonidis[159], D. Sampsonidou[159], J. Sánchez[171], A. Sanchez Pineda[64a,64c], H. Sandaker[130], C.O. Sander[44], M. Sandhoff[179], C. Sandoval[22], D.P.C. Sankey[141], M. Sannino[53b,53a], Y. Sano[115], A. Sansoni[49], C. Santoni[37], H. Santos[136a], I. Santoyo Castillo[153], A. Sapronov[77], J.G. Saraiva[136a,136d], O. Sasaki[79], K. Sato[166], E. Sauvan[5], P. Savard[164,as], N. Savic[113], R. Sawada[160], C. Sawyer[141], L. Sawyer[93,ai], C. Sbarra[23b], A. Sbrizzi[23b,23a], T. Scanlon[92], J. Schaarschmidt[145], P. Schacht[113], B.M. Schachtner[112], D. Schaefer[36], L. Schaefer[133], J. Schaeffer[97], S. Schaepe[35], U. Schäfer[97], A.C. Schaffer[128], D. Schaile[112], R.D. Schamberger[152], N. Scharmberg[98], V.A. Schegelsky[134], D. Scheirich[139], F. Schenck[19], M. Schernau[168], C. Schiavi[53b,53a], S. Schier[143], L.K. Schildgen[24], Z.M. Schillaci[26], E.J. Schioppa[35], M. Schioppa[40b,40a], K.E. Schleicher[50], S. Schlenker[35], K.R. Schmidt-Sommerfeld[113], K. Schmieden[35], C. Schmitt[97], S. Schmitt[44], S. Schmitz[97], U. Schnoor[50], L. Schoeffel[142], A. Schoening[59b], E. Schopf[24], M. Schott[97], J.F.P. Schouwenberg[117], J. Schovancova[35], S. Schramm[52], A. Schulte[97], H-C. Schultz-Coulon[59a], M. Schumacher[50], B.A. Schumm[143], Ph. Schune[142], A. Schwartzman[150], T.A. Schwarz[103], H. Schweiger[98], Ph. Schwemling[142], R. Schwienhorst[104], A. Sciandra[24], G. Sciolla[26], M. Scornajenghi[40b,40a], F. Scuri[69a], F. Scutti[102], L.M. Scyboz[113], J. Searcy[103], C.D. Sebastiani[70a,70b], P. Seema[24], S.C. Seidel[116], A. Seiden[143], T. Seiss[36], J.M. Seixas[78b], G. Sekhniaidze[67a], K. Sekhon[103], S.J. Sekula[41], N. Semprini-Cesari[23b,23a], S. Sen[47], S. Senkin[37], C. Serfon[130], L. Serin[128], L. Serkin[64a,64b],

M. Sessa[72a,72b], H. Severini[124], F. Sforza[167], A. Sfyrla[52], E. Shabalina[51], J.D. Shahinian[143], N.W. Shaikh[43a,43b], L.Y. Shan[15a], R. Shang[170], J.T. Shank[25], M. Shapiro[18], A.S. Sharma[1], A. Sharma[131], P.B. Shatalov[109], K. Shaw[153], S.M. Shaw[98], A. Shcherbakova[134], Y. Shen[124], N. Sherafati[33], A.D. Sherman[25], P. Sherwood[92], L. Shi[155,ao], S. Shimizu[80], C.O. Shimmin[180], M. Shimojima[114], I.P.J. Shipsey[131], S. Shirabe[85], M. Shiyakova[77], J. Shlomi[177], A. Shmeleva[108], D. Shoaleh Saadi[107], M.J. Shochet[36], S. Shojaii[102], D.R. Shope[124], S. Shrestha[122], E. Shulga[110], P. Sicho[137], A.M. Sickles[170], P.E. Sidebo[151], E. Sideras Haddad[32c], O. Sidiropoulou[174], A. Sidoti[23b,23a], F. Siegert[46], Dj. Sijacki[16], J. Silva[136a], M. Silva Jr.[178], M.V. Silva Oliveira[78a], S.B. Silverstein[43a], L. Simic[77], S. Simion[128], E. Simioni[97], M. Simon[97], R. Simoniello[97], P. Sinervo[164], N.B. Sinev[127], M. Sioli[23b,23a], G. Siragusa[174], I. Siral[103], S.Yu. Sivoklokov[111], J. Sjölin[43a,43b], M.B. Skinner[87], P. Skubic[124], M. Slater[21], T. Slavicek[138], M. Slawinska[82], K. Sliwa[167], R. Slovak[139], V. Smakhtin[177], B.H. Smart[5], J. Smiesko[28a], N. Smirnov[110], S.Yu. Smirnov[110], Y. Smirnov[110], L.N. Smirnova[111], O. Smirnova[94], J.W. Smith[51], M.N.K. Smith[38], R.W. Smith[38], M. Smizanska[87], K. Smolek[138], A. Smykiewicz[82], A.A. Snesarev[108], I.M. Snyder[127], S. Snyder[29], R. Sobie[173,ac], A.M. Soffa[168], A. Soffer[158], A. Søgaard[48], D.A. Soh[155], G. Sokhrannyi[89], C.A. Solans Sanchez[35], M. Solar[138], E.Yu. Soldatov[110], U. Soldevila[171], A.A. Solodkov[140], A. Soloshenko[77], O.V. Solovyanov[140], V. Solovyev[134], P. Sommer[146], H. Son[167], W. Song[141], A. Sopczak[138], F. Sopkova[28b], D. Sosa[59b], C.L. Sotiropoulou[69a,69b], S. Sottocornola[68a,68b], R. Soualah[64a,64c,h], A.M. Soukharev[120b,120a], D. South[44], B.C. Sowden[91], S. Spagnolo[65a,65b], M. Spalla[113], M. Spangenberg[175], F. Spanò[91], D. Sperlich[19], F. Spettel[113], T.M. Spieker[59a], R. Spighi[23b], G. Spigo[35], L.A. Spiller[102], D.P. Spiteri[55], M. Spousta[139], A. Stabile[66a,66b], R. Stamen[59a], S. Stamm[19], E. Stanecka[82], R.W. Stanek[6], C. Stanescu[72a], B. Stanislaus[131], M.M. Stanitzki[44], B. Stapf[118], S. Stapnes[130], E.A. Starchenko[140], G.H. Stark[36], J. Stark[56], S.H Stark[39], P. Staroba[137], P. Starovoitov[59a], S. Stärz[35], R. Staszewski[82], M. Stegler[44], P. Steinberg[29], B. Stelzer[149], H.J. Stelzer[35], O. Stelzer-Chilton[165a], H. Stenzel[54], T.J. Stevenson[90], G.A. Stewart[55], M.C. Stockton[127], G. Stoicea[27b], P. Stolte[51], S. Stonjek[113], A. Straessner[46], J. Strandberg[151], S. Strandberg[43a,43b], M. Strauss[124], P. Strizenec[28b], R. Ströhmer[174], D.M. Strom[127], R. Stroynowski[41], A. Strubig[48], S.A. Stucci[29], B. Stugu[17], J. Stupak[124], N.A. Styles[44], D. Su[150], J. Su[135], S. Suchek[59a], Y. Sugaya[129], M. Suk[138], V.V. Sulin[108], D.M.S. Sultan[52], S. Sultansoy[4c], T. Sumida[83], S. Sun[103], X. Sun[3], K. Suruliz[153], C.J.E. Suster[154], M.R. Sutton[153], S. Suzuki[79], M. Svatos[137], M. Swiatlowski[36], S.P. Swift[2], A. Sydorenko[97], I. Sykora[28a], T. Sykora[139], D. Ta[97], K. Tackmann[44,z], J. Taenzer[158], A. Taffard[168], R. Tafirout[165a], E. Tahirovic[90], N. Taiblum[158], H. Takai[29], R. Takashima[84], E.H. Takasugi[113], K. Takeda[80], T. Takeshita[147], Y. Takubo[79], M. Talby[99], A.A. Talyshev[120b,120a], J. Tanaka[160], M. Tanaka[162], R. Tanaka[128], R. Tanioka[80], B.B. Tannenwald[122], S. Tapia Araya[144b], S. Tapprogge[97], A. Tarek Abouelfadl Mohamed[132], S. Tarem[157], G. Tarna[27b,d], G.F. Tartarelli[66a], P. Tas[139], M. Tasevsky[137], T. Tashiro[83], E. Tassi[40b,40a], A. Tavares Delgado[136a,136b], Y. Tayalati[34e], A.C. Taylor[116], A.J. Taylor[48], G.N. Taylor[102], P.T.E. Taylor[102], W. Taylor[165b], A.S. Tee[87], P. Teixeira-Dias[91], H. Ten Kate[35], P.K. Teng[155], J.J. Teoh[118], F. Tepel[179], S. Terada[79], K. Terashi[160], J. Terron[96], S. Terzo[14], M. Testa[49], R.J. Teuscher[164,ac], S.J. Thais[180], T. Theveneaux-Pelzer[44], F. Thiele[39], D.W. Thomas[91], J.P. Thomas[21], A.S. Thompson[55], P.D. Thompson[21], L.A. Thomsen[180], E. Thomson[133], Y. Tian[38], R.E. Ticse Torres[51], V.O. Tikhomirov[108,al], Yu.A. Tikhonov[120b,120a], S. Timoshenko[110], P. Tipton[180], S. Tisserant[99], K. Todome[162], S. Todorova-Nova[5], S. Todt[46], J. Tojo[85], S. Tokár[28a], K. Tokushuku[79], E. Tolley[122], K.G. Tomiwa[32c], M. Tomoto[115], L. Tompkins[150,p], K. Toms[116], B. Tong[57], P. Tornambe[50], E. Torrence[127], H. Torres[46], E. Torró Pastor[145], C. Tosciri[131], J. Toth[99,ab], F. Touchard[99], D.R. Tovey[146], C.J. Treado[121], T. Trefzger[174], F. Tresoldi[153], A. Tricoli[29], I.M. Trigger[165a], S. Trincaz-Duvoid[132], M.F. Tripiana[14], W. Trischuk[164], B. Trocmé[56], A. Trofymov[128], C. Troncon[66a], M. Trovatelli[173], F. Trovato[153], L. Truong[32b], M. Trzebinski[82], A. Trzupek[82], F. Tsai[44], J.C-L. Tseng[131], P.V. Tsiareshka[105], N. Tsirintanis[9], V. Tsiskaridze[152], E.G. Tskhadadze[156a], I.I. Tsukerman[109],

V. Tsulaia[18], S. Tsuno[79], D. Tsybychev[152], Y. Tu[61b], A. Tudorache[27b], V. Tudorache[27b], T.T. Tulbure[27a], A.N. Tuna[57], S. Turchikhin[77], D. Turgeman[177], I. Turk Cakir[4b,t], R. Turra[66a], P.M. Tuts[38], E. Tzovara[97], G. Ucchielli[23b,23a], I. Ueda[79], M. Ughetto[43a,43b], F. Ukegawa[166], G. Unal[35], A. Undrus[29], G. Unel[168], F.C. Ungaro[102], Y. Unno[79], K. Uno[160], J. Urban[28b], P. Urquijo[102], P. Urrejola[97], G. Usai[8], J. Usui[79], L. Vacavant[99], V. Vacek[138], B. Vachon[101], K.O.H. Vadla[130], A. Vaidya[92], C. Valderanis[112], E. Valdes Santurio[43a,43b], M. Valente[52], S. Valentinetti[23b,23a], A. Valero[171], L. Valéry[44], R.A. Vallance[21], A. Vallier[5], J.A. Valls Ferrer[171], T.R. Van Daalen[14], W. Van Den Wollenberg[118], H. Van der Graaf[118], P. Van Gemmeren[6], J. Van Nieuwkoop[149], I. Van Vulpen[118], M. Vanadia[71a,71b], W. Vandelli[35], A. Vaniachine[163], P. Vankov[118], R. Vari[70a], E.W. Varnes[7], C. Varni[53b,53a], T. Varol[41], D. Varouchas[128], K.E. Varvell[154], G.A. Vasquez[144b], J.G. Vasquez[180], F. Vazeille[37], D. Vazquez Furelos[14], T. Vazquez Schroeder[101], J. Veatch[51], V. Vecchio[72a,72b], L.M. Veloce[164], F. Veloso[136a,136c], S. Veneziano[70a], A. Ventura[65a,65b], M. Venturi[173], N. Venturi[35], V. Vercesi[68a], M. Verducci[72a,72b], C.M. Vergel Infante[76], W. Verkerke[118], A.T. Vermeulen[118], J.C. Vermeulen[118], M.C. Vetterli[149,as], N. Viaux Maira[144b], M. Vicente Barreto Pinto[52], I. Vichou[170,*], T. Vickey[146], O.E. Vickey Boeriu[146], G.H.A. Viehhauser[131], S. Viel[18], L. Vigani[131], M. Villa[23b,23a], M. Villaplana Perez[66a,66b], E. Vilucchi[49], M.G. Vincter[33], V.B. Vinogradov[77], A. Vishwakarma[44], C. Vittori[23b,23a], I. Vivarelli[153], S. Vlachos[10], M. Vogel[179], P. Vokac[138], G. Volpi[14], S.E. von Buddenbrock[32c], E. Von Toerne[24], V. Vorobel[139], K. Vorobev[110], M. Vos[171], J.H. Vossebeld[88], N. Vranjes[16], M. Vranjes Milosavljevic[16], V. Vrba[138], M. Vreeswijk[118], T. Šfiligoj[89], R. Vuillermet[35], I. Vukotic[36], T. Ženiš[28a], L. Živković[16], P. Wagner[24], W. Wagner[179], J. Wagner-Kuhr[112], H. Wahlberg[86], S. Wahrmund[46], K. Wakamiya[80], V.M. Walbrecht[113], J. Walder[87], R. Walker[112], S.D. Walker[91], W. Walkowiak[148], V. Wallangen[43a,43b], A.M. Wang[57], C. Wang[58b,d], F. Wang[178], H. Wang[18], H. Wang[3], J. Wang[154], J. Wang[59b], P. Wang[41], Q. Wang[124], R.-J. Wang[132], R. Wang[58a], R. Wang[6], S.M. Wang[155], W.T. Wang[58a], W. Wang[15c,ad], W.X. Wang[58a,ad], Y. Wang[58a], Z. Wang[58c], C. Wanotayaroj[44], A. Warburton[101], C.P. Ward[31], D.R. Wardrope[92], A. Washbrook[48], P.M. Watkins[21], A.T. Watson[21], M.F. Watson[21], G. Watts[145], S. Watts[98], B.M. Waugh[92], A.F. Webb[11], S. Webb[97], C. Weber[180], M.S. Weber[20], S.A. Weber[33], S.M. Weber[59a], A.R. Weidberg[131], B. Weinert[63], J. Weingarten[51], M. Weirich[97], C. Weiser[50], P.S. Wells[35], T. Wenaus[29], T. Wengler[35], S. Wenig[35], N. Wermes[24], M.D. Werner[76], P. Werner[35], M. Wessels[59a], T.D. Weston[20], K. Whalen[127], N.L. Whallon[145], A.M. Wharton[87], A.S. White[103], A. White[8], M.J. White[1], R. White[144b], D. Whiteson[168], B.W. Whitmore[87], F.J. Wickens[141], W. Wiedenmann[178], M. Wielers[141], C. Wiglesworth[39], L.A.M. Wiik-Fuchs[50], A. Wildauer[113], F. Wilk[98], H.G. Wilkens[35], L.J. Wilkins[91], H.H. Williams[133], S. Williams[31], C. Willis[104], S. Willocq[100], J.A. Wilson[21], I. Wingerter-Seez[5], E. Winkels[153], F. Winklmeier[127], O.J. Winston[153], B.T. Winter[24], M. Wittgen[150], M. Wobisch[93], A. Wolf[97], T.M.H. Wolf[118], R. Wolff[99], M.W. Wolter[82], H. Wolters[136a,136c], V.W.S. Wong[172], N.L. Woods[143], S.D. Worm[21], B.K. Wosiek[82], K.W. Woźniak[82], K. Wraight[55], M. Wu[36], S.L. Wu[178], X. Wu[52], Y. Wu[58a], T.R. Wyatt[98], B.M. Wynne[48], S. Xella[39], Z. Xi[103], L. Xia[175], D. Xu[15a], H. Xu[58a], L. Xu[29], T. Xu[142], W. Xu[103], B. Yabsley[154], S. Yacoob[32a], K. Yajima[129], D.P. Yallup[92], D. Yamaguchi[162], Y. Yamaguchi[162], A. Yamamoto[79], T. Yamanaka[160], F. Yamane[80], M. Yamatani[160], T. Yamazaki[160], Y. Yamazaki[80], Z. Yan[25], H.J. Yang[58c,58d], H.T. Yang[18], S. Yang[75], X. Yang[58b], Y. Yang[160], Z. Yang[17], W-M. Yao[18], Y.C. Yap[44], Y. Yasu[79], E. Yatsenko[58c,58d], J. Ye[41], S. Ye[29], I. Yeletskikh[77], E. Yigitbasi[25], E. Yildirim[97], K. Yorita[176], K. Yoshihara[133], C.J.S. Young[35], C. Young[150], J. Yu[8], J. Yu[76], X. Yue[59a], S.P.Y. Yuen[24], B. Zabinski[82], G. Zacharis[10], E. Zaffaroni[52], R. Zaidan[14], A.M. Zaitsev[140,ak], N. Zakharchuk[44], J. Zalieckas[17], S. Zambito[57], D. Zanzi[35], D.R. Zaripovas[55], S.V. Zeißner[45], C. Zeitnitz[179], G. Zemaityte[131], J.C. Zeng[170], Q. Zeng[150], O. Zenin[140], D. Zerwas[128], M. Zgubič[131], D.F. Zhang[58b], D. Zhang[103], F. Zhang[178], G. Zhang[58a], H. Zhang[15c], J. Zhang[6], L. Zhang[15c], L. Zhang[58a], M. Zhang[170], P. Zhang[15c], R. Zhang[58a], R. Zhang[24], X. Zhang[58b], Y. Zhang[15d], Z. Zhang[128], P. Zhao[47], X. Zhao[41], Y. Zhao[58b,128,ah], Z. Zhao[58a], A. Zhemchugov[77], B. Zhou[103], C. Zhou[178],

L. Zhou[41], M.S. Zhou[15d], M. Zhou[152], N. Zhou[58c], Y. Zhou[7], C.G. Zhu[58b], H.L. Zhu[58a], H. Zhu[15a], J. Zhu[103], Y. Zhu[58a], X. Zhuang[15a], K. Zhukov[108], V. Zhulanov[120b,120a], A. Zibell[174], D. Zieminska[63], N.I. Zimine[77], S. Zimmermann[50], Z. Zinonos[113], M. Zinser[97], M. Ziolkowski[148], G. Zobernig[178], A. Zoccoli[23b,23a], K. Zoch[51], T.G. Zorbas[146], R. Zou[36], M. Zur Nedden[19], L. Zwalinski[35].

[1]Department of Physics, University of Adelaide, Adelaide; Australia.
[2]Physics Department, SUNY Albany, Albany NY; United States of America.
[3]Department of Physics, University of Alberta, Edmonton AB; Canada.
[4(a)]Department of Physics, Ankara University, Ankara;[(b)]Istanbul Aydin University, Istanbul;[(c)]Division of Physics, TOBB University of Economics and Technology, Ankara; Turkey.
[5]LAPP, Université Grenoble Alpes, Université Savoie Mont Blanc, CNRS/IN2P3, Annecy; France.
[6]High Energy Physics Division, Argonne National Laboratory, Argonne IL; United States of America.
[7]Department of Physics, University of Arizona, Tucson AZ; United States of America.
[8]Department of Physics, University of Texas at Arlington, Arlington TX; United States of America.
[9]Physics Department, National and Kapodistrian University of Athens, Athens; Greece.
[10]Physics Department, National Technical University of Athens, Zografou; Greece.
[11]Department of Physics, University of Texas at Austin, Austin TX; United States of America.
[12(a)]Bahcesehir University, Faculty of Engineering and Natural Sciences, Istanbul;[(b)]Istanbul Bilgi University, Faculty of Engineering and Natural Sciences, Istanbul;[(c)]Department of Physics, Bogazici University, Istanbul;[(d)]Department of Physics Engineering, Gaziantep University, Gaziantep; Turkey.
[13]Institute of Physics, Azerbaijan Academy of Sciences, Baku; Azerbaijan.
[14]Institut de Física d'Altes Energies (IFAE), Barcelona Institute of Science and Technology, Barcelona; Spain.
[15(a)]Institute of High Energy Physics, Chinese Academy of Sciences, Beijing;[(b)]Physics Department, Tsinghua University, Beijing;[(c)]Department of Physics, Nanjing University, Nanjing;[(d)]University of Chinese Academy of Science (UCAS), Beijing; China.
[16]Institute of Physics, University of Belgrade, Belgrade; Serbia.
[17]Department for Physics and Technology, University of Bergen, Bergen; Norway.
[18]Physics Division, Lawrence Berkeley National Laboratory and University of California, Berkeley CA; United States of America.
[19]Institut für Physik, Humboldt Universität zu Berlin, Berlin; Germany.
[20]Albert Einstein Center for Fundamental Physics and Laboratory for High Energy Physics, University of Bern, Bern; Switzerland.
[21]School of Physics and Astronomy, University of Birmingham, Birmingham; United Kingdom.
[22]Centro de Investigaciónes, Universidad Antonio Nariño, Bogota; Colombia.
[23(a)]Dipartimento di Fisica e Astronomia, Università di Bologna, Bologna;[(b)]INFN Sezione di Bologna; Italy.
[24]Physikalisches Institut, Universität Bonn, Bonn; Germany.
[25]Department of Physics, Boston University, Boston MA; United States of America.
[26]Department of Physics, Brandeis University, Waltham MA; United States of America.
[27(a)]Transilvania University of Brasov, Brasov;[(b)]Horia Hulubei National Institute of Physics and Nuclear Engineering, Bucharest;[(c)]Department of Physics, Alexandru Ioan Cuza University of Iasi, Iasi;[(d)]National Institute for Research and Development of Isotopic and Molecular Technologies, Physics Department, Cluj-Napoca;[(e)]University Politehnica Bucharest, Bucharest;[(f)]West University in Timisoara, Timisoara; Romania.
[28(a)]Faculty of Mathematics, Physics and Informatics, Comenius University, Bratislava;[(b)]Department of Subnuclear Physics, Institute of Experimental Physics of the Slovak Academy of Sciences, Kosice;

Slovak Republic.
[29]Physics Department, Brookhaven National Laboratory, Upton NY; United States of America.
[30]Departamento de Física, Universidad de Buenos Aires, Buenos Aires; Argentina.
[31]Cavendish Laboratory, University of Cambridge, Cambridge; United Kingdom.
[32(a)]Department of Physics, University of Cape Town, Cape Town;[(b)]Department of Mechanical Engineering Science, University of Johannesburg, Johannesburg;[(c)]School of Physics, University of the Witwatersrand, Johannesburg; South Africa.
[33]Department of Physics, Carleton University, Ottawa ON; Canada.
[34(a)]Faculté des Sciences Ain Chock, Réseau Universitaire de Physique des Hautes Energies - Université Hassan II, Casablanca;[(b)]Centre National de l'Energie des Sciences Techniques Nucleaires (CNESTEN), Rabat;[(c)]Faculté des Sciences Semlalia, Université Cadi Ayyad, LPHEA-Marrakech;[(d)]Faculté des Sciences, Université Mohamed Premier and LPTPM, Oujda;[(e)]Faculté des sciences, Université Mohammed V, Rabat; Morocco.
[35]CERN, Geneva; Switzerland.
[36]Enrico Fermi Institute, University of Chicago, Chicago IL; United States of America.
[37]LPC, Université Clermont Auvergne, CNRS/IN2P3, Clermont-Ferrand; France.
[38]Nevis Laboratory, Columbia University, Irvington NY; United States of America.
[39]Niels Bohr Institute, University of Copenhagen, Copenhagen; Denmark.
[40(a)]Dipartimento di Fisica, Università della Calabria, Rende;[(b)]INFN Gruppo Collegato di Cosenza, Laboratori Nazionali di Frascati; Italy.
[41]Physics Department, Southern Methodist University, Dallas TX; United States of America.
[42]Physics Department, University of Texas at Dallas, Richardson TX; United States of America.
[43(a)]Department of Physics, Stockholm University;[(b)]Oskar Klein Centre, Stockholm; Sweden.
[44]Deutsches Elektronen-Synchrotron DESY, Hamburg and Zeuthen; Germany.
[45]Lehrstuhl für Experimentelle Physik IV, Technische Universität Dortmund, Dortmund; Germany.
[46]Institut für Kern- und Teilchenphysik, Technische Universität Dresden, Dresden; Germany.
[47]Department of Physics, Duke University, Durham NC; United States of America.
[48]SUPA - School of Physics and Astronomy, University of Edinburgh, Edinburgh; United Kingdom.
[49]INFN e Laboratori Nazionali di Frascati, Frascati; Italy.
[50]Physikalisches Institut, Albert-Ludwigs-Universität Freiburg, Freiburg; Germany.
[51]II. Physikalisches Institut, Georg-August-Universität Göttingen, Göttingen; Germany.
[52]Département de Physique Nucléaire et Corpusculaire, Université de Genève, Genève; Switzerland.
[53(a)]Dipartimento di Fisica, Università di Genova, Genova;[(b)]INFN Sezione di Genova; Italy.
[54]II. Physikalisches Institut, Justus-Liebig-Universität Giessen, Giessen; Germany.
[55]SUPA - School of Physics and Astronomy, University of Glasgow, Glasgow; United Kingdom.
[56]LPSC, Université Grenoble Alpes, CNRS/IN2P3, Grenoble INP, Grenoble; France.
[57]Laboratory for Particle Physics and Cosmology, Harvard University, Cambridge MA; United States of America.
[58(a)]Department of Modern Physics and State Key Laboratory of Particle Detection and Electronics, University of Science and Technology of China, Hefei;[(b)]Institute of Frontier and Interdisciplinary Science and Key Laboratory of Particle Physics and Particle Irradiation (MOE), Shandong University, Qingdao;[(c)]School of Physics and Astronomy, Shanghai Jiao Tong University, KLPPAC-MoE, SKLPPC, Shanghai;[(d)]Tsung-Dao Lee Institute, Shanghai; China.
[59(a)]Kirchhoff-Institut für Physik, Ruprecht-Karls-Universität Heidelberg, Heidelberg;[(b)]Physikalisches Institut, Ruprecht-Karls-Universität Heidelberg, Heidelberg; Germany.
[60]Faculty of Applied Information Science, Hiroshima Institute of Technology, Hiroshima; Japan.
[61(a)]Department of Physics, Chinese University of Hong Kong, Shatin, N.T., Hong Kong;[(b)]Department

of Physics, University of Hong Kong, Hong Kong;[(c)]Department of Physics and Institute for Advanced Study, Hong Kong University of Science and Technology, Clear Water Bay, Kowloon, Hong Kong; China.
[62]Department of Physics, National Tsing Hua University, Hsinchu; Taiwan.
[63]Department of Physics, Indiana University, Bloomington IN; United States of America.
[64(a)]INFN Gruppo Collegato di Udine, Sezione di Trieste, Udine;[(b)]ICTP, Trieste;[(c)]Dipartimento di Chimica, Fisica e Ambiente, Università di Udine, Udine; Italy.
[65(a)]INFN Sezione di Lecce;[(b)]Dipartimento di Matematica e Fisica, Università del Salento, Lecce; Italy.
[66(a)]INFN Sezione di Milano;[(b)]Dipartimento di Fisica, Università di Milano, Milano; Italy.
[67(a)]INFN Sezione di Napoli;[(b)]Dipartimento di Fisica, Università di Napoli, Napoli; Italy.
[68(a)]INFN Sezione di Pavia;[(b)]Dipartimento di Fisica, Università di Pavia, Pavia; Italy.
[69(a)]INFN Sezione di Pisa;[(b)]Dipartimento di Fisica E. Fermi, Università di Pisa, Pisa; Italy.
[70(a)]INFN Sezione di Roma;[(b)]Dipartimento di Fisica, Sapienza Università di Roma, Roma; Italy.
[71(a)]INFN Sezione di Roma Tor Vergata;[(b)]Dipartimento di Fisica, Università di Roma Tor Vergata, Roma; Italy.
[72(a)]INFN Sezione di Roma Tre;[(b)]Dipartimento di Matematica e Fisica, Università Roma Tre, Roma; Italy.
[73(a)]INFN-TIFPA;[(b)]Università degli Studi di Trento, Trento; Italy.
[74]Institut für Astro- und Teilchenphysik, Leopold-Franzens-Universität, Innsbruck; Austria.
[75]University of Iowa, Iowa City IA; United States of America.
[76]Department of Physics and Astronomy, Iowa State University, Ames IA; United States of America.
[77]Joint Institute for Nuclear Research, Dubna; Russia.
[78(a)]Departamento de Engenharia Elétrica, Universidade Federal de Juiz de Fora (UFJF), Juiz de Fora;[(b)]Universidade Federal do Rio De Janeiro COPPE/EE/IF, Rio de Janeiro;[(c)]Universidade Federal de São João del Rei (UFSJ), São João del Rei;[(d)]Instituto de Física, Universidade de São Paulo, São Paulo; Brazil.
[79]KEK, High Energy Accelerator Research Organization, Tsukuba; Japan.
[80]Graduate School of Science, Kobe University, Kobe; Japan.
[81(a)]AGH University of Science and Technology, Faculty of Physics and Applied Computer Science, Krakow;[(b)]Marian Smoluchowski Institute of Physics, Jagiellonian University, Krakow; Poland.
[82]Institute of Nuclear Physics Polish Academy of Sciences, Krakow; Poland.
[83]Faculty of Science, Kyoto University, Kyoto; Japan.
[84]Kyoto University of Education, Kyoto; Japan.
[85]Research Center for Advanced Particle Physics and Department of Physics, Kyushu University, Fukuoka ; Japan.
[86]Instituto de Física La Plata, Universidad Nacional de La Plata and CONICET, La Plata; Argentina.
[87]Physics Department, Lancaster University, Lancaster; United Kingdom.
[88]Oliver Lodge Laboratory, University of Liverpool, Liverpool; United Kingdom.
[89]Department of Experimental Particle Physics, Jožef Stefan Institute and Department of Physics, University of Ljubljana, Ljubljana; Slovenia.
[90]School of Physics and Astronomy, Queen Mary University of London, London; United Kingdom.
[91]Department of Physics, Royal Holloway University of London, Egham; United Kingdom.
[92]Department of Physics and Astronomy, University College London, London; United Kingdom.
[93]Louisiana Tech University, Ruston LA; United States of America.
[94]Fysiska institutionen, Lunds universitet, Lund; Sweden.
[95]Centre de Calcul de l'Institut National de Physique Nucléaire et de Physique des Particules (IN2P3), Villeurbanne; France.

[96]Departamento de Física Teorica C-15 and CIAFF, Universidad Autónoma de Madrid, Madrid; Spain.
[97]Institut für Physik, Universität Mainz, Mainz; Germany.
[98]School of Physics and Astronomy, University of Manchester, Manchester; United Kingdom.
[99]CPPM, Aix-Marseille Université, CNRS/IN2P3, Marseille; France.
[100]Department of Physics, University of Massachusetts, Amherst MA; United States of America.
[101]Department of Physics, McGill University, Montreal QC; Canada.
[102]School of Physics, University of Melbourne, Victoria; Australia.
[103]Department of Physics, University of Michigan, Ann Arbor MI; United States of America.
[104]Department of Physics and Astronomy, Michigan State University, East Lansing MI; United States of America.
[105]B.I. Stepanov Institute of Physics, National Academy of Sciences of Belarus, Minsk; Belarus.
[106]Research Institute for Nuclear Problems of Byelorussian State University, Minsk; Belarus.
[107]Group of Particle Physics, University of Montreal, Montreal QC; Canada.
[108]P.N. Lebedev Physical Institute of the Russian Academy of Sciences, Moscow; Russia.
[109]Institute for Theoretical and Experimental Physics (ITEP), Moscow; Russia.
[110]National Research Nuclear University MEPhI, Moscow; Russia.
[111]D.V. Skobeltsyn Institute of Nuclear Physics, M.V. Lomonosov Moscow State University, Moscow; Russia.
[112]Fakultät für Physik, Ludwig-Maximilians-Universität München, München; Germany.
[113]Max-Planck-Institut für Physik (Werner-Heisenberg-Institut), München; Germany.
[114]Nagasaki Institute of Applied Science, Nagasaki; Japan.
[115]Graduate School of Science and Kobayashi-Maskawa Institute, Nagoya University, Nagoya; Japan.
[116]Department of Physics and Astronomy, University of New Mexico, Albuquerque NM; United States of America.
[117]Institute for Mathematics, Astrophysics and Particle Physics, Radboud University Nijmegen/Nikhef, Nijmegen; Netherlands.
[118]Nikhef National Institute for Subatomic Physics and University of Amsterdam, Amsterdam; Netherlands.
[119]Department of Physics, Northern Illinois University, DeKalb IL; United States of America.
[120(a)]Budker Institute of Nuclear Physics, SB RAS, Novosibirsk;[(b)]Novosibirsk State University Novosibirsk; Russia.
[121]Department of Physics, New York University, New York NY; United States of America.
[122]Ohio State University, Columbus OH; United States of America.
[123]Faculty of Science, Okayama University, Okayama; Japan.
[124]Homer L. Dodge Department of Physics and Astronomy, University of Oklahoma, Norman OK; United States of America.
[125]Department of Physics, Oklahoma State University, Stillwater OK; United States of America.
[126]Palacký University, RCPTM, Joint Laboratory of Optics, Olomouc; Czech Republic.
[127]Center for High Energy Physics, University of Oregon, Eugene OR; United States of America.
[128]LAL, Université Paris-Sud, CNRS/IN2P3, Université Paris-Saclay, Orsay; France.
[129]Graduate School of Science, Osaka University, Osaka; Japan.
[130]Department of Physics, University of Oslo, Oslo; Norway.
[131]Department of Physics, Oxford University, Oxford; United Kingdom.
[132]LPNHE, Sorbonne Université, Paris Diderot Sorbonne Paris Cité, CNRS/IN2P3, Paris; France.
[133]Department of Physics, University of Pennsylvania, Philadelphia PA; United States of America.
[134]Konstantinov Nuclear Physics Institute of National Research Centre "Kurchatov Institute", PNPI, St. Petersburg; Russia.

[135]Department of Physics and Astronomy, University of Pittsburgh, Pittsburgh PA; United States of America.
[136(a)]Laboratório de Instrumentação e Física Experimental de Partículas - LIP;[(b)]Departamento de Física, Faculdade de Ciências, Universidade de Lisboa, Lisboa;[(c)]Departamento de Física, Universidade de Coimbra, Coimbra;[(d)]Centro de Física Nuclear da Universidade de Lisboa, Lisboa;[(e)]Departamento de Física, Universidade do Minho, Braga;[(f)]Departamento de Física Teorica y del Cosmos, Universidad de Granada, Granada (Spain);[(g)]Dep Física and CEFITEC of Faculdade de Ciências e Tecnologia, Universidade Nova de Lisboa, Caparica; Portugal.
[137]Institute of Physics, Academy of Sciences of the Czech Republic, Prague; Czech Republic.
[138]Czech Technical University in Prague, Prague; Czech Republic.
[139]Charles University, Faculty of Mathematics and Physics, Prague; Czech Republic.
[140]State Research Center Institute for High Energy Physics, NRC KI, Protvino; Russia.
[141]Particle Physics Department, Rutherford Appleton Laboratory, Didcot; United Kingdom.
[142]IRFU, CEA, Université Paris-Saclay, Gif-sur-Yvette; France.
[143]Santa Cruz Institute for Particle Physics, University of California Santa Cruz, Santa Cruz CA; United States of America.
[144(a)]Departamento de Física, Pontificia Universidad Católica de Chile, Santiago;[(b)]Departamento de Física, Universidad Técnica Federico Santa María, Valparaíso; Chile.
[145]Department of Physics, University of Washington, Seattle WA; United States of America.
[146]Department of Physics and Astronomy, University of Sheffield, Sheffield; United Kingdom.
[147]Department of Physics, Shinshu University, Nagano; Japan.
[148]Department Physik, Universität Siegen, Siegen; Germany.
[149]Department of Physics, Simon Fraser University, Burnaby BC; Canada.
[150]SLAC National Accelerator Laboratory, Stanford CA; United States of America.
[151]Physics Department, Royal Institute of Technology, Stockholm; Sweden.
[152]Departments of Physics and Astronomy, Stony Brook University, Stony Brook NY; United States of America.
[153]Department of Physics and Astronomy, University of Sussex, Brighton; United Kingdom.
[154]School of Physics, University of Sydney, Sydney; Australia.
[155]Institute of Physics, Academia Sinica, Taipei; Taiwan.
[156(a)]E. Andronikashvili Institute of Physics, Iv. Javakhishvili Tbilisi State University, Tbilisi;[(b)]High Energy Physics Institute, Tbilisi State University, Tbilisi; Georgia.
[157]Department of Physics, Technion, Israel Institute of Technology, Haifa; Israel.
[158]Raymond and Beverly Sackler School of Physics and Astronomy, Tel Aviv University, Tel Aviv; Israel.
[159]Department of Physics, Aristotle University of Thessaloniki, Thessaloniki; Greece.
[160]International Center for Elementary Particle Physics and Department of Physics, University of Tokyo, Tokyo; Japan.
[161]Graduate School of Science and Technology, Tokyo Metropolitan University, Tokyo; Japan.
[162]Department of Physics, Tokyo Institute of Technology, Tokyo; Japan.
[163]Tomsk State University, Tomsk; Russia.
[164]Department of Physics, University of Toronto, Toronto ON; Canada.
[165(a)]TRIUMF, Vancouver BC;[(b)]Department of Physics and Astronomy, York University, Toronto ON; Canada.
[166]Division of Physics and Tomonaga Center for the History of the Universe, Faculty of Pure and Applied Sciences, University of Tsukuba, Tsukuba; Japan.
[167]Department of Physics and Astronomy, Tufts University, Medford MA; United States of America.
[168]Department of Physics and Astronomy, University of California Irvine, Irvine CA; United States of

America.
[169]Department of Physics and Astronomy, University of Uppsala, Uppsala; Sweden.
[170]Department of Physics, University of Illinois, Urbana IL; United States of America.
[171]Instituto de Física Corpuscular (IFIC), Centro Mixto Universidad de Valencia - CSIC, Valencia; Spain.
[172]Department of Physics, University of British Columbia, Vancouver BC; Canada.
[173]Department of Physics and Astronomy, University of Victoria, Victoria BC; Canada.
[174]Fakultät für Physik und Astronomie, Julius-Maximilians-Universität Würzburg, Würzburg; Germany.
[175]Department of Physics, University of Warwick, Coventry; United Kingdom.
[176]Waseda University, Tokyo; Japan.
[177]Department of Particle Physics, Weizmann Institute of Science, Rehovot; Israel.
[178]Department of Physics, University of Wisconsin, Madison WI; United States of America.
[179]Fakultät für Mathematik und Naturwissenschaften, Fachgruppe Physik, Bergische Universität Wuppertal, Wuppertal; Germany.
[180]Department of Physics, Yale University, New Haven CT; United States of America.
[181]Yerevan Physics Institute, Yerevan; Armenia.
[a] Also at Borough of Manhattan Community College, City University of New York, NY; United States of America.
[b] Also at Centre for High Performance Computing, CSIR Campus, Rosebank, Cape Town; South Africa.
[c] Also at CERN, Geneva; Switzerland.
[d] Also at CPPM, Aix-Marseille Université, CNRS/IN2P3, Marseille; France.
[e] Also at Département de Physique Nucléaire et Corpusculaire, Université de Genève, Genève; Switzerland.
[f] Also at Departament de Fisica de la Universitat Autonoma de Barcelona, Barcelona; Spain.
[g] Also at Departamento de Física Teorica y del Cosmos, Universidad de Granada, Granada (Spain); Spain.
[h] Also at Department of Applied Physics and Astronomy, University of Sharjah, Sharjah; United Arab Emirates.
[i] Also at Department of Financial and Management Engineering, University of the Aegean, Chios; Greece.
[j] Also at Department of Physics and Astronomy, University of Louisville, Louisville, KY; United States of America.
[k] Also at Department of Physics and Astronomy, University of Sheffield, Sheffield; United Kingdom.
[l] Also at Department of Physics, California State University, Fresno CA; United States of America.
[m] Also at Department of Physics, California State University, Sacramento CA; United States of America.
[n] Also at Department of Physics, King's College London, London; United Kingdom.
[o] Also at Department of Physics, St. Petersburg State Polytechnical University, St. Petersburg; Russia.
[p] Also at Department of Physics, Stanford University; United States of America.
[q] Also at Department of Physics, University of Fribourg, Fribourg; Switzerland.
[r] Also at Department of Physics, University of Michigan, Ann Arbor MI; United States of America.
[s] Also at Dipartimento di Fisica E. Fermi, Università di Pisa, Pisa; Italy.
[t] Also at Giresun University, Faculty of Engineering, Giresun; Turkey.
[u] Also at Graduate School of Science, Osaka University, Osaka; Japan.
[v] Also at Hellenic Open University, Patras; Greece.
[w] Also at Horia Hulubei National Institute of Physics and Nuclear Engineering, Bucharest; Romania.
[x] Also at II. Physikalisches Institut, Georg-August-Universität Göttingen, Göttingen; Germany.
[y] Also at Institucio Catalana de Recerca i Estudis Avancats, ICREA, Barcelona; Spain.
[z] Also at Institut für Experimentalphysik, Universität Hamburg, Hamburg; Germany.

[aa] Also at Institute for Mathematics, Astrophysics and Particle Physics, Radboud University Nijmegen/Nikhef, Nijmegen; Netherlands.
[ab] Also at Institute for Particle and Nuclear Physics, Wigner Research Centre for Physics, Budapest; Hungary.
[ac] Also at Institute of Particle Physics (IPP); Canada.
[ad] Also at Institute of Physics, Academia Sinica, Taipei; Taiwan.
[ae] Also at Institute of Physics, Azerbaijan Academy of Sciences, Baku; Azerbaijan.
[af] Also at Institute of Theoretical Physics, Ilia State University, Tbilisi; Georgia.
[ag] Also at Istanbul University, Dept. of Physics, Istanbul; Turkey.
[ah] Also at LAL, Université Paris-Sud, CNRS/IN2P3, Université Paris-Saclay, Orsay; France.
[ai] Also at Louisiana Tech University, Ruston LA; United States of America.
[aj] Also at Manhattan College, New York NY; United States of America.
[ak] Also at Moscow Institute of Physics and Technology State University, Dolgoprudny; Russia.
[al] Also at National Research Nuclear University MEPhI, Moscow; Russia.
[am] Also at Near East University, Nicosia, North Cyprus, Mersin; Turkey.
[an] Also at Physikalisches Institut, Albert-Ludwigs-Universität Freiburg, Freiburg; Germany.
[ao] Also at School of Physics, Sun Yat-sen University, Guangzhou; China.
[ap] Also at The City College of New York, New York NY; United States of America.
[aq] Also at The Collaborative Innovation Center of Quantum Matter (CICQM), Beijing; China.
[ar] Also at Tomsk State University, Tomsk, and Moscow Institute of Physics and Technology State University, Dolgoprudny; Russia.
[as] Also at TRIUMF, Vancouver BC; Canada.
[at] Also at Universita di Napoli Parthenope, Napoli; Italy.
[*] Deceased